

NOTE TO USERS

This reproduction is the best copy available.

UMI[®]

University of Alberta

**Sub-cellular Localization and Trafficking of Neuronal Nitric Oxide Synthase
(nNOS) in Primary Cortical Neurons**

By



Elsa Ximena Corso-Diaz

**A thesis submitted to the Faculty of Graduate Studies and Research in partial
fulfillment of requirements for the degree of *Master of Science***

Centre for Neuroscience

**Edmonton, Alberta
Fall 2008**



Library and
Archives Canada

Published Heritage
Branch

395 Wellington Street
Ottawa ON K1A 0N4
Canada

Bibliothèque et
Archives Canada

Direction du
Patrimoine de l'édition

395, rue Wellington
Ottawa ON K1A 0N4
Canada

Your file *Votre référence*
ISBN: 978-0-494-47197-5
Our file *Notre référence*
ISBN: 978-0-494-47197-5

NOTICE:

The author has granted a non-exclusive license allowing Library and Archives Canada to reproduce, publish, archive, preserve, conserve, communicate to the public by telecommunication or on the Internet, loan, distribute and sell theses worldwide, for commercial or non-commercial purposes, in microform, paper, electronic and/or any other formats.

The author retains copyright ownership and moral rights in this thesis. Neither the thesis nor substantial extracts from it may be printed or otherwise reproduced without the author's permission.

AVIS:

L'auteur a accordé une licence non exclusive permettant à la Bibliothèque et Archives Canada de reproduire, publier, archiver, sauvegarder, conserver, transmettre au public par télécommunication ou par l'Internet, prêter, distribuer et vendre des thèses partout dans le monde, à des fins commerciales ou autres, sur support microforme, papier, électronique et/ou autres formats.

L'auteur conserve la propriété du droit d'auteur et des droits moraux qui protègent cette thèse. Ni la thèse ni des extraits substantiels de celle-ci ne doivent être imprimés ou autrement reproduits sans son autorisation.

In compliance with the Canadian Privacy Act some supporting forms may have been removed from this thesis.

Conformément à la loi canadienne sur la protection de la vie privée, quelques formulaires secondaires ont été enlevés de cette thèse.

While these forms may be included in the document page count, their removal does not represent any loss of content from the thesis.

Bien que ces formulaires aient inclus dans la pagination, il n'y aura aucun contenu manquant.


Canada

**To my parents, who shared with me their admiration for life and encouraged my
absurd attempt to understand it.**

ABSTRACT

In neurons, the signaling molecule nitric oxide (NO) is produced by neuronal nitric oxide synthase (nNOS). nNOS full length (nNOS α), and nNOS splice variant beta (nNOS β), are the only nNOS forms active in the brain. nNOS β lacks the PDZ domain which is important for nNOS α interactions with regulatory proteins such as the postsynaptic density 95 (PSD95). To better understand the regulatory mechanisms of nNOS α and nNOS β , chimeras of nNOS α and nNOS β were expressed in primary neurons. nNOS α and nNOS β chimeras localized to all neuronal compartments and co-localized with PSD95-EGFP clusters. Trafficking studies revealed that nNOS α mobility is affected by the chaperone, Heat Shock Protein 90 (HSP90), and the hormone, estrogen. nNOS α and nNOS β were also present in aggresome-like inclusions and their aggregation was induced by HSP90 inhibition. These results suggest that nNOS β is another constituent of the synapse and that nNOS aggregation is a mechanism for its regulation.

ACKNOWLEDGEMENTS

I would like to express my gratitude to Dr. Teresa Krukoff for giving me the opportunity to get involved in the neuroscience field. I would also like to thank my committee members, Dr. Satya Kar and Dr. Kathryn Todd, for their support and advice during this process. In addition, I want to thank my lab-mates for creating a good environment to work in during these years. I also want to thank the Department of Cell Biology for their academic and technical support. Finally, I want to thank the University of Alberta and the Centre for Neuroscience for their financial support.

TABLE OF CONTENTS

CHAPTER 1: INTRODUCTION	1
1.1. Nitric Oxide (NO) discovery and synthesis	2
1.2. Physiological effects of Nitric Oxide (NO)	2
1.2.1. NO in the brain	5
1.3. Nitric Oxide Synthases (NOS)	8
1.3.1. Neuronal NOS (nNOS)	9
1.3.2. Endothelial NOS (eNOS)	9
1.3.3. Inducible NOS (iNOS)	10
1.4. nNOS signaling in neurons	11
1.4.1. Activation of soluble guanylate cyclase (sGC)	11
1.4.2. S-nitrosylation	13
1.5. nNOS regulation	14
1.5.1. nNOS gene regulation	14
1.5.1.1. nNOS splice variants	14
1.5.2. Protein-protein interactions	17
1.5.3. Post-transcriptional modifications	21
1.5.4. Degradation	22
1.6. nNOS sub-cellular localization	23
1.7. Estrogen effects on nNOS	24
1.8. Objectives	24

CHAPTER 2: MATERIALS AND METHODS	26
2.1. Materials	27
2.1.1. Reagents and supplies	27
2.1.2. Oligonucleotides and plasmids	29
2.1.3. Antibodies	29
2.1.4. Animals	30
2.1.5. Commonly used buffers	30
2.2. Cell cultures	31
2.2.1. Primary rat cortical culture	31
2.2.2. Human embryonic kidney cells (HEK293) culture	31
2.2.3. <i>E.coli</i> culture	32
2.3. DNA and RNA analysis	32
2.3.1. Isolation of DNA from <i>E.coli</i>	32
2.3.2. Restriction endonuclease digestion and dephosphorylation of 5', 3' overhangs	33
2.3.3. Ligation of DNA	33
2.3.4. Isolation of RNA from primary neurons	33
2.3.5. Reverse transcriptase polymerase chain reaction	34
2.3.6. Polymerase chain reaction	35
2.3.7. Agarose gel electrophoresis	36
2.4. Construction of tagged nNOS proteins	36
2.4.1. nNOS α -EGFP and nNOS β -EGFP	36
2.4.2. nNOS α -HA and nNOS β -HA	37

2.4.3.	mCherry expression vector	37
2.5.	Plasmid delivery	38
2.5.1.	Transformation of chemically competent <i>E.coli</i>	38
2.5.2.	Transfection of HEK293 cells and primary cortical neurons	38
2.6.	Protein electrophoresis and detection	39
2.6.1.	Whole cell extracts	39
2.6.2.	Sodium Dodecyl-sulfate polyacrylamide gel electrophoresis (SDS-PAGE)	39
2.6.3.	Western blot	39
2.6.4.	Membrane stripping	40
2.6.5.	Immunofluorescence	40
2.7.	Fluorescence microscopy	41
2.7.1.	Fixed-cell confocal microscopy	41
2.7.2.	Live-cell confocal microscopy	42
2.7.3.	Fluorescence recovery after photobleaching (FRAP)	42
2.8.	Experimental design	43
2.8.1.	Determining the percentage of cells containing nNOS aggregates in primary cortical neurons	43
2.8.2.	Effect of HSP90 on nNOS aggregations	44
2.8.3.	Effect of estrogen and HSP90 on nNOS α -EGFP trafficking in primary neuronal cultures	44
2.9.	Statistics	44

CHAPTER 3: RESULTS	45
3.1. Characterization of nNOS chimeras	46
3.1.1. nNOS α -GFP, nNOS β -GFP, nNOS α -HA and nNOS β -HA sizes and phosphorylation	46
3.1.2. nNOS α -HA and nNOS β -HA interaction with PSD95	46
3.2. nNOS expression and distribution in primary cortical neurons	48
3.2.1. nNOS α and nNOS β transcripts	48
3.2.2. Distribution of nNOS	48
3.2.2.1. Localization of endogenous nNOS	48
3.2.2.2. Localization of nNOS chimeras	51
3.2.2.3. Localization of nNOS to the nuclear compartment	54
3.3. nNOS trafficking in primary cortical cultures	54
3.3.1. Effects of HSP90 on nNOS trafficking	58
3.3.2. Effects of estrogen on nNOS trafficking	58
3.4. nNOS localization to aggregates	58
3.4.1. Characterization of nNOS aggregates	58
3.4.1.1. Correlation between nNOS aggregates and aggresomes	60
3.4.2. nNOS aggregations and neuronal survival	60
3.4.3. Correlation between nNOS aggregates and nNOS localization to neuronal compartments	64
3.4.4. α -synulcein and nNOS aggregations	64
3.4.5. HSP90 effects on nNOS aggregation	64

CHAPTER 4: DISCUSSION	70
4.1. Overview	71
4.2. Subcellular localization and trafficking of nNOS	72
4.2.1. Sub-cellular localization of neuronal nitric oxide synthase alpha (nNOS α)	72
4.2.2. Trafficking of neuronal nitric oxide synthase alpha (nNOS α)	74
4.2.3. Sub-cellular localization of neuronal nitric oxide synthase beta (nNOS β)	76
4.2.4. Interactions of neuronal nitric oxide synthase alpha (nNOS α) and beta (nNOS β) with PSD95	77
4.3. nNOS is trafficked to aggregates in primary cortical neurons	78
4.3.1. nNOS aggregations are aggresome-like structures	78
4.3.2. Neurons containing nNOS aggregations are not degenerating	80
4.3.3. Mechanism of aggresome-like inclusion formation	80
4.3.4. Implications of nNOS aggregations	83
4.4. Concluding remarks	86
4.5. Future directions	87
4.5.1. What is the physiological significance of nNOS trafficking to the nuclear compartment?	88
4.5.2. How is nNOS β trafficked to PSD95 puncta?	88
4.5.3. What are the characteristics of nNOS α and nNOS β aggregates in neurons?	89
REFERENCES	90

LIST OF TABLES

Table 1. Known protein interactors for nNOS in neurons.	18
Table 2. Reagents and supplies	27
Table 3. Multi-component systems	28
Table 4. DNA modifying enzymes	28
Table 5. Oligonucleotides	29
Table 6. Plasmids	29
Table 7. Primary antibodies	29
Table 8. Secondary antibodies	30
Table 9. Buffers	30

LIST OF FIGURES

Figure 1. Nitric oxide production	3
Figure 2. NO signaling at the synapse	12
Figure 3. nNOS splice variants	15
Figure 4. nNOS chimeras are phosphorylated	47
Figure 5. nNOS α -HA and nNOS β -HA interact with PSD95-GFP	49
Figure 6. Expression and distribution of endogenous nNOS in primary cortical cultures	50
Figure 7. Distribution of nNOS α -EGFP and nNOS β -EGFP chimeras in primary cortical neurons	52
Figure 8. Distribution of nNOS α -HA and nNOS β -HA chimeras in primary cortical neurons	53
Figure 9. Nuclear localization of nNOS	55
Figure 10. Fluorescence recovery after photobleaching (FRAP) of nNOS α -EGFP in primary cortical neurons	56
Figure 11. Effect of HSP90 on nNOS α -EGFP trafficking in primary cortical neurons	57
Figure 12. Effect of estrogen on nNOS α -EGFP trafficking in primary cortical neurons	59
Figure 13. Endogenous nNOS aggregates in primary cortical cultures.	61
Figure 14. Characterization of nNOS aggregates	62
Figure 15. Survival of neurons containing nNOS aggregates	63

Figure 16. Golgi apparatus and nNOS aggregations	65
Figure 17. Correlation between nNOS aggregates and nNOS localization to neuronal compartments	66
Figure 18. α -synuclein and nNOS aggregations	67
Figure 19. HSP90 inhibition induces nNOS aggregation	69
Figure 20. nNOS monomerization induces aggregation	84

LIST OF ABBREVIATIONS

°C	Degrees Celcius
µg	Microgram
µl	Microlitre
µM	Micromolar
ACTH	Adrenocorticotropic hormone
AMP	Adenosine monophosphate
BH4	Tetrabiopterin
Ca ²⁺	Calcium
CaM	Calmodulin
CaM-K II	Calcium/calmodulin-dependent protein kinase II
cDNA	Complimentary deoxyribonucleic acid
cGC	Cyclic guanylate cyclase
cGMP	Cyclic guanosine monophosphate
COX	Hemoprotein cyclooxygenase
CREB	cyclic AMP responsive element binding protein
CRF	Corticotropin-releasing factor
CtBP	C-terminal binding protein
DIV	Days in vitro
DMEM	Dulbecco's modified essential media
DNA	Deoxyribonucleic acid
dNTP	Deoxyribunocleotide triphosphate

DTT	Dithiothreitol
e-	Electron
E2	Estrogen
ECL	Enhanced chemiluminescence
EGF	Epidermal growth factor
EGFP	Enhanced GFP
eNOS	Endothelial nitric oxide synthase
ERK-1	Extracellular signal-regulated kinase-1
FAD	Flavin adenine dinucleotide
FBS	Fetal bovine serum
FMN	Flavin mononucleotide
fmol	Femtomole ($\times 10^{-15}$)
GABA	Gamma-aminobutyric acid
GFP	Green fluorescent protein
GluR1	Glutamate receptor subunit 1
GSNO	S-nitroso-L-glutathione
GTP	Guanosine triphosphate
HA	Hemeagglutinin
HEK293	Human embryonic kidney cells 293
HSP70	Heat shock protein 70
HSP90	The heat shock protein 90
iNOS	Inducible nitric oxide synthase
IPTG	Isopropyl-thio-2-D-galactopyranoside

JNK	c-Jun N-terminal kinases
L-NAME	N-Nitro-L-Arginine Methyl Ester
LPS	Lipopolysaccharide
LTD	Long term depression
LTP	Long term potentiation
MAP-2	Microtubule associated protein 2
MAPK	Mitogen-activated protein kinase
ml	Milliliter
MMP9	Matrix metalloproteinase-9
mRNA	Messenger ribonucleic acid
NADPH	Nicotinamide adenine dinucleotide phosphate
NB	Neurobasal media
NCPs	Neuronal cell precursors
nM	Nanomolar
NMDA	N-methyl-D-aspartate
nNOS	Neuronal nitric oxide synthase
nNOS α	Neuronal nitric oxide synthase alpha
nNOS β	Neuronal nitric oxide synthase beta
N-terminal	Amino terminal
NO	Nitric oxide
NOS	Nitric oxide synthase
NOSIP	Nitric oxide synthase-interacting protein
ONOO-	Peroxynitrite

PBS	Phosphate-buffered saline
PCR	Polymerase chain reaction
PDZ	PSD/Disc-large/ZO-1
PI3K	Phosphoinositide 3-kinase
PIN	Protein inhibitor of nNOS
PKG	Protein kinase G
PKK-M	Muscle phosphofructokinase
PSD93	Postsynaptic density protein 93
PSD95	Postsynaptic density protein 95
RIPA	Radioimmunoprecipitation buffer
RISK-1	Ribosomal S6 kinase 1
RT-PCR	Reverse transcriptase-Polymerase chain reaction
SDS-PAGE	Sodium Dodecyl-sulfate polyacrylamide gel electrophoresis
SERT	Serotonin transporter
SFM	Serum-free media
TBS	Tris buffer saline
VP	Vasopressin

CHAPTER 1

INTRODUCTION

1.1. Nitric Oxide (NO) discovery and synthesis

Nitric oxide (NO) is a highly reactive gas first described by Ignarro and collaborators as a mediator of vasodilation in 1987 (Ignarro et al., 1987). NO is a free radical with a high diffusion rate and lipophilicity (Reiter et al., 2006). NO is also a signaling molecule that reacts with heme proteins, metalloenzymes and other free radicals. In excess, NO can generate harmful oxidative and nitrosative species (Szabo et al., 2007). NO is mainly generated by nitric oxide synthase (NOS) that uses L-arginine and oxygen to generate L-citrulline and NO (Knowles et al., 1994). A representation of the reaction involved in NO production is depicted in Figure 1. To date, three isoforms of NOS have been characterized. One of them is the inducible, calcium-independent nitric oxide synthase (iNOS). The other two are endothelial (eNOS) and neuronal (nNOS) NOS, both calcium-dependent. All three isoforms share approximately 50% homology but their regulation is quite distinct and complex (Alderton et al., 2001).

Since the discovery of NO as an important mediator of vasodilation, a great number of studies have supported its role in astonishingly different physiological processes. For example, NO is involved in apoptosis (Afanas'ev et al., 2007), differentiation (Stroissnigg et al., 2007), blood pressure regulation (Gingerich et al., 2006), and synaptic plasticity (Sergeeva et al., 2007), among others.

1.2. Physiological effects of Nitric Oxide (NO)

NO has various physiological effects and modulates different body functions. NO is important for the proper functioning of the cardiovascular, respiratory, renal,

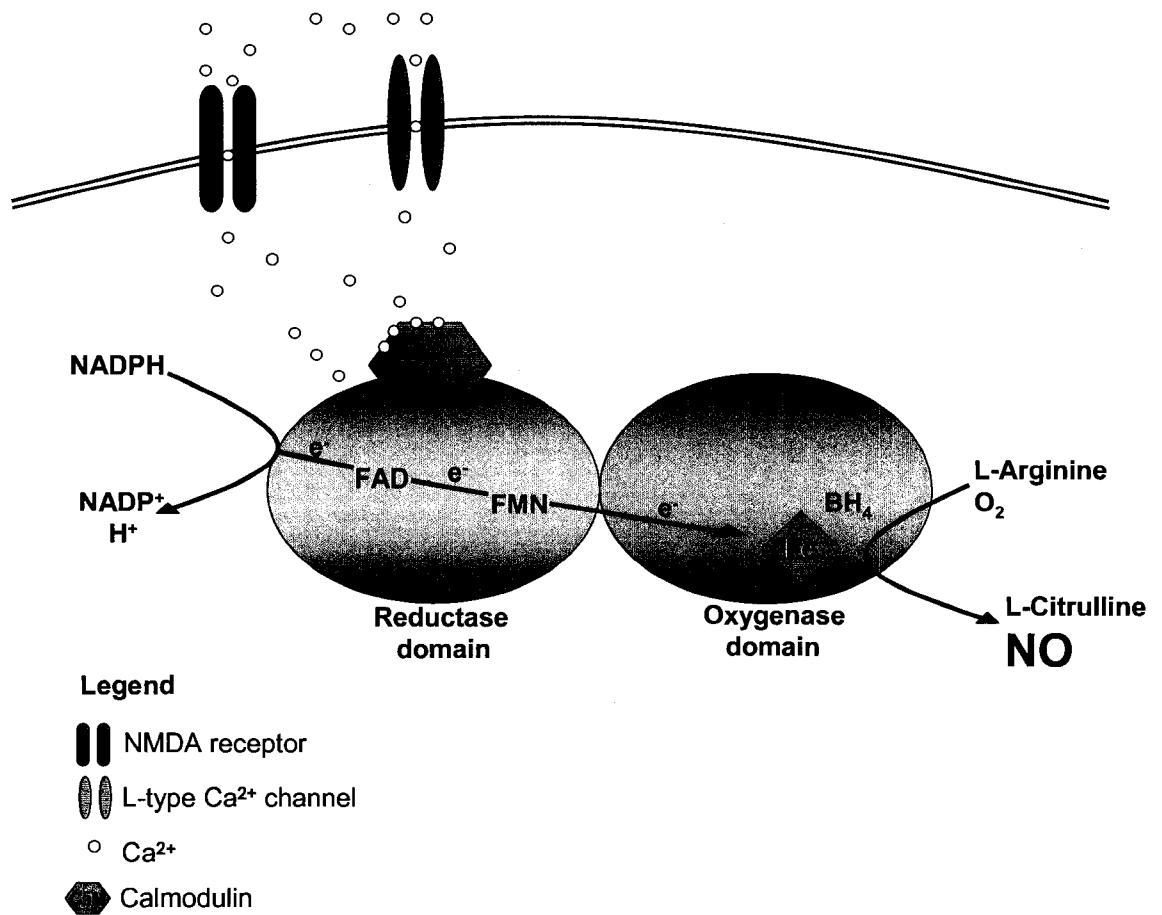


Figure 1. Nitric oxide production. At the level of the reductase domain of nitric oxide synthase, NADPH donates electrons (e⁻) that are carried via FAD and FMN to the oxygenase domain. At the active site, they interact with the heme iron and tetrahydrobiopterin (BH₄) to catalyse the reaction of oxygen with L-arginine. This reaction generates NO and L-citrulline. Electron flow through the reductase domain requires bound calcium/calmodulin (Ca²⁺/CaM) for both eNOS and nNOS.

reproductive, muscular, digestive, immune, and nervous systems. The first known physiological effect of NO was its participation in vascular relaxation through its direct action on the vascular smooth muscle (Ignarro et al., 1987). Subsequent studies showed that NO is the principal regulator of blood pressure (Griffith et al., 1987). NO effects in the cardiovascular system also depend on its actions in the brain. For example, inhibition of NOS in autonomic centers leads to an increase in blood pressure and heart rate in anesthetized rats (Nurminen et al., 1997). NO also has a direct effect on the cardiovascular system through the regulation of myocardial contractility. For example, NO inhibits L-type Ca^{2+} channels and stimulates Ca^{2+} release from sarcoplasmic reticulum in cardiomyocytes (Barouch et al., 2002).

The effect of NO on vascular relaxation greatly affects other systems as well such as the renal system, having a relaxing effect on the glomerular microcirculation (Hirata et al., 1995); reproductive system, producing penile erection (Toda et al., 2005); and the respiratory system, increasing lung blood flow and gas exchange (Walters et al., 2008). NO is also directly involved in respiratory rhythmogenesis facilitating ventilation under physiological conditions of increased oxygen demand (Pierrefiche et al., 2007).

In skeletal muscle, NO mediates different processes such as excitation-contraction coupling, glucose metabolism and mitochondrial energy production to increase muscle relaxation (Grozdanovic, 2001).

NO is also a key player in the immune system, being involved in processes such as proliferation, differentiation and apoptosis of macrophages, thymocytes, lymphocytes and endothelial cells (Duan et al., 2007). NO can also form

peroxynitrate (ONOO⁻), which is a powerful anti-microbial and anti-tumoral agent (Xie et al., 1994). NO is also an important neurotransmitter and neuromodulator of the central and peripheral nervous systems (Bredt et al., 1994). NO has varied effects on different neural populations including neurons (Oess et al., 2006), astrocytes (Saha et al., 2006), microglia (Gebicke-Haerter et al., 2001), and oligodendrocytes (Boullerne et al., 2006).

1.2.1. NO in the brain

Due to its effects on all cell populations in the brain, NO can greatly affect brain function. nNOS is the main enzyme responsible for NO production in neurons and has been detected in different areas of the brain including the cerebral cortex, the hippocampus, hypothalamus and thalamus (Calabrese et al., 2007).

NO effects in the brain were first described by Garthwaite in 1988, who observed that activation of N-methyl-D-aspartate (NMDA) receptors results in the release of NO (Garthwaite et al., 1988). NO functions in the brain include induction and maintenance of synaptic plasticity (Dinerman et al., 1994), control of sleep, appetite and, body temperature (Monti et al., 2004), modulation of the hypothalamic–pituitary–adrenal axis (Rivier et al., 2001), and control of neural development (Cheng et al., 2003).

NO involvement in synaptic transmission requires its diffusion to the presynaptic neuron and activation of cyclic guanylate cyclase (cGC) thus increasing the release of glutamate and strengthening the synapse (Yang et al., 1999). In this way, NO modulates long term potentiation (LTP), a physiological form of memory formation (Schuman et al., 1991).

In addition to its role as a neurotransmitter, NO has been shown to affect the release of other neurotransmitters such as acetylcholine (Prast et al., 1998), gamma-aminobutyric acid (GABA) (Getting et al., 1996), noradrenaline, glutamate (Lonart et al., 1992), dopamine, and serotonin (Lorrain et al., 1993) through the activation of soluble guanylyl cyclases (sGC).

In addition, NO has a role in the sleep pattern. Intracerebroventricular administration of L-arginine during the dark phase of the light-dark cycle significantly increased slow-wave sleep and reduced waking in adult rats (Monti et al., 2004). In addition, acute intraperitoneal administration of the NOS inhibitor, L-NAME, reduced food intake in lean rats (Squadrito et al., 1994), suggesting a strong effect of NO in modulating feeding behaviours. Furthermore, NO also regulates body temperature. Intravenous injection of L-NAME significantly attenuated the elevation in body temperature elicited by stress in adult rats (Soszynski et al., 2006).

NO affects the hypothalamic–pituitary–adrenal axis by inhibiting adrenocorticotrophic hormone (ACTH) responses to pro-inflammatory cytokines or vasopressin (VP), and stimulating the synthesis of the hypothalamic peptides, corticotropin-releasing factor (CRF) and VP (Rivier et al., 2001). NO affects sympathetic output through different hypothalamic regions including the paraventricular nucleus and posterior hypothalamus, and regions that participate in the baroreflex such as ventrolateral medulla and nucleus of the tractus solitarius. NO regulation of sympathetic function can result in changes in arterial pressure and heart rate (Krukoff, 1999).

NO also influences neuronal differentiation. Treatment of dissociated cortical neuroepithelium cells from embryonic day 10 mice with the NOS inhibitor L-NAME increases proliferation of neuronal cell precursors (NCPs) and decreases differentiation into neurons, whereas the NO donor, sodium nitroprusside, inhibits NCPs proliferation and increases neuronal differentiation (Cheng et al., 2003).

Besides its ability to modulate neuronal signaling, NO also participates in brain homeostasis. For example, NO released from endothelial cells through eNOS decreases vascular tone and increases cerebral blood flow (Bauser et al., 2007). NO also influences the permeability of the blood-brain barrier, inhibits hypertrophy of vascular muscle, and promotes angiogenesis and neurogenesis (Faraci et al., 2006).

NO has also a role in neuronal survival, being neuroprotective or toxic depending on its concentration. NO can be neuroprotective through different mechanisms. NO activates protein kinase B (AKT) and cyclic AMP responsive element binding protein (CREB), both of which are involved in neuroprotection (Contestabile et al., 2004). NO also inhibits NMDA receptors, reducing the formation of peroxynitrite or excessive calcium influx that can cause cell death (Jaffrey et al., 2001). NO can also be neuroprotective through the inhibition of the pro-apoptotic protein caspase-3 (Melino et al., 1997) or through the up-regulation of heme oxygenase 1 (Kitamura et al., 1998).

On the other hand, if NO is produced in excess, nitric oxide becomes cytotoxic. For example, NO can react with superoxide anions to form peroxynitrite, which in turn causes protein damage by nitration (Pacher et al., 2007). NO is also known to affect proteins such as matrix metalloproteinase-9 (MMP9) (Gu et al.,

2002) and the E3 ligase, Parkin, (Yao et al., 2004), both of which are involved in neuronal cell death. Activation of the haemoprotein cyclooxygenase (COX) by NO also produces free-radicals and prostaglandins contributing to inflammatory processes (Mancuso et al., 2007). Oxidative and nitrosative (i.e. N_2O_3 formation) stress have been related to different neurodegenerative diseases such as Alzheimer (Sultana et al., 2006), Parkinson and Huntington disease (Browne et al., 2006).

1.3. Nitric Oxide Synthases (NOS)

NOS enzymes are dimeric proteins that require calmodulin (CaM) for their activation. Three different isoforms of NOS have been identified so far: nNOS, eNOS and iNOS. These isoforms are products of different genes, are regulated in different ways, have different catalytic properties, and share 51-57% homology (Wendy et al., 2001).

The three isoforms are differentially expressed in different tissues: nNOS is mainly present in neurons and muscle, eNOS mainly in endothelial cells, and iNOS mainly in immune cells (Knowles et al., 1994). nNOS and eNOS are constitutively expressed and need calcium for their activation whereas iNOS is inducible and calcium independent.

NOS has an N-terminal oxygenase domain that contains binding sites for heme, tetrahydrobiopterin (BH_4) and L-arginine. This domain is linked by a CaM-recognition site to a C-terminal reductase domain that contains binding sites for flavin adenine dinucleotide (FAD), flavin mononucleotide (FMN) and nicotinamide adenine dinucleotide phosphate (NADPH) (McMillan et al., 1995) (Fig. 1).

1.3.1. Neuronal NOS (nNOS)

nNOS gene is located on chromosome 12 in the human genome and has 29 exons and 28 introns which produce a protein of 160 kDa (Alderton et al., 2001). To date, it is known that nNOS is activated by glutamate, acetylcholine (Mungrue et al., 2004), catecholamines (Balligand et al., 1997) and sex hormones (Weiner et al., 1994). nNOS is expressed in neurons, skeletal muscle, cardiac muscle, and arterial smooth muscle. nNOS has an PSD/Disc-large/ZO-1 homologous (PDZ) binding domain in its amino terminal end. This domain allows the interaction of nNOS with different proteins including the postsynaptic density protein 95 (PSD95), which binds to the cytosolic tail of the NMDAR in neurons (Brenman et al., 1996). In this way, NO is produced following nNOS activation by calcium influx through the NMDAR (Satler et al., 1999).

NO from nNOS increases glucose uptake into skeletal muscle cells (Roberts et al., 1997) and participates in vascular relaxation and cardiac contractility (Barouch et al., 2002). In the brain, NO from nNOS regulates synaptic transmission (Yang et al., 1999) and neuronal survival (Contestabile et al., 2004).

1.3.2. Endothelial NOS (eNOS)

The eNOS gene is located on chromosome 7 in the human genome and has 26 exons, 25 introns and produces a protein of 133 kDa (Alderton et al., 2001). Agonists of different G-protein-coupled cell surface receptors, hemodynamic shear stress and oxygenation can activate eNOS (Shaul et al., 1996). eNOS is highly expressed in the vascular endothelium, airway epithelium and cardiomyocytes, and is mainly involved in the regulation of the cardio-respiratory system (Förstermann et al., 2006). eNOS is

localized to microdomains of the plasmalemmal membrane called caveolae (Shaul et al., 1996). It directly interacts with caveolin-1 in endothelial cells and caveolin-3 in the sarcolemma of cardiomyocytes (Feron et al., 1996). eNOS has also been shown to be trafficked to other cellular compartments such as the Golgi apparatus, nucleus, mitochondria, and peroxisomes (Oess et al., 2006). eNOS undergoes acylation by both myristate and palmitate, which regulate its subcellular localization (Michel et al., 1999).

1.3.3. Inducible NOS (iNOS)

The iNOS gene is located on chromosome 17 in the human genome and has 26 exons and 25 introns which produce a protein of 131 kDa (Alderton et al., 2001). iNOS activity does not depend on calcium and its expression is not constitutive. The iNOS gene is under transcriptional control of different inflammatory mediators such as cytokines and lipopolysaccharide (LPS) (Kröncke et al., 1995). iNOS is expressed in different cellular types including macrophages and microglia (Kröncke et al., 1998). iNOS trafficking can be regulated by palmitoylation which results in its tethering to the plasma membrane (Navarro-Lérida et al., 2004). NO from iNOS plays a very important role in the immune system as a defense molecule against pathogens and as a regulator of the survival of immune cells but its activity has detrimental effects in autoimmune or chronically inflammatory processes (Kröncke et al., 1998).

1.4. nNOS signaling in neurons

In neurons, NO interacts with many intracellular targets to activate a range of different signal transduction pathways that result in stimulatory or inhibitory output signals. The most established mechanisms of NO signaling in neurons are the activation of guanylate cyclase (GC) and protein modifications such as S-nitrosylation (Calabrese et al., 2007). An example of GC activation and S-nitrosylation events occurring at the synapse is depicted in Figure 2.

1.4.1. Activation of soluble guanylate cyclase (sGC)

sGC is a heterodimeric hemoprotein that catalyzes the conversion of guanosine triphosphate (GTP) to cyclic guanosine monophosphate (cGMP). cGMP mediates several effects of NO in the central nervous system (Poulos et al., 2006). NO activates sGC by binding to its heme prosthetic group (Denninger et al., 1999). There are three known targets for cGMP that mediate the transmission of the NO/cGMP pathway signal downstream from guanylate cyclase: cGMP-dependent protein kinase (Lohmann et al., 1997), cGMP-regulated phosphodiesterase (Degerman et al., 1997) and cGMP-gated ion channels (Zagotta et al., 1996). In neurons, NO activates cGMP-dependent protein kinase G (PKG) I and II, which are involved in the control of calcium and sodium influx (Guix et al, 2005). At the neuronal synapse, NO diffuses retrogradely to the presynaptic neuron and stimulates the NO/cGMP/PKG pathway that ultimately induces the release of the neurotransmitter glutamate. This mechanism is important for LTP and long term depression (LTD), both mechanisms of learning and memory formation (Domek-Łopacińska et al., 2005). In addition, cGMP mediates NO-induced

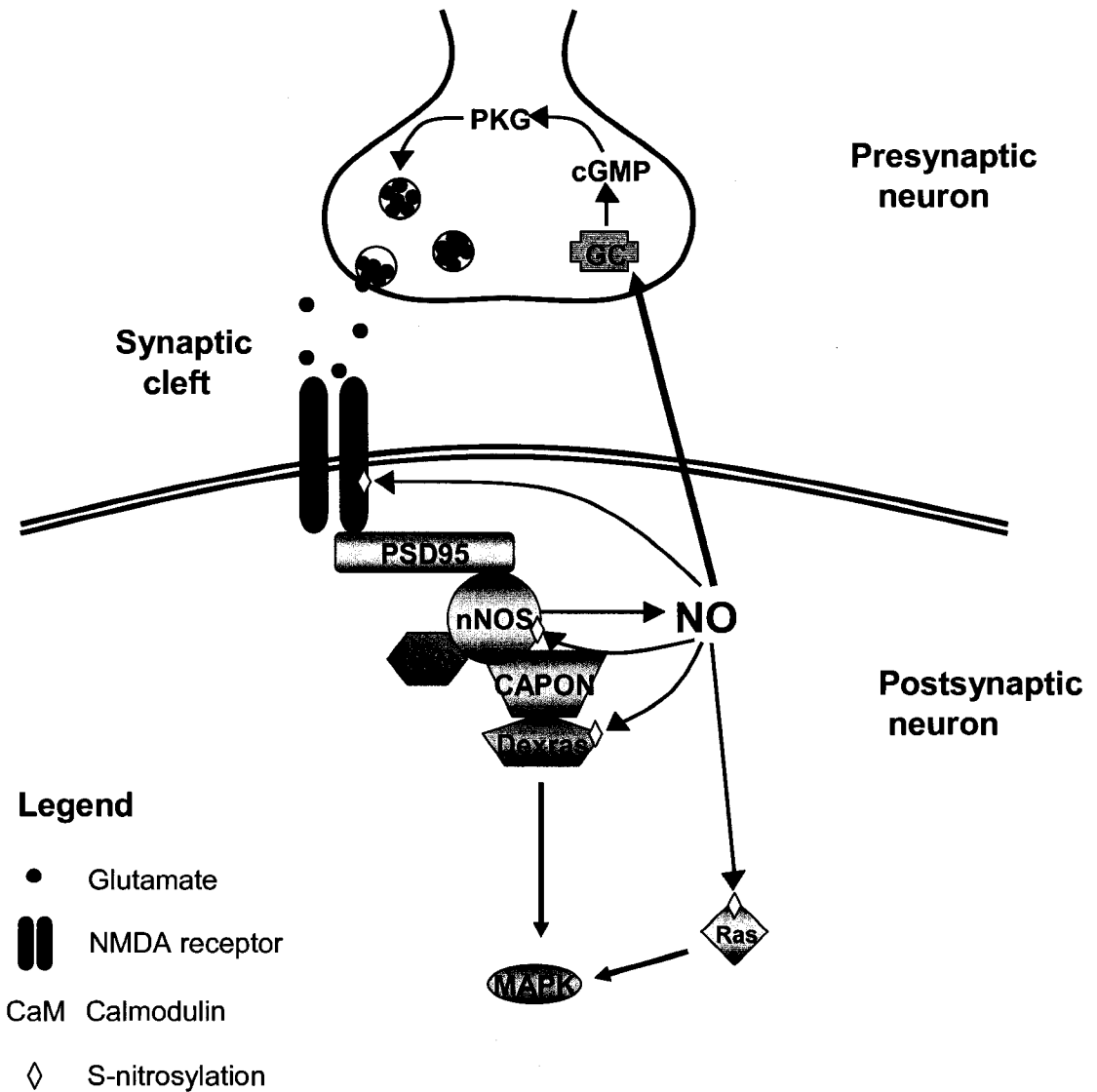


Figure 2. NO signaling at the synapse. Glutamate released by the pre-synaptic neuron activates the NMDAR in the post-synaptic neuron. This activation results in the influx of calcium through the NMDAR calcium channel. In the cytosol, calcium binds calmodulin which, in turn, binds nNOS inducing the production of NO. Nitric oxide diffuses back to the pre-synaptic neuron activating sGC. Activated sGC initiates a cascade of events terminating in the release of glutamate from synaptic vesicles. These events will ultimately strengthen the synapse. In addition to the activation of sGC, NO also reacts with cystein thiol groups of the NMDAR and nNOS, which will lead to their inhibition. Furthermore, S-nitrosylation of the G-protein Ras will activate MAPK. S-nitrosylation of the G-protein Dexras can also occur.

release of other neurotransmitters such as acetylcholine (Prast et al., 1998), GABA (Getting et al., 1996), noradrenaline, dopamine, and serotonin (Lorrain et al., 1993).

1.4.2. S-nitrosylation

S-nitrosylation is a covalent attachment of a nitrogen monoxide group to the thiol side chain of cysteine. This post-translational protein modification is reversible and tightly regulated in time and space (Hess et al., 2005). S-nitrosylation can change protein conformation affecting different protein properties such as electrostatic environment and ability to form disulfide linkages within or between proteins (Hess et al., 2005). The NO moiety can be provided by NO itself whereas de-nitrosylation is carried out by an enzyme, oxidoreductase thioredoxine (Kahlos et al., 2003). Examples of proteins affected by S-nitrosylation are N-Methyl-D-Aspartate receptor (NMDAR) and nNOS itself. Calcium influx through the stimulated NMDAR activates nNOS which produces NO. Nitric oxide generated in this process can inhibit NMDAR and nNOS by S-nitrosylation (Kim et al., 1999; Hess et al., 2005) (Figure 2). Other targets for S-nitrosylation are enzymes such as caspases and aromatases, G-proteins such as cdc42, Ras, Dexas, and kinases such as extracellular signal-regulated kinase-1 (ERK) and p38 (Guix et al., 2005). S-nitrosylation can also confer neuroprotection through the formation of the antioxidant and NO-storing molecule, S-nitroso-L-glutathione (GSNO) (Rauhala et al., 1998). S-nitrosylation can also be detrimental for neurons. An example is the activation of matrix metalloproteases during stroke and neurodegeneration (Gu et al., 2002; Chung et al., 2004).

1.5. nNOS regulation

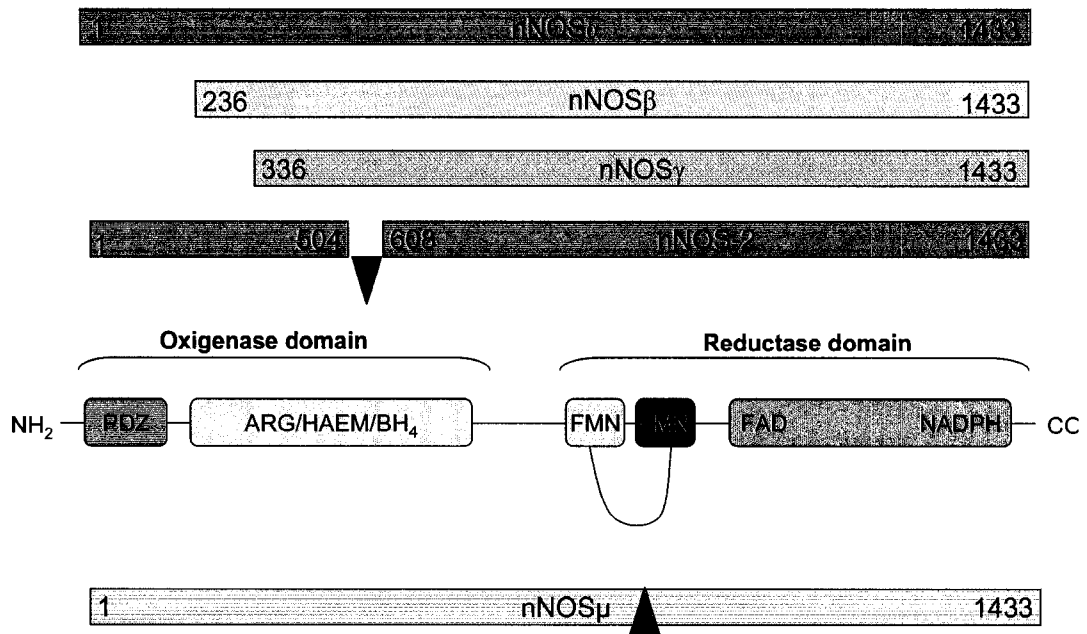
1.5.1. nNOS gene regulation

The nNOS gene is regulated at transcriptional and translational levels. Therefore, it is considered one of the most structurally diverse human genes (Wang et al., 1999). This diversity confers a highly regulated spatial and temporal expression. The nNOS promoter is particularly regulated through the variability of exon 1, which confers nNOS promoter diversity in a tissue- and differentiation-specific manner (Panda et al., 2003).

nNOS mRNA is also alternatively spliced. To date, five primary insertion/deletion nNOS splice variants have been reported in the brain and skeletal muscle (Alderton et al., 2001) (Figure 3). Even though nNOS gene complexity has been extensively studied, the mechanisms and physiological relevance of different splice variants are poorly understood.

1.5.1.1. nNOS splice variants

In 1993, Huang and collaborators generated the first nNOS α null mouse. Surprisingly, this mouse seemed almost completely normal except for digestive and behavioral anomalies (Huang et al., 1993). It was shown later that some residual NO was being produced by different nNOS splice variant isoforms in the brain. These variants were reported to account for 5% of the total NO production in the wild type brain (Brenman et al., 1996). In 1997, Eliasson and collaborators showed that the splice variant beta (nNOS β) is actually an important source of NO in discrete regions of the wild type brain such as cortex and striatum. nNOS β is produced by translation



Legend

- ▼ 104 aa deletion
- ▲ 34 aa insertion

Figure 3. nNOS splice variants. nNOS gene undergoes alternative splicing in the brain and skeletal muscle. nNOS α is a 160 kDa protein and the main splice variant in the brain. It contains 1433 amino acids. nNOS β transcript produces a 136 kDa protein that lacks the PDZ domain. It is comprised of aminoacids 236-1433. nNOS γ transcript produces a 125 kDa protein comprised of aminoacids 336-1433. nNOS-2 transcript produces a 144 kDa protein that has a deletion of 104 amino acids between amino acids 504 and 608. nNOS μ transcript produces a 165 kDa protein with an insert of 34 amino acids in the reductase domain. This protein is mainly expressed in the skeletal muscle. Boxes indicate the PDZ, oxygenase and reductase domains of rat nNOS.

initiation within exon 1a, which gives rise to a protein lacking the first 236 N-terminal amino acids of the full length nNOS (See Fig. 3). Therefore, nNOS β lacks the important PDZ domain which, in the full length isoform, is responsible for mediating interactions with important regulators such as carboxy-terminal PDZ ligand of nNOS (CAPON) (Jaffrey et al., 2002), protein inhibitor of nNOS (PIN) (Jaffrey et al., 1996) and PSD95 (Brenman et al., 1996). The absence of this important domain raises a lot of intriguing questions regarding the physiological role of nNOS β and the molecular mechanisms that allow its functioning in neurons.

To date, very little is known about the role of nNOS β in the brain. It was reported that nNOS β has 80% of nNOS α activity (Brenman et al., 1996). It is also known that its dimerization capability, which is indispensable for the enzyme activation, is not affected by the lack of N-terminal leader sequences (Panda et al., 2003). In addition, nNOS β up-regulation was observed in the spinal cord of humans suffering from amyotrophic lateral sclerosis (Catania et al., 2001).

Another nNOS splice variant, nNOS γ , produces a 125 kDa protein with the deletion of the first 335 amino acids of nNOS α (Eliasson et al., 1997). nNOS γ was shown to have just 3% of nNOS α activity and it is speculated that it can regulate the catalytic activity of nNOS α and nNOS β (Brenman et al., 1996). nNOS-2 is another nNOS splice variant expressed in mouse brain and neuroblastoma cells that lacks 104 amino acids of nNOS α (Brenman et al., 1997). Evidence of opposing effects of nNOS α and nNOS-2 on morphine analgesia and tolerance in mice suggests a dominant negative role of the latter in regulating other nNOS isoforms (Kolesnikov et al., 1997).

nNOS μ is another nNOS splice variant expressed in rat heart, skeletal muscle, penis and urethra (Silvagno et al., 1996), and in human penis and urethra (Magee et al., 1996). nNOS μ is the best characterized nNOS variant. It has additional 34 amino acids present between the CaM and flavin binding domains (Silvagno et al., 1996).

1.5.2. Protein-protein interactions

nNOS must be regulated at different levels to ensure the precise temporal and spatial production of NO. Regulation of protein-protein interactions is an essential strategy to establish nNOS spatial organization within the cell. There are several nNOS interactors that regulate nNOS trafficking and activity in neurons. A list of all known neuronal interactors of nNOS and their significance is shown in Table 1. At least half of nNOS interactors bind to its PDZ domain located at the N-terminal (Fig. 3).

Postsynaptic density protein 95 (PSD95) is a scaffold protein with multiple protein-protein interaction domains. It is the backbone of a protein complex that organizes receptors and signal transduction molecules at the synapse (Dosemeci et al., 2007). nNOS has been shown to interact with PSD95 through its PDZ domain. This interaction allows nNOS to be present at the synaptic active site, especially close to the NMDAR, thus coupling NMDAR activity to NO production (Brenman et al., 1996). nNOS also interacts with postsynaptic density protein 93 (PSD93), another important scaffold present in the postsynaptic density complex (Kim et al., 2004). The exact significance of this interaction is not known.

Another protein that interacts with nNOS PDZ domain is carboxy-terminal PDZ ligand of nNOS (CAPON), which is thought to regulate nNOS association with

Table 1. Known protein interactors for nNOS in neurons. The nNOS region responsible for nNOS binding to the corresponding protein, and the most important outcome of the interaction of nNOS with other proteins are mentioned.

Protein name	Interaction site	Main function of the interaction	Reference
Akt	Unknown	nNOS phosphorylation at serine 1412	Adak et al., 2001
CaM	Reductase domain	nNOS activation	Persechini et al., 1994
CamKII	Unknown	nNOS phosphorylation at serine 847	Komeima et al., 2000
CAPON	PDZ domain	Couples nNOS to Dexras1 nNOS localization to the presynaptic membrane.	Fang et al., 2000 Jaffrey et al., 2002
CtBP	PDZ domain	CtBP subcellular localization	Riefler et al., 2001
HSP90	Unknown	Enhance nNOS/calmodulin association. Modulates nNOS degradation	Song et al., 2001 Avena et al., 2007
NIDD	PDZ domain	Targets nNOS to synaptic compartments	Saitoh et al., 2004
NOSIP	N-terminus	nNOS subcellular localization	Dreyer et al., 2004
PIN	Met-228 to His-244	Inhibits nNOS activity	Jaffrey et al., 1996
PFK-M	PDZ domain	Neuroprotection?	Firestein et al., 1999
PSD93	PDZ domain	Targeting of nNOS to postsynaptic density	Brenman et al., 1996
PSD95	PDZ domain	Targets nNOS to the NMDA receptor	Brenman et al., 1996
RSK1	Unknown	nNOS phosphorylation at serine 847	Song et al., 2007
SERT	PDZ domain	Negative modulation of SERT activity	Chanrion et al., 2006

PSD95 (Jaffrey et al., 1998). CAPON was also found to form a ternary complex with nNOS and synapsin I, which is exclusively a presynaptic protein that mediates neurotransmitter release and synaptic plasticity (Evergren et al., 2007). CAPON-mediated targeting of nNOS to synapsin may expose different synapsin-associated proteins to NO and regulate neurotransmitter release in neurons (Jaffrey et al., 2001). CAPON also forms a ternary complex with nNOS and Dexras 1, a member of the Ras family of monomeric G- proteins. This association allows Dexras 1 to be activated by NO through S-nitrosylation (Fang et al., 2000). Even though the physiological importance of Dexras1 as a target of nNOS is not clear, some studies suggest that nNOS activation of Dexras 1 could be involved in iron-mediated neurotoxicity since activation of Dexras 1 increases iron uptake (Cheah et al., 2006).

The heat shock protein 90 (HSP90) also binds to nNOS (Bender et al., 1999). HSP90 is a chaperone that contributes to proper protein folding. It is different from other chaperones because it induces conformational changes in folded native-like proteins (Wandinger et al., 2008). It has been shown that HSP90 increases nNOS activity by enhancing calcium/calmodulin binding (Song et al., 2001). HSP90 binding to nNOS is very dynamic and is also important to facilitate the binding of the heme group to nNOS (Bender et al., 1999). This binding contributes to the stabilization of the nNOS homodimer. Therefore, inhibition of HSP90 with the antibiotic geldanamycin causes nNOS dimer destabilization and degradation through the proteasome pathway (Osawa et al., 2002). On the other hand, HSP90 is also involved in modulating the proteolytic degradation of nNOS by the enzyme calpain. HSP90-

nNOS complexes recruit calpain, reducing the extent of nNOS proteolysis through this enzyme (Averna et al., 2007).

Another nNOS PDZ domain-interacting protein is nNOS-interacting DHHC domain-containing protein with dendritic mRNA (NIDD). It was reported that NIDD regulates nNOS activity by targeting it to the postsynaptic membrane (Fuminori et al., 2004). nNOS was also reported to bind an isoform of the muscle phosphofructokinase (PFK-M) in brain and skeletal muscle (Firestein et al., 1999). nNOS and PFK-M are enriched in synaptosomes and are present in the same neurons in the brain. nNOS binding to PFK-M may be involved in neuronal survival since the product of PFK-M, fructose-1, 6-biphosphate, is neuroprotective (Firestein et al., 1999). Nevertheless, clear evidence for the purpose of this interaction is lacking.

Interaction of nNOS with the serotonin transporter (SERT) has also been recently reported. nNOS was shown to modulate the membrane localization of SERT and subsequent 5-hydroxytryptamine (5-HT) uptake. Uptake of 5-HT also increased nNOS activity. Therefore, this interaction confers reciprocal functional modulation for nNOS and SERT (Chanrion et al., 2007).

nNOS also interacts with nitric oxide synthase-interacting protein (NOSIP). NOSIP reduces nNOS activity and regulates nNOS localization to terminal dendrites (Dreyer et al., 2004). Protein inhibitor of nNOS, PIN, is another nNOS interactor that inhibits nNOS activity possible through destabilization of nNOS dimer (Jaffrey et al., 1996). nNOS has also been shown to affect the localization of other proteins. For example, it interacts with C-terminal binding protein (CtBP), a transcriptional co-

repressor, changing its localization from the nuclear to the cytosolic compartment (Riefler et al., 2001).

1.5.3. Post-transcriptional modifications

nNOS is also regulated by post-transcriptional modifications that allow the modulation of its activity in response to the changing physiological environment. One of these modifications is phosphorylation. nNOS can be phosphorylated at two different residues. Serine 847 phosphorylation is carried out by calcium/calmodulin-dependent protein kinase II (CaM-K II) resulting in inhibition of nNOS (Komeima et al., 2000). It has been shown that PSD95 promotes CaM-K II-mediated nNOS phosphorylation at this site (Watanabe et al., 2003). This phosphorylation is also strongly regulated by the NMDAR. It has been shown that physiological concentrations of glutamate induce phosphorylation of nNOS at serine 847 but pathological activation of NMDAR by excitotoxic concentrations of glutamate does not induce the phosphorylation of nNOS at this residue (Rameau et al., 2004).

Recently, ribosomal S6 kinase 1 (RSK-1), a downstream effector of mitogen-activated protein kinase (MAPK) (Grove et al., 1993), was also shown to directly phosphorylate nNOS in response to mitogens. Treatment of rat hippocampal neurons with epidermal growth factor (EGF) induced the phosphorylation of nNOS at serine 847. This phosphorylation was prevented by MAPK/extracellular-signal-regulated kinase kinase (MEK) inhibitor PD98059 (Song et al., 2007).

nNOS serine 1412 is phosphorylated by AKT (Adak et al., 2001). Recent studies suggest that NMDAR activation leads to increased phosphorylation of serine

1412 by AKT, which in turn increases nNOS sensitivity to calcium/calmodulin (Rameau et al., 2007). Therefore, nNOS phosphorylation is tightly regulated by the NMDAR since both, serine 847 and serine 1412, are phosphorylated after glutamate transmission.

Another important post-translational modification of nNOS is S-nitrosylation (Hess et al., 2006). This modification has not been studied but it was previously shown that S-nitrosylation of eNOS leads to dimer collapse with a resultant loss of enzyme activity (Ravi et al., 2003).

1.5.4. Degradation

Protein degradation is another mechanism by which nNOS is regulated. The ubiquitin-proteasome and calpain pathways are the major proteolytic systems regulating nNOS turnover (Osawa et al., 2003). The exact mechanism that triggers nNOS proteolysis is not known. Nevertheless, there are studies suggesting that the activation of calpain after excitotoxic insults leads to the proteolytic cleavage of nNOS in rat cerebrocortical cells (Hajimohammadreza et al., 1997). In addition, it was suggested that the heme-deficient monomeric form of nNOS is preferentially ubiquitylated to favour nNOS proteosomal degradation (Osawa et al., 2002). There are different conditions in which the nNOS monomeric form could increase and trigger nNOS degradation. These include NOS inhibitors such as (2,6-dichlorophenyl)-methylidene-amino-imino-methane-diamine (Guanabenz) (Noguchi et al., 2000), heme availability (Albakri et al., 1996), tetrahydrobiopterin depletion (Reif et al., 1999), dimerization inhibition (McMillan et al., 2000) and S-nitrosylation (Ravi et al., 2003).

nNOS degradation is also strongly regulated by HSP90. This chaperone has been shown to prevent both, calpain- and proteasome-induced nNOS degradation (Osawa et al., 2002; Averna et al., 2007).

1.6. nNOS sub-cellular localization

Due to its highly reactive nature and its different effects within the cell, NO sub-cellular production, and therefore nNOS subcellular localization, must be tightly regulated. Most of the studies regarding nNOS localization in neurons have been related to the targeting of nNOS to the post-synaptic plasma membrane through its interaction with the scaffold PSD95 (Brenman et al., 1996). Nevertheless, nNOS is also an important regulator of neurotransmitter release and is also found in the presynaptic vesicles (Loesch et al., 1994). nNOS has also been found in the neuronal mitochondria (Loesch et al., 1994; Batista et al., 2001), endoplasmic reticulum, cytosol (Batista et al., 2001) and presynaptic cytoskeleton (Loesch et al., 1994).

nNOS expression has also been reported in reactive astrocytes (Cantoni et al., 2008). In cultured cerebral cortical astrocytes of rats, nNOS was reported to translocate to the nuclear compartment in astrocytes cultured for 7 days (Yuan et al., 2004).

Despite evidence for nNOS subcellular localization to different neuronal compartments, the consequences of its presence on certain compartments and how it is trafficked to them remains unclear.

1.7. Estrogen effects on nNOS

Estrogen is a steroid hormone that plays different physiological roles in the female and male reproductive systems (Luconi et al., 2002), non-reproductive systems (Mendelsohn et al., 2002), and the initiation and proliferation of reproductive cancer cells (Pike et al., 2004). Some of the physiological processes in which NO mediates estrogen effects include the attenuation of blood pressure responses to psychological stress (Cherney et al., 2003), neuroprotection (Lee et al., 2003; Wen et al., 2004) and learning and memory (Audesirk et al., 2003).

Estrogen exerts most of its effects by increasing nNOS expression in both, endothelial and neuronal cells (Okamura et al., 1994; Sanchez et al., 1998; McNeill et al., 1999; Yang et al., 2000;). Estrogen also activates nNOS by increasing its phosphorylation at serine 1412 through a mechanism that involves calcium mobilization and activation of phosphoinositide 3-kinases (PI3K) (Alexaki et al., 2004).

Whether estrogen affects NO production in other ways remains to be elucidated. Nevertheless, there is evidence suggesting that estrogen regulates nNOS protein-protein interactions. For example, estrogen was found to enhance the association of nNOS with PSD95 in the rat hypothalamus (d'Anglemont de Tassigny et al., 2007).

1.8. Objectives

- nNOS α and nNOS β are the only active forms of nNOS in the brain. Even though it is well established that nNOS α localizes to almost all neuronal compartments, little is known about the signaling that mediates nNOS trafficking to

each compartment where NO is produced locally. In addition, nNOS β sub-cellular distribution in neurons is poorly understood. Therefore, **my first aim is to use primary cortical neuron cultures to study nNOS α and nNOS β subcellular localization.**

- HSP90 is an important chaperone and modulator of protein trafficking that has been shown to interact with nNOS (Bender et al, 1999). HSP90 has also been shown to influence cell signaling by affecting protein conformation and protein-protein interactions (Stravopodis et al., 2007). In addition, HSP90 inhibitors have been proposed to ameliorate neurodegeneration (Luo et al., 2007). **Therefore, my second aim is to determine whether HSP90 affects nNOS α and nNOS β subcellular localization and nNOS α trafficking in primary cortical neurons.**

- Even though estrogen effects are known to be partly mediated by NO, the mechanisms through which estrogen can modulate NOS are not clear. In addition to affect nNOS phosphorylation, estrogen may promote nNOS protein-protein interactions. For example, estrogen enhances the association of nNOS with PSD95 in the rat hypothalamus (d'Anglemon de Tassigny et al., 2007) and promotes the binding of HSP90 to eNOS in endothelial cells (Schulz et al., 2005). To investigate whether estrogen affects nNOS protein-protein interactions, **my third aim is to study the effects of estrogen on nNOS α trafficking in primary cortical neurons.**

CHAPTER 2

MATERIALS AND METHODS

2.1. Materials

2.1.2. Reagents and supplies

Reagents and supplies were used as recommended by the manufacturer unless otherwise stated.

Table 2. Reagents and supplies

Name of Reagent	Source of Reagent
1 kb DNA ladder	Invitrogen
3,8-Diamino-5-ethyl-6-phenylphenanthridinium bromide (Ethidium bromide)	Sigma
17 β -estradiol	Sigma
40% Acrylamide/Bis-acrylamide solution (29:1)	Sigma
4'-6-diamidino-2-phenylindole (DAPI)	Vector
Agar bacteriological	Gibco
Agarose A, electrophoresis grade	Rose Scientific
Ammonium persulfate	BDH
Ampicillin	Sigma
B27 supplement	Invitrogen
Bradford assay	BioRad Laboratories
Bacto-tryptone	Difco
Bacto-yeast extract	Difco
Bromophenol blue	BDH
Complete EDTA-free protease inhibitors	Roche
D-glucose	Invitrogen
Dimethyl sulfoxide (DMSO)	Sigma
Dithioethreitol (DTT)	Sigma
Dulbecco's modified essential media (DMEM)	Invitrogen
dNTPs	Invitrogen
Ethanol	Comercial Alcohols
Ethylenediaminetetraacetic acid (EDTA)	Sigma
Fetal bovine serum (FBS)	Invitrogen
Glycerol	BDH
Halothane	Halocarbon
Hank's balanced salt solution (HBSS)	Invitrogen
HEPES buffer solution	Invitrogen
Hydrogen Peroxide	Sigma
Isopropanol	Fisher
Isopropyl-thio-2-D-galactopyranoside (IPTG)	Quiagen
Kanamycin	Sigma
L-glutamic acid	Sigma
Lipofectamine 2000	Invitrogen
Mercaptoethanol	Sigma-Aldrich
Methanol	Fisher
N,N,N',N'-tetramethylethylenediamine (TEMED)	Invitrogen
Neurobasal medium	Invitrogen
Nonfat dry milk	Carnation
oligo(dT) ₁₂₋₁₈	Invitrogen

Table 2. Reagent and supplies (continued)

Name of Reagent	Source of Reagent
Paraformaldehyde	Sigma-Aldrich
Penicillin-streptomycin	Invitrogen
Poly-D-lysine	Sigma
Pre-stained protein ladder (20-25- kDa)	Fermentas
Rx film (Western blot)	Fuji
Sodium bicarbonate	Invitrogen
Sodium Chloride	Sigma
Sodium deoxycholate	Sigma
Sodium dodecyl sulfate	Sigma
Sodium orthovanadate	Sigma
Sodium pyruvate solution	Invitrogen
Trans-blot Transfer medium-nitrocellulose membrane	Bio-Rad
Tris base	Roche
Triton-X 100	Sigma
Trizol	Invitrogen
Trypsin	Invitrogen
Tween-20	Sigma
Vectashield-DAPI solution	Vector Labs
Western Lightning chemiluminescence kit	PerkinElmer
5-bromo-4-chloro-3-indolyl- β -D-galactopyranoside (X-gal)	Quiagen

Table 3. Multi-component systems

System	Source
QUIAEXII Gel extraction kit	Quiagen
QUIAGEN plasmid Maxi Kit	Quiagen
SuperScript™ III RT	Invitrogen

Table 4. DNA modifying enzymes

Enzymes	Source
Calf intestinal alkaline phosphatase	Roche
Platinum Taq High fidelity DNA polymerase	Invitrogen
Restriction endonucleases	Invitrogen
T4 DNA ligase	Invitrogen

2.1.2. Oligonucleotides and plasmids

Table 5. Oligonucleotides

Primer name	Primer sequence	Engineered sites
1. nNOS α F	5'ACCGCTCGAGACCATGGAGAACACGTTTG3'	XhoI
2. nNOS α R GFP	5'CCGGAATTCGGTGATGGTGATGGTGATGATGGGAGC TGAAAACCTCATCTGC3'	EcoRI
3. nNOS β F	5'ATATTGAATTCACCATGCGCGGGCTCGGCAGCAGAG ACCTCGATGGCAAAC3'	EcoRI
4. nNOS β R GFP	5'ATATGAATTCGGGAGGCGGAGCTGAAAACCTCATC3'	EcoRI
5. nNOS R HA	5'ATATGAATTCTTATACCCATACGATGTTCCAGATTAC GCTGGCGGAGGGGGCGGAGGAGCTGAAAACCTCATCT G3'	EcoRI
6. Cherry F	5'ATATGAATTCATGGGCGGAGGCGGAGGCATGGT GAGCAAGGGCGCATC3'	EcoRI
7. Cherry R	5'ATATGCGGCCGCTTACTTGTACAGCTCGTCCATG3'	NotI
8. nNOS α RT F	5'AGGTGGACAGAGACCTCGAT3'	
9. nNOS β RT F	5'CTGCGCGGGCTCGGCAG3'	
10. nNOS RT R	5'AGCATGATCGAGCCCATGC3'	
11. L-19 F	5'GAAATCGCCAATGCCAACTC3'	
12. L-19 R	5'ACCTCCAGGTACAGGCTGTG3'	

Table 6. Plasmids

Vector	Source	Institution
pGEM-T	Promega	N/A
pEGFP-N1	Clontech	N/A
PSD95-GFP	Dr. Alaa El-Huseinni	University of British Columbia, Vancouver, Canada
pnNOS-cDNA	Dr. Solomon Snyder	Johns Hopkins University, Baltimore, USA
pAALN-Cherry	Dr. Tom Hobman	University of Alberta, Edmonton, Canada

2.1.3. Antibodies

Table 7. Primary antibodies

Specificity	Dilution	Source	Institution
Rabbit anti-nNOS (R-20)	1:100/500/6000	Santa Cruz	N/A
Mouse anti-Neurofilament M	1:50	Santa Cruz	N/A
Mouse anti-Ubiquitin	1:10	Santa Cruz	N/A
Mouse anti HSP90	1:50	Cell Signaling	N/A
Rabbit anti-phospho nNOS (Ser ¹⁴¹²)	1:500	Abcam	N/A
Rabbit anti-phospho nNOS (Ser ⁸⁴⁷)	1:500	Abcam	N/A
Mouse anti-p115	1:50	Dr. Melançon	University of Alberta, Canada
Mouse anti- α -synuclein	1:50	Cell Signaling	N/A
Mouse anti-MAP-2	1:50	Cell Signaling	N/A
Rabbit anti-cleaved caspase 3	1:50	Cell Signaling	N/A
Mouse anti- β -actin	1:4000	Jackson ImmunoResearch	N/A

Table 8. Secondary antibodies

Specificity	Source
Donkey anti- rabbit Alexa Fluor 488	Invitrogen
Donkey anti- mouse Alexa Fluor 568	Invitrogen
Donkey anti-rabbit Alexa Fluor 568	Invitrogen
Goat anti-mouse HRP	Jackson Immunoresearch
Donkey anti-rabbit HRP	Jackson Immunoresearch

2.1.4. Animals

Pregnant female Sprague-Dawley rats (day 18 of gestation) were purchased from Charles River Laboratories (Saint-Constant, Quebec). All procedures were approved by the local Animal Welfare Committee.

2.1.5. Commonly used buffers

Table 9. Buffers

Buffer	Ingredients
4 x protein sample buffer	400 mM DTT, 8% SDS, 0.4% bromophenol blue, 20% glycerol, 200 mM Tris-HCL, pH 6.8
6 x DNA loading buffer	40% sucrose, 0.25% bromophenol blue, 0.25% xylene cyanol FF
Phosphate buffered saline (PBS)	137 mM NaCl, 2.7 mM KCl, 8 mM Na ₂ HPO ₄
Protein transfer buffer	200 mM glycine, 25 mM Tris Base, 20% methanol
Radioimmunoprecipitation buffer (RIPA)	150 mM NaCl, 0.5% sodium deoxyate, 0.1 % SDS, 1% NP40, 50 mM tris-HCl, pH 8.0
SDS-PAGE resolving gel buffer	0.1 % SDS, , 374 mM Tris-HCl, pH 8.8
SDS-PAGE running buffer	250 mM Glycine, 0.1 % SDS, 100 mM Tris Base
SDS-PAGE stacking gel buffer	0.1 % SDS, , 250 mM Tris-HCl, pH 6.8
Solution I (miniprep)	50 mM tris-HCl pH 8.0, 10 mM EDTA, 100 µg/ml RNase A
Solution II (miniprep)	200 mM NaOH, 1 % SDS
Solution III (miniprep)	3 M Potassium acetate pH 5.5
TAE	40 mM Tris acetate. 1 mM EDTA, pH 8.0
TE	1 mM EDTA, 10 mM Tris-HCL, pH 7.5

2.2. Cell culture

2.2.1. Primary rat cortical culture

Primary cortical neurons were obtained from embryonic day 18 rat pups and cultured as described previously (Brewer et al., 1993). Briefly, brains were dissected and the forebrain separated from the rest of the brain. The cortex was obtained by removing adjacent tissue (meninges, basal ganglia, thalamus, hypothalamus, and hippocampus). Cortices were rinsed 3 times in Hank's balanced salt solution (HBSS, containing 15 mM HEPES and 30 µg/mL penicillin-streptomycin) followed by digestion with 0.125% trypsin for 15 minutes at 37°C. Cortical tissue was then rinsed with HBSS followed by trypsin inactivation with fetal bovine serum (FBS) for 30 seconds. Tissue was rinsed again 3 times in HBSS and then mechanically dissociated by trituration. Cortical neurons were re-suspended in serum-free media (SFM) consisting of phenol-red free Neurobasal medium, 15 mM Hepes, 1.5 mM sodium pyruvate, 0.6 mM L-glutamine, 30 µg/mL penicillin/streptomycin and 2% B27 supplement.

Cells were plated onto culture dishes or cover-slips coated with poly-D-Lysine (Sigma) at a density of 1400 cells/mm², and incubated at 37°C in 5% CO₂ and 95% air. On day 3, medium was changed to SFM without L-glutamine. Medium was changed three times per week. Cultures were maintained for 14 days in vitro (DIV). Culture materials were purchased from Invitrogen unless otherwise stated.

2.2.2. Human embryonic kidney cells (HEK293) culture

HEK293 cells (Clontech) were grown in DMEM medium supplemented with

10% fetal bovine serum and 30 µg/mL penicillin/streptomycin. Medium was changed every 3 days. Cells were grown in 6-well plates or 24-well plates according to the experimental design. Culture materials were purchased from Invitrogen.

2.2.3. *E.coli* culture

DH5α chemicompetent cells (Invitrogen) were grown on LB (0.5g/ml Bacto tryptone, 0.25 g/ml bacto-yeast extract, 40 mM NaCl) antibiotic-selective plates for 16 hours. Colonies from plates were then grown in 5 ml of antibiotic-selective LB media and processed later for plasmid purification. Bacteria transformed with pGEM-T vector (Table 6) were grown on plates containing 0.1 mM of X-gal and 0.1 mM IPTG (Table 2).

2.3. DNA and RNA analysis

2.3.1. Isolation of DNA from *E.coli*

High yield plasmid DNA (~500 µg) was purified using a commercially available kit from Qiagen (Table 3). DNA minipreparations were made as follows. Bacterial pellets were resuspended in 250 µl of solution I (Table 9). Then, 250 µl of solution II (Table 9) were added. The tube was then inverted 4 times and incubated for 5 minutes at room temperature to allow the lysis of bacteria. Proteins were precipitated upon the addition of 350 µl of solution III (Table 9). The tube was centrifuged at 14,000 g for 15 minutes to pellet proteins and chromosomal DNA. The supernatant was transferred to a new tube and 0.6 volumes of isopropanol were added to precipitate the plasmid DNA. The tube was centrifuged at 15,000 g for 15 minutes.

The pellet was washed with 70% of Isopropanol and air-dried. Subsequently, the pellet was resuspended in 30 μ l of TE (Table 9).

2.3.2. Restriction endonuclease digestion and dephosphorylation of 5', 3' overhangs

Prior to the ligation of insert and vector, a restriction digestion was carried out. Reaction volumes of 20 μ l were used to completely digest 0.5 to 3.0 μ g of DNA with EcoR1 or Xho1 as per manufacturer's specifications.

To enrich for positive clones and minimize the occurrence of vector self-ligation when using single cut vectors, calf intestinal alkaline phosphatase (Table 4) was used to dephosphorylate the ends of linearized vectors. The reaction was carried out according to the manufacturer's instructions. The inserts and vectors were then ligated as described below (section 2.3.4).

2.3.3. Ligation of DNA

T4 DNA ligase (Table 4) was used to ligate DNA fragments. All reactions were carried out according to manufacturer's recommendations. Normally, 20 μ l of the reaction contained 10 fmol of vector and 30 fmol of insert. Reactions were carried out for 16 hours at 15 $^{\circ}$ C.

2.3.4. Isolation of RNA from primary neurons

In order to determine whether primary cortical neurons express nNOS α and/or nNOS β in culture, the corresponding RNA transcripts were amplified by RT-PCR (see below). RNA was extracted from 14 DIV cells grown in 6-well plates using the Trizol reagent (Table 2) according to the manufacturer's instructions. Briefly, cells

were washed twice with PBS and 1 ml of Trizol reagent was added to homogenize the cells. After 5 minutes of incubation at room temperature, 0.2 ml of chloroform were added and samples incubated for 3 more minutes at room temperature. Subsequently, samples were centrifuged at 10,000 g for 15 minutes at 4°C. The aqueous phase was transferred to a new tube and the RNA was precipitated by the addition of 0.5 ml of isopropanol. Samples were incubated for 30 minutes at room temperature and centrifuged at 10,000 g for 10 minutes. Subsequently, the supernatant was removed and the RNA pellet was washed with 1 ml of 75% ethanol. Samples were further centrifuged at 7,000 g for 10 minutes. The pellet was air-dried and dissolved in RNase-free water. Samples were stored at -80°C until use.

2.3.5. Reverse transcriptase polymerase chain reaction

To assess the presence of nNOS α and nNOS β transcripts, cDNA was generated from RNA obtained from primary cortical neurons using first strand synthesis followed by PCR. Thirteen μ l of a reaction containing 500 ng of oligo(dT)₁₂₋₁₈ (Table 2), 5 μ g total RNA, 1 μ l of 10 mM dNTPs mix (Table 2) and Millipore water were heated to 65°C for 5 minutes and incubated on ice for 1 minute. A second reaction mix containing 4 μ l of 5X First-Strand Buffer, 1 μ l 0.1 M DTT (Table 2), 1 μ l RNaseOUT™, and 1 μ l of SuperScript™ III RT (200 units/ μ l) (Table 3) was added and mixed with gentle pipetting. The sample was incubated at 50°C for 60 minutes followed by incubation at 70°C for 15 minutes. The cDNA was used for PCR amplification of nNOS isoforms.

2.3.6. Polymerase chain reaction

To assess the presence of nNOS α and nNOS β transcripts in cultured neurons, the cDNA generated from RNA of primary cortical neurons was used as a template. The sets of primers were constructed to span an intron between exon 2 and 3. A region of ~290 bp for nNOS α was amplified using primers 8 and 10 (Table 5). A region of ~310 bp for nNOS β was amplified using primers 9 and 10 (Table 5). Amplification of a 290 bp fragment of the L-19 ribosomal protein mRNA was used as a control and carried out using the primer pair 11 and 12 (Table 5). The 50 μ l reaction normally contained 1 μ g of cDNA template, 10 μ M of dNTPs, 1 unit of Platinum High Fidelity Taq polymerase (Table 4), 1X reaction buffer and 20 μ l of mineral oil. DNA amplification was performed using a PTC-100 programmable thermal controller (NJ Research, Inc.). A PCR reaction consisted of a denaturing cycle at 94°C for 2 minutes, followed by 35 cycles of amplification defined by denaturation at 94°C for 45 seconds, annealing at 50°C for 45 seconds, and extension at 68°C for 5 minutes. A final extension cycle of 68°C for 10 minutes was included. The PCR product was run on an agarose gel.

For the construction of nNOS chimeras (section 2.4), nNOS cDNA (Table 6) was amplified by PCR. The amplification of nNOS α and nNOS β sequences was performed with corresponding primers (Table 5): 1,2 for nNOS α -EGFP; 3,4 for nNOS β -EGFP; 1,5 for nNOS α -HA; 3,5 for nNOS β -HA. The reaction was carried on in a 50 μ l solution containing high fidelity polymerase according to the manufacturer's specifications. The PCR was carried out as described above except for an extension time of 5 minutes. The PCR product (4.4 Kb for nNOS α ; 3.7 KB for

nNOS β) was run on agarose gel and purified using a gel purification kit (Table 3) before it was subjected to restriction endonuclease digestion.

For the construction of a mCherry expression vector, mCherry sequence was amplified from pAALN-Cherry (Table 6) by PCR. The amplification of mCherry was carried out using the primers 6 and 7 (table 5) which amplify a 711 bp fragment. The PCR reaction was carried on as described above using an extension time of 1 minute.

2.3.7. Agarose gel electrophoresis

Gels were prepared by adding 1% of electrophoresis grade agarose to TAE buffer (Table 9) and heating to dissolve. Prior to congealing of the gel, 0.3 μ g/ml ethidium bromide (Table 2) was added. DNA samples mixed with 6X gel loading dye (Table 9) were resolved while immersed in TAE. The fragments were visualized and images captured using a FluoroChem imaging system (Alpha Innotech Corporation).

2.4. Construction of tagged nNOS proteins

2.4.1. nNOS α -EGFP and nNOS β -EGFP

To generate nNOS α -EGFP and nNOS β -EGFP chimeras, nNOS cDNAs were amplified by PCR (section 2.3.7) and cloned into the EGFP-N1 vector (Table 6). Briefly, nNOS α and nNOS β PCR products were run on agarose gels and purified using a gel purification kit (Table 3). Purified nNOS α DNA was ligated into pGEM-T (section 2.3.4) to facilitate restriction endonuclease activity of Xho1. Bacteria were transformed and grown on IPTG/XGal plates (section 2.2.3) for blue/white selection. Plasmid DNA from positive colonies (white color) was extracted. Purified pGEM-T-

nNOS α and EGFP-N1 vectors (Table 6) were subjected to restriction endonuclease digestion using Xho1 and EcoR1. The samples were run again on agarose gels and purified. Ligation of the fragments was performed using T4 DNA ligase (section 2.3.4). The ligated vector was then transformed in bacteria and grown on antibiotic-selective plates (section 2.5.1). Colonies were grown in antibiotic-selective LB media and plasmid DNA was purified for restriction digestion screening.

Purified nNOS β DNA and EGFP-N1 vector were subjected to restriction endonuclease digestion using EcoR1. The samples were gel-purified and cloned as described above.

2.4.2. nNOS α -HA and nNOS β -HA

nNOS α and nNOS β DNA were amplified from nNOS cDNA by PCR (section 2.3.7) and cloned into the EGFP-N1 vector (Table 6). The cloning protocol was followed as explained above (section 2.4.1). Expression of the EGF protein was prevented by the insertion of a stop codon in front of the EGFP coding region.

2.4.3. mCherry expression vector

A red fluorescent protein (mCherry) was used as a control for protein localization in primary cortical cultures. mCherry DNA was amplified from pAALN-Cherry by PCR (section 2.3.7) and cloned into the EGFP-N1 vector (Table 6). Purified mCherry PCR product and EGFP-N1 vectors were subjected to restriction endonuclease digestion using Xho1 and Not1. The cloning protocol was followed as described above (section 2.4.1)

2.5. Plasmid delivery

2.5.1. Transformation of chemically competent *E.coli*

Fifty μl of chemically competent *E.coli* DH5 α were transformed by adding 1 μl of appropriate plasmids (1 $\mu\text{g}/\text{ml}$) and incubating them on ice for 20 minutes. Heat-shock was carried out at 37°C for 20 seconds. Subsequently, cells were placed on ice for 2 minutes followed by the addition of 1 ml of LB media. Cells were incubated at 37°C for 45-60 minutes. Afterwards, cells were precipitated by centrifugation, resuspended in 100 μl of LB media and plated on LB Ampycillin+ or Kanamycin+ (Table 2) plates.

2.5.2. Transfection of HEK293 and primary cortical neurons

HEK293 cells and primary cortical neurons were grown in 24-well or 6-well and transfected with Lipofectamine 2000 (Table 2) according to the manufacturer's instructions. Briefly, 3.4 $\mu\text{l}/\text{ml}$ of Lipofectamine were dissolved in 50 μl (24-well) or 200 μl (6-well) of Neurobasal media (NB). The mixture was incubated at room temperature for 5 minutes. A solution containing appropriate DNA in 50 μl or 200 μl of NB was added to the lipofectamine mixture so that the final concentration of DNA per well was 8 $\mu\text{g}/\text{ml}$. The final mixture was incubated for 20 minutes at room temperature and added to the wells. Normally, cells were used for experiments after 24 hours of transfection.

2.6. Protein electrophoresis and detection

2.6.1. Whole cell extracts

In order to evaluate the sizes and phosphorylation states of the nNOS chimeras, HEK293 cells were grown in 6-wells and transfected with the respective nNOS plasmids. After 24 hours, cells were lysed in RIPA buffer containing complete protease inhibitor cocktail and sodium orthovanadate (Table 2). After incubation on ice for 20 minutes, genomic DNA was sheared by passing the lysate through a 16 gauge needle. Lysates were cleared by centrifugation (4000 x g) for 15 minutes at 4°C. The supernatant was used for protein quantification with the Bradford assay. The supernatant was subsequently stored at -80°C.

2.6.2. Sodium Dodecyl-sulfate polyacrylamide gel electrophoresis (SDS-PAGE)

Sample buffer (Table 9) was added to the protein samples extracted from HEK293 cells. Proteins were then denatured at 95°C for 6 minutes and separated by gel electrophoresis. To prepare the stacking gel, 4% of acrylamide/bis-acrylamide (Table 2) was added to the SDS-PAGE stacking buffer (Table 9). The resolving gel was comprised of 8% acrylamide/bis-acrylamide added to the SDS resolving buffer (Table 9). Prior to gel casting, 0.1% TEMED (v/v) and 0.1% ammonium persulfate (w/v) (Table 9) were added. Electrophoresis was conducted in SDS-PAGE buffer (Table 9).

2.6.3. Western blot

Proteins were transferred to a nitrocellulose membrane after being separated

on an SDS-PAGE gel. Transfer was achieved using a Bio-Rad Mini Trans-Blot™ electrophoretic transfer cell at 120 mV for 80 minutes. During the transfer, the apparatus was chilled in an iced water bath. After transfer of proteins, membranes were washed in TBS-T for 10 minutes and then blocked in TBS-T containing 5% milk for 1 hour at room temperature. Respective primary antibodies (Table 7) were diluted in blocking solution. Membranes were incubated overnight at 4°C.

Subsequently, membranes were washed in TBS-T for 1 hour, incubated with peroxidase-conjugated secondary antibody (Table 8) and washed again in TBS-T for 1 hour. Membranes were subsequently incubated with a chemiluminescent reagent (PerkinElmer, Boston, MA) for 1 minute and exposed to an autoradiography film.

2.6.4. Membrane stripping

To blot against phosphorylated nNOS at both, serine 847 and serine 1412 residues, membranes containing antibody against nNOS were exposed to a stripping solution comprised of 350 µl of 4.3 M Mercaptoethanol, 10 ml of 10% SDS, 31.25 ml of 1M Tris-HCl pH 6.7 and 8.75 ml of di distilled water. The incubation was performed for 1 hour at 50°C. Membranes were then washed 3 times in TBS and subsequently blocked and treated as in section 2.5.4.

2.6.5. Immunofluorescence

Immunocytochemistry was used to study nNOS distribution and viability of primary cortical cultures. Cultures were washed twice with PBS (Table 9) and fixed with 3% paraformaldehyde (Table 2) for 20 minutes. After a subsequent wash with PBS, free aldehydes were quenched with 50 mM NH₄Cl/PBS for 10 minutes.

Neurons were then permeablized in 0.1% Triton-X 100/PBS (table 2) for 4 minutes, washed twice with PBS and incubated in blocking solution (PBS containing 0.1% Tween 20 and 1% nonfat dry milk) for 30 more minutes. Subsequently, neurons were incubated overnight at 4°C with the respective primary antibodies (Table 7) diluted in blocking solution. After three washes with blocking solution, respective secondary antibodies conjugated to fluorophores (Table 8) were added. Cultures were then washed twice with blocking solution for 10 minutes and twice with PBS for 20 more minutes. For double labeling experiments with α -synuclein and activated caspase-3, cultures were blocked again and the procedure was repeated with anti-nNOS antibody. After the final washing, fixed-cells were mounted and imaged as described in section 2.6.1.

2.7. Fluorescence Microscopy

2.7.1. Fixed-cell confocal microscopy

Confocal microscopy was performed on cells grown on cover-slips in 24-well plates. Imaging was carried out in transfected primary cortical neurons and HEK293 cells, or in neurons processed for immunofluorescence and fixed with paraformaldehyde. Cover-slips were mounted onto slides over a drop of Vectashield-DAPI solution (Table 2). Imaging was achieved using a Zeiss LSM510 confocal microscope.

2.7.2. Live-cell confocal microscopy

With the purpose of assessing nNOS distribution in live HEK293 cells and

trafficking in primary cortical cultures, cells were grown on 22 mm cover-slips and transfected with nNOS α -EGFP. Twenty four hours after transfection, cover-slips were transferred to an Attofluor cell chamber (Invitrogen). The chamber was kept at 37°C using a lens heater and stage heater while images were taken using a Zeiss LSM510 confocal microscope.

2.7.3. Fluorescence recovery after photobleaching (FRAP)

In order to study nNOS trafficking in live-cells, primary cortical neurons were grown for 13 DIV, transfected with nNOS α -EGFP and imaged as in section 2.6.2. A confocal image of the transfected neuron of interest was taken before starting the photobleaching procedure. The zoom-up function (2X) was used to limit the scanned region to the dendrites (3 μ m pinhole) of interest or nucleus (8 μ m pinhole). A chosen dendrite from the neuron of interest was bleached by directing a high power (100%) argon laser onto an area of 20 x 20 μ m². The dendrite was imaged before bleaching and every 10 seconds after bleaching over 290 seconds. The fluorescence recovery was studied by measuring the signal intensities obtained every 10 seconds after bleaching. The signal intensities were studied in an area of 10 μ m² in the bleached field using LSM510 software. To normalize for fluorescence loss, another region not adjacent to the bleached dendrite was monitored for changes in intensity. Data from 6 neurons per treatment were used for analysis. The amount of recovery (R) at each time point (t) was normalized with the fluorescence in a non-bleached area (control) using the following formula: $R = (F'0/F't) * (Ft/F0)$.

F'0 = fluorescence of the 10 μ m² control area before bleaching

F't = fluorescence at every time point of the control area

F0 = fluorescence of the bleached area before bleaching

Ft = fluorescence at each time point of the 10 μm^2 bleached area

With the aim of assessing nNOS nuclear localization in HEK293 cells, cells were transfected with nNOS α -EGFP and treated as in section 2.6.2. The nucleus was bleached in an area of 8 X 8 μm^2 corresponding to approximately half of the nuclear compartment. Two images before bleaching and 1 image 10 seconds after bleaching were taken.

2.8. Experimental design

2.8.1. Determining the percentage of cells containing nNOS aggregates in primary cortical neurons

In order to assess the numbers of cells containing nNOS aggregates in culture at different times, cells at 6, 10 and 14 DIV were processed for indirect immunofluorescence against endogenous nNOS and visualized under a fluorescence microscope. To assess the numbers of neurons with nNOS aggregations at different DIV, neurons with aggregates and total nuclei were counted under the microscope. Using the 63X lens, approximately 1000 cells were counted per cover-slip. Ten fields were counted through the middle of the cover slip following a straight line that corresponded to the cover-slip diameter. All DAPI-stained nuclei were counted regardless of the nuclear integrity. The percentage of nNOS-containing aggregates relative to the total number of nuclei counted was used for comparison among 6, 10 and 14 DIV. Four different cultures were used per treatment.

2.8.2. Effect of HSP90 on nNOS aggregations

To induce aggresome formation of nNOS α and nNOS β , HEK293 cells and primary cortical cultures were transfected with nNOS α -EGFP, nNOS β -EGFP or EGFP and treated with 10 μ M of an HSP90 inhibitor, geldanamycin. The drug or vehicle was added to the cultures for 6 hours. Subsequently, cells were fixed and processed for confocal imaging.

2.8.3. Effect of estrogen and HSP90 on nNOS α -EGFP trafficking in primary neuronal cultures

To study the effect of HSP90 and estrogen on nNOS trafficking, 13 DIV primary cortical neurons grown on 22 mm cover-slips were transfected with nNOS α -EGFP. Twenty four hours after transfection, cultures were treated with 10 μ M of the HSP90 inhibitor geldanamycin or vehicle for 3 hours. Other cultures were treated with 5, 500 or 1000 nM of 17- β -estradiol (E2) or vehicle for 10 minutes. To determine the duration of action of E2, another set of cultures was treated for 1 or 2 hours with 1000 nM of E2 or vehicle. Trafficking was then studied as described in section 2.6.3.

2.9. Statistics

Statistical analysis was carried out using XLSTAT. All data are presented as mean \pm SEM. Significant differences were determined by one-way ANOVA followed by the posthoc Dunnet test and were considered significant when $P < 0.05$.

CHAPTER 3

RESULTS

3.1. Characterization of nNOS chimeras

To test whether the nNOS chimeras produced in this study have similar characteristics as their endogenous counterparts, all nNOS chimeras were tested for protein size and phosphorylation. In addition, the ability of nNOS α and nNOS β to interact with the scaffold protein, PSD95, was assessed.

3.1.1. nNOS α -GFP, nNOS β -GFP, nNOS α -HA and nNOS β -HA sizes and phosphorylation

To verify the correct protein sizes of the constructs developed, each chimera was transfected into HEK293 cells. A western blot was performed using proteins collected 24 hours post transfection. Membranes were first probed with antibody against nNOS. The sizes of nNOS α -EGFP (~180 kDa) and nNOS β -EGFP (~160 kDa) corresponded to the sizes of nNOS α and nNOS β proteins (~155 kDa; ~136 kDa) plus the EGFP tag (~27 kDa). Similarly, the sizes of nNOS α -HA and nNOS β -HA corresponded to the size of nNOS α and nNOS β proteins, respectively. The size of the HA tag is negligible (~0.9 kDa).

In addition, membranes were stripped and probed with antibodies against the known phosphorylated sites of nNOS (serine 847 and serine 1412) as an indication of correct folding and interaction with proper kinases (Akt and CamKII). All the constructs were phosphorylated at both serine 847 and serine 1412 residues (Figure 4).

3.1.2. nNOS α -HA and nNOS β -HA interaction with PSD95

To further test for the functionality of the generated nNOS chimeras, I

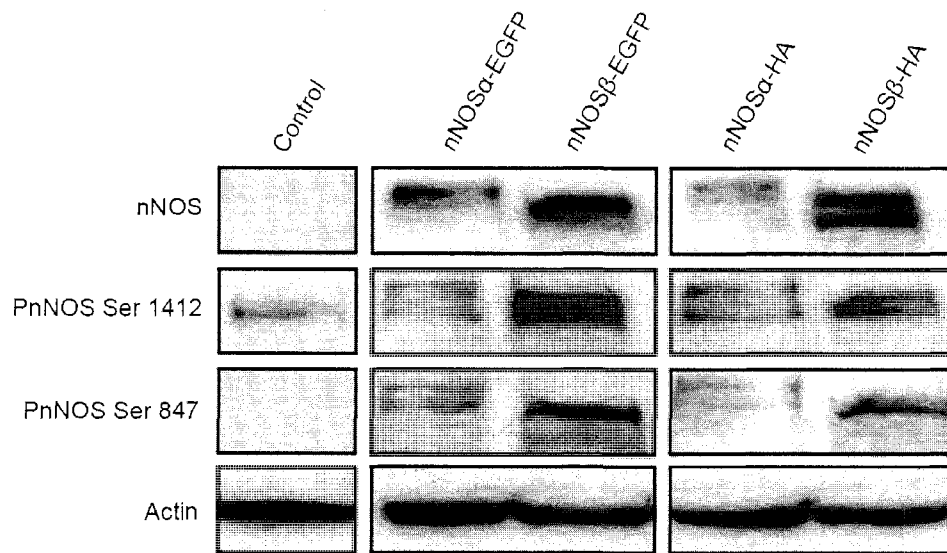


Figure 4. nNOS chimeras are phosphorylated. In order to evaluate the functionality of the nNOS chimeras developed, the phosphorylation of nNOS at serine 847 and serine 1412 was evaluated. HEK293 cells were transfected with each nNOS chimera. Proteins were collected 24 hours after transfection, separated by SDS-PAGE and subjected to immunoblot analysis. Membranes were probed with anti-nNOS, stripped and probed for phosphorylated serine 847 or phosphorylated serine 1412. All chimeras were phosphorylated at both phosphorylation sites. Negative controls were run on a different gel.

evaluated whether they could co-localize with PSD95 in the neuronal intracellular environment. nNOS α -HA or nNOS β -HA were co-transfected with PSD95-GFP into 13 DIV primary cortical neurons. nNOS α -HA and PSD95-EGFP colocalized in puncta along dendritic shafts (Figure 5A). This co-localization result argues for appropriate folding of the over-expressed nNOS chimeras. Furthermore, nNOS β -HA also co-localized with PSD95 in puncta (Figure 5B).

3.2. nNOS expression and distribution in primary cortical neurons

3.2.1. nNOS α and nNOS β transcripts

While nNOS β transcripts have been found in the mouse brain (Eliasson et al., 1997), their presence in primary brain neuronal cultures was not established. To detect nNOS β transcripts in 14 DIV rat cortical cultures, total mRNA was purified and the correspondent cDNA generated. A RT-PCR reaction was performed to amplify a fragment of ~300 bp of nNOS α and nNOS β DNA. As shown in Figure 6A, both splice variants are expressed in mature cortical cultures. The ribosomal subunit L-19 was used as a positive control.

3.2.2. Distribution of nNOS

3.2.2.1. Localization of endogenous nNOS

Primary cortical cultures at 8 and 14 DIV were fixed and processed for indirect immunofluorescence against total nNOS. Figure 6B shows that nNOS is present predominantly in the cytoplasm. Faint nuclear staining can also be detected. Overall, nNOS distribution in the cytoplasm is mainly punctate. Even though mature neurons

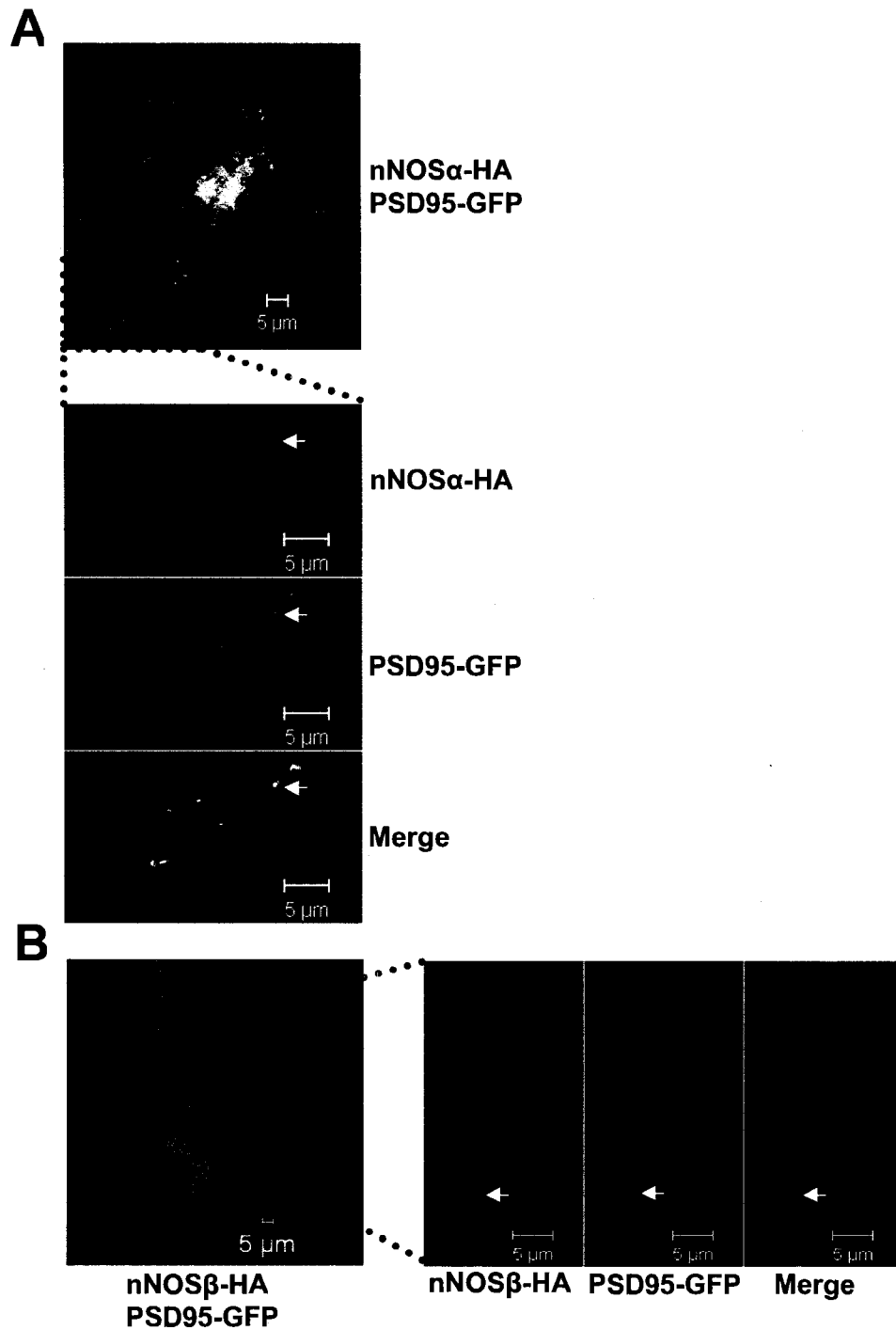


Figure 5. nNOS α -HA and nNOS β -HA interact with PSD95-GFP. To evaluate nNOS α -HA functionality, its interaction with PSD95-GFP was studied. Primary cortical neurons were transfected with nNOS α -HA or nNOS β -HA at 13 DIV. After 24 hours of transfection, rat anti-nNOS was used to detect nNOS α -HA and nNOS β -HA chimeras by immunocytochemistry. **A)** nNOS α -HA co-localizes with PSD-95 in puncta (arrows); **B)** nNOS β -HA also co-localizes with PSD-95 in puncta (arrows).

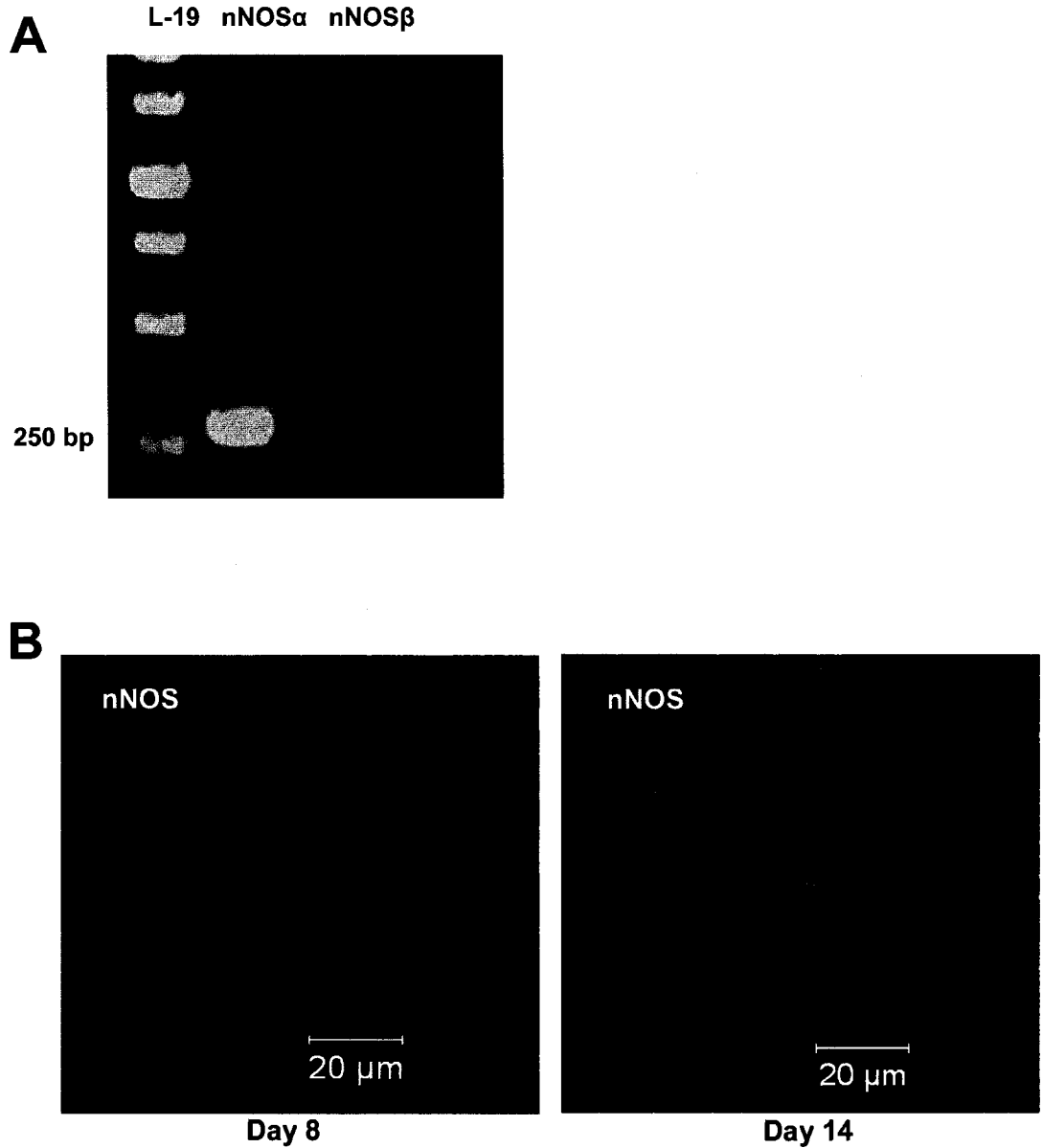


Figure 6. Expression and distribution of endogenous nNOS in primary cortical cultures. **A)** An RT-PCR was performed to study the expression of nNOS α and nNOS β in primary cortical cultures. RNA was collected from 14 DIV cortical cells and used as a template for cDNA generation. Short fragments of the ribosomal subunit L-19 (control), nNOS α and nNOS β were amplified by PCR. All transcripts are present in primary cortical neurons. **B)** Endogenous nNOS subcellular distribution was studied by immunofluorescence. nNOS distribution is punctate throughout the neuronal cytoplasm and similar at 8 and 14 DIV.

showed more dendritic area and spines than young neurons, a similar nNOS distribution was observed in both neuronal populations.

3.2.2.2. Localization of nNOS chimeras

Since cultured neurons express both, nNOS α and nNOS β proteins, HA and EGFP tagged chimeras of each splice variant were engineered to study their distributions. nNOS α -EGFP, nNOS β -EGFP, nNOS α -HA, or nNOS β -HA were co-transfected each together with mCherry into 7 and 13 DIV primary cortical neurons. Twenty four hours post transfection, neurons were fixed and, in the case of HA chimeras, processed for indirect immunofluorescence against nNOS (1:6000). mCherry is a small red fluorescent protein that diffuses throughout the cytoplasm (Shu et al., 2006) and was used to visualize all neuronal compartments. The distribution of nNOS α -EGFP is diffuse throughout the neuron (Figure 7A) and present with mCherry in dendrites and spines (Figure 7B). To confirm that this distribution is not due to the EGFP tag, another chimera with the small HA tag was also transfected in primary neurons. nNOS α -HA displayed a similar distribution as that of nNOS α -EGFP (Figure 8A and 8B) suggesting that the localization of the over-expressed chimeras is not influenced by the tag.

nNOS β -EGFP distribution was similar to that of nNOS α chimeras shown in Figures 7A and 8A. nNOS β -EGFP was diffuse throughout the neuron (Figures 7C) and present in neurites and dendritic spines (Figure 7D). This distribution was also similar to that of nNOS β -HA (Figures 8D and 8E). A confocal slice of 3 μ m through the middle of the neuronal nuclear compartment shows that nNOS α (Figure 8C) and nNOS β (Figure 8F) are indeed present in the neuronal nucleus.

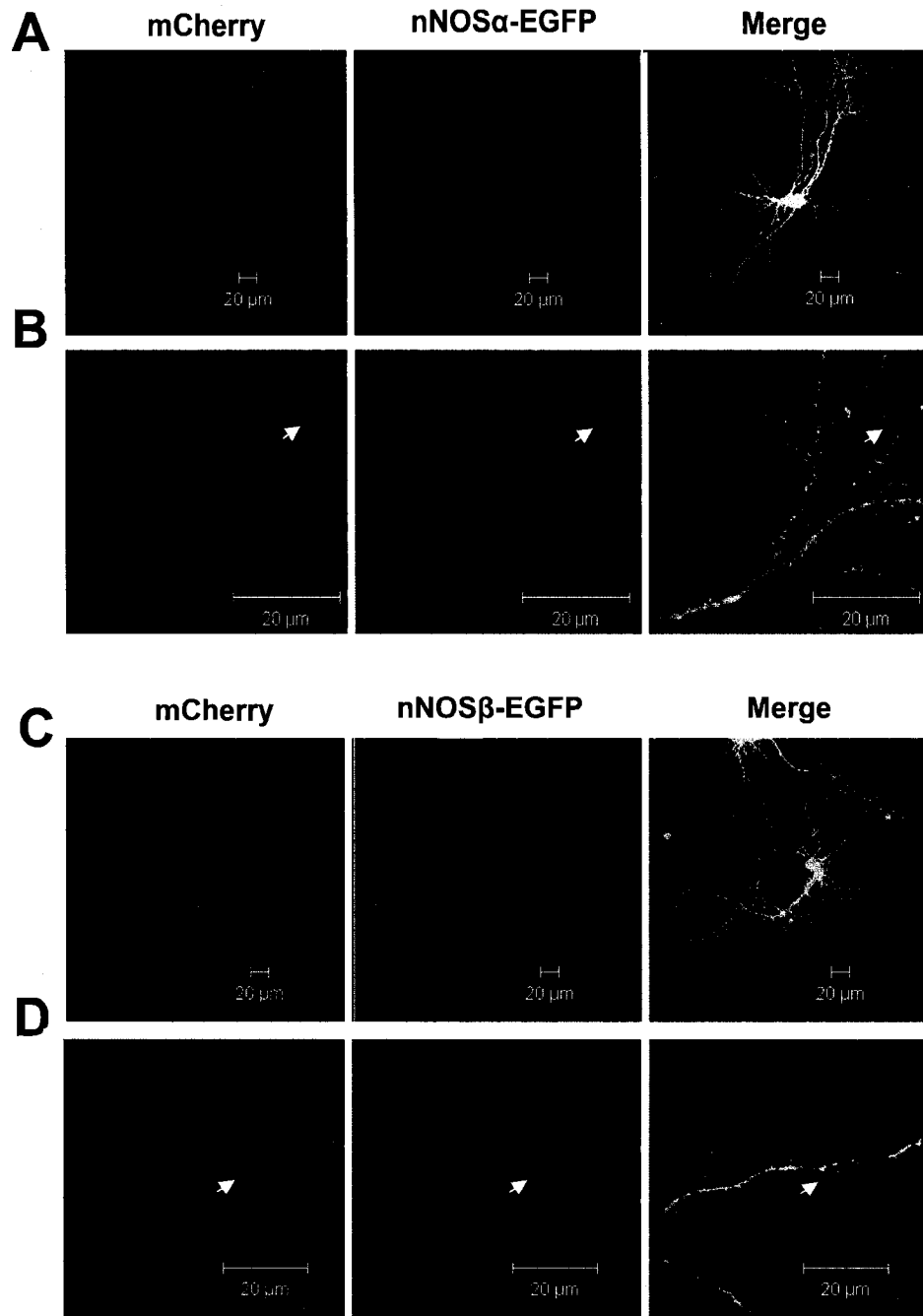


Figure 7. Distribution of nNOS α -EGFP and nNOS β -EGFP chimeras in primary cortical neurons. Neurons were grown for 13 DIV and transfected with either nNOS chimera plus a red fluorescent protein (mCherry). nNOS α -EGFP is distributed in the cell soma (A) and neuritic compartments (B) including spines (arrows). nNOS β -EGFP has a similar distribution to nNOS α -EGFP. nNOS β -EGFP is distributed in the cell soma (C) and neuritic compartments (D) including spines (arrows).

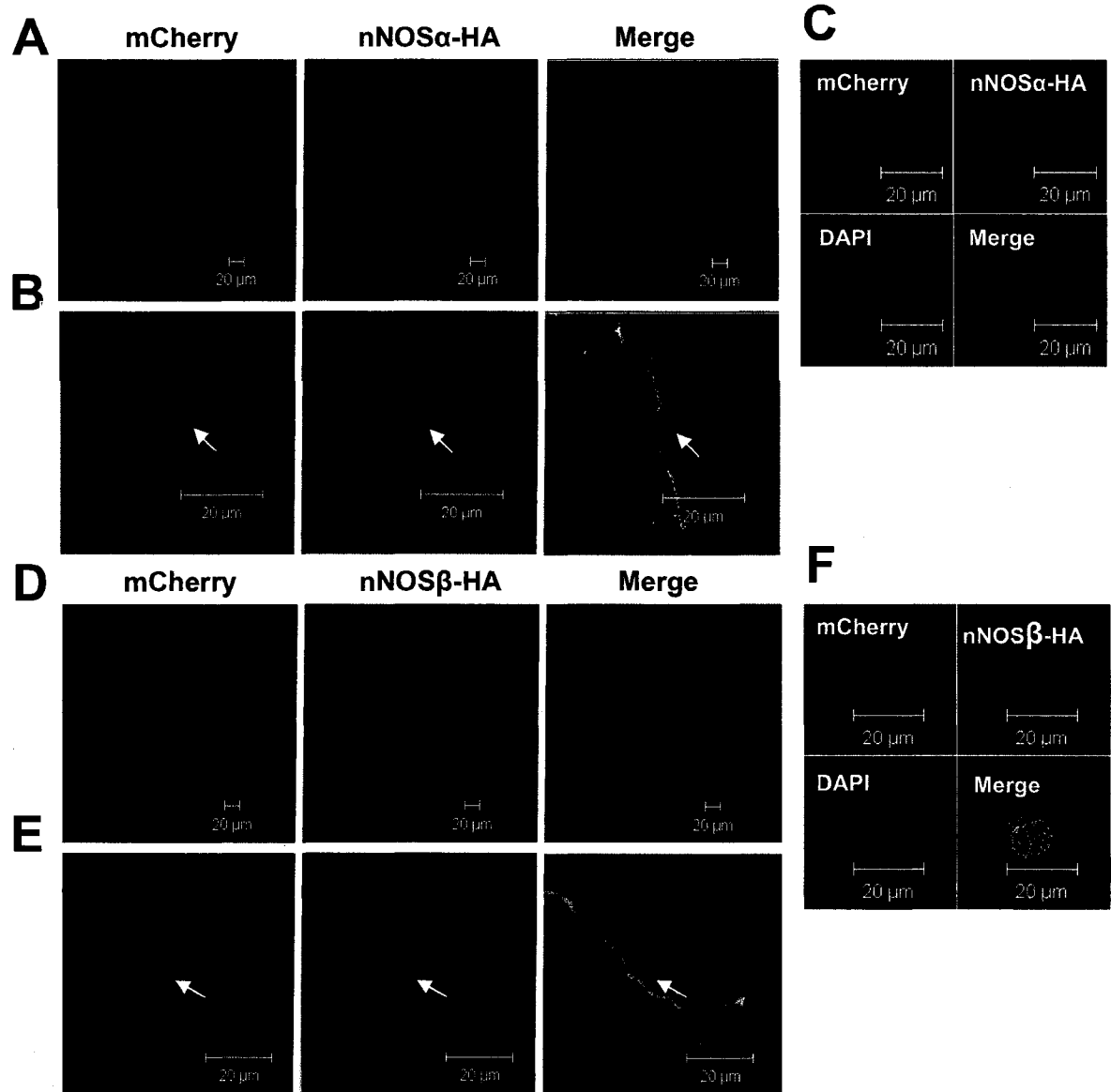


Figure 8. Distribution of nNOS α -HA and nNOS β -HA chimeras in primary cortical neurons. To corroborate the distribution of nNOS-EGFP chimaeras using another tag, neurons grown for 13 DIV were transfected with either nNOS-HA chimera plus mCherry. nNOS-HA chimaeras were distributed similarly to nNOS-EGFP chimaeras. nNOS α -HA is distributed in the cell soma (**A**) and neuritic compartments (**B**) including spines (arrows). nNOS α -HA signal is also detectable in the nuclear compartment (**C**). nNOS β -HA is distributed in the cell soma (**D**), neurites (**E**) spines (arrows) and nucleus (**F**). C and F represent single confocal slices.

3.2.2.3. Localization of nNOS to the nuclear compartment

Occasionally, 14 DIV primary cortical cells processed for immunofluorescence against nNOS showed extensive nNOS nuclear accumulation accompanied by complete loss of nNOS signal in the cytoplasm (Figure 9B). The conditions under which this accumulation occurred or the phenotype of the cells involved were not determined. This type of nuclear localization was also seen occasionally in HEK293 cells transfected with nNOS α -EGFP (Figure 9A) and primary cortical neurons transfected with nNOS β -EGFP (Figure 9C), which demonstrates that both nNOS α and nNOS β can be trafficked to the nuclear compartment. In addition, photobleaching of half of the nuclear compartment of HEK293 cells expressing nNOS α -EGFP rapidly decreased nNOS α -EGFP signal in the entire nuclear compartment confirming that a pool of nNOS was indeed confined to this compartment and that the majority of nNOS within the nucleus was freely mobile (Figure 9A).

3.3. nNOS trafficking in primary cortical cultures

To investigate the mechanism of nNOS trafficking in neurons, nNOS α -EGFP or EGFP were transfected into 13 DIV primary cortical neurons. Twenty four hours post-transfection, cells were transferred to a live-cell chamber for confocal imaging. A Z-stack of the selected neuron was taken and one of its dendrites was bleached in an area of 20 X 20 μM^2 (Figure 10). nNOS-EGFP fluorescence recovery after bleaching was very rapid with a complete recovery after 260 seconds post-bleaching (Figure 10 and 11A). This recovery was similar to EGFP alone (Figure 11A).

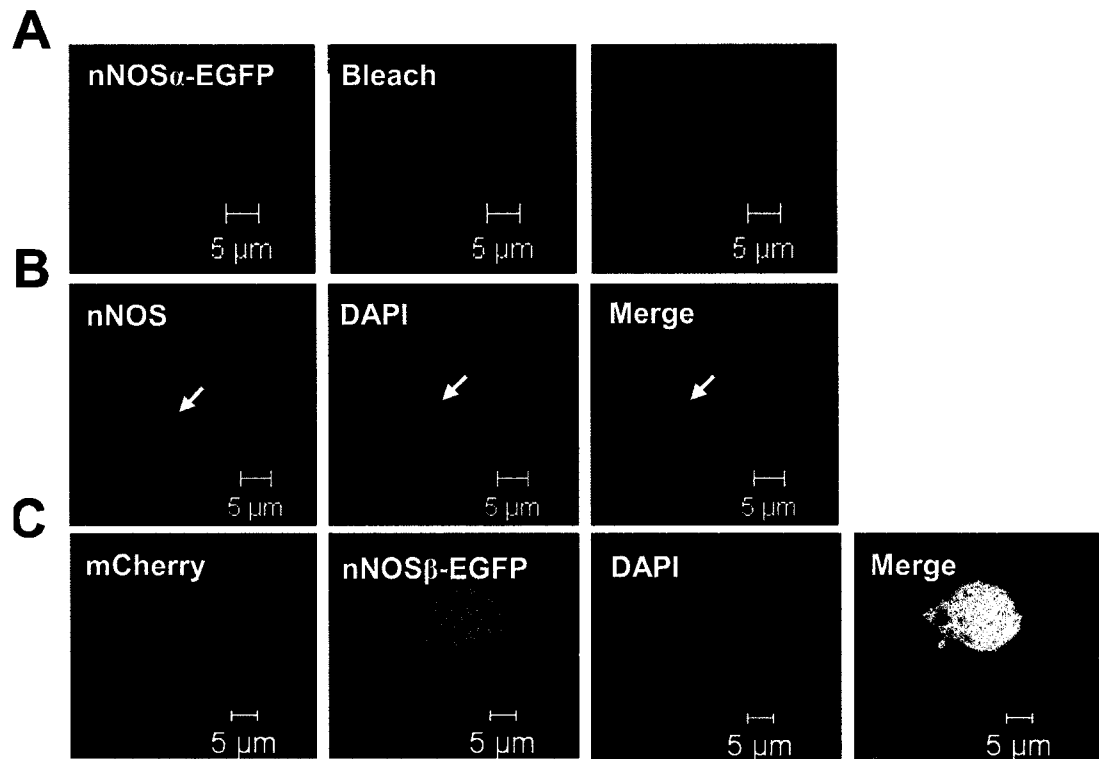


Figure 9. Nuclear localization of nNOS. **A)** HEK293 cells were transfected with nNOS α -EGFP. After 24 hours cells were fixed and transferred to a live-cell chamber for confocal imaging. Approximately half of the nuclear compartment was photobleached (red square) and an image was obtained 10 sec after bleaching. Note the selective nuclear bleaching indicating that nNOS is confined to the nuclear compartment. **B)** Primary cortical neurons were fixed at 14 DIV and processed for immunofluorescence against nNOS. Accumulation of nNOS was seen in the nuclei of some cells (arrows). **C)** Primary cortical neurons were transfected with nNOS β -EGFP and mCherry at 13 DIV. Twenty four hours post transfection, cells were fixed and imaged. nNOS β -EGFP signal was detected within a 3 μ m confocal slice through the middle of the neuronal nucleus. The characteristic mCherry nuclear localization is also evident.

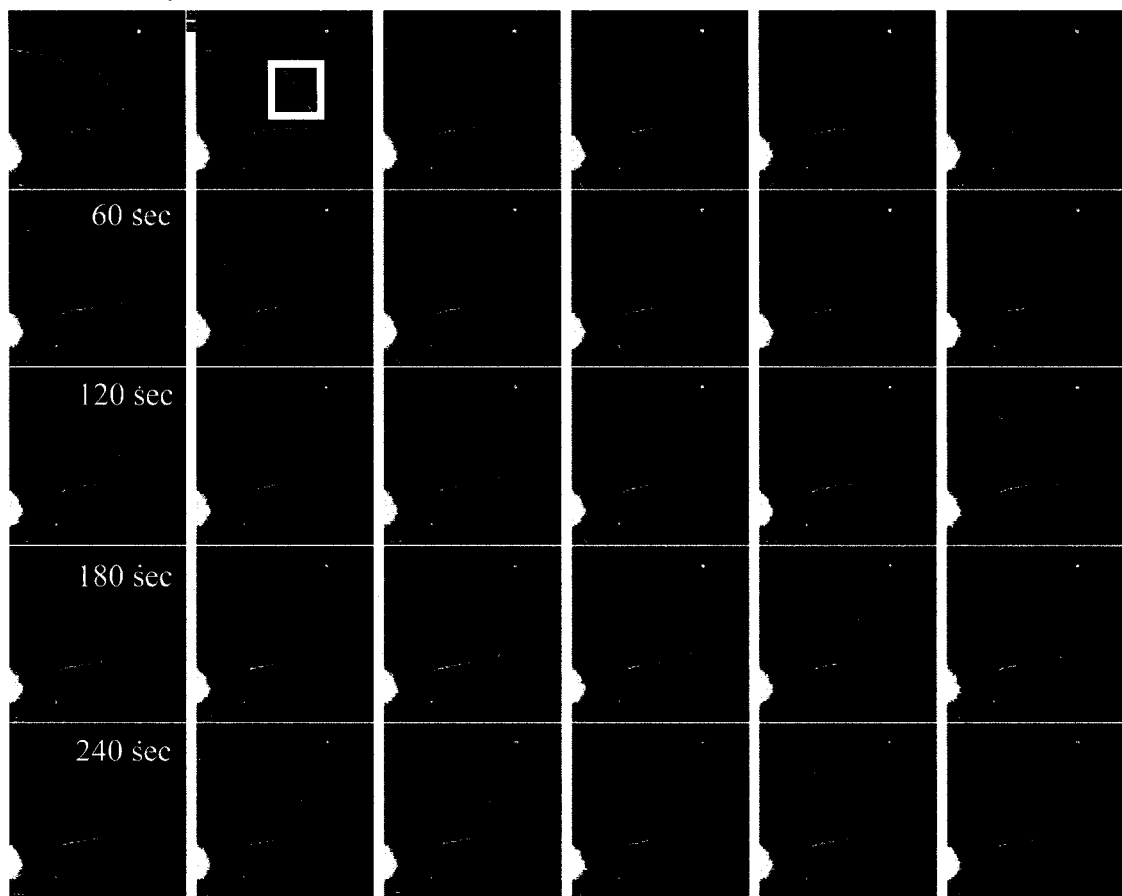
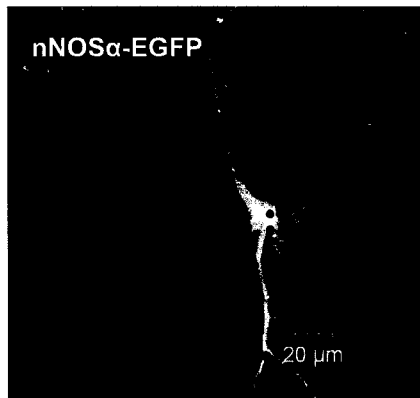


Figure 10. Fluorescence recovery after photobleaching (FRAP) of nNOS α -EGFP in primary cortical neurons. In order to study nNOS trafficking in neurons, primary cortical cultures at 13 DIV were transfected with nNOS α -EGFP. After 24 hours, cultures were transferred to a chamber for live-cell microscopy. A region of the neuronal dendrite was scanned with the 2X zoom-up function (red square) and an area of 20 X 20 μM^2 was bleached (yellow square). A time series at 10 second intervals was taken over 290 sec. Fluorescence recovery for nNOS α -EGFP occurred very quickly, within the 290 sec of imaging.

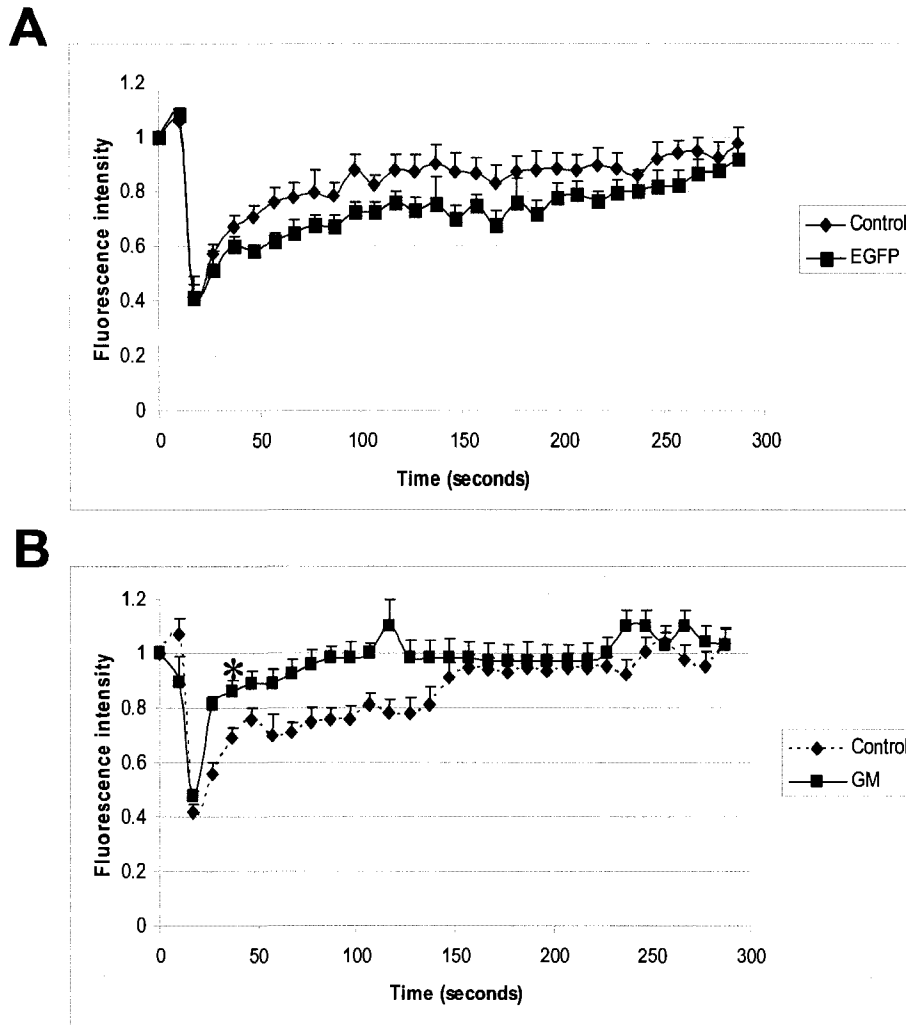


Figure 11. Effect of HSP90 on nNOS α -EGFP trafficking in primary cortical neurons. nNOS α -EGFP or EGFP were transfected into 13 DIV primary cortical neurons. The FRAP experiment was carried out as described in Figure 10. Statistical testing was performed comparing the fluorescence only at 40 sec (half of the recovery) and at 290 sec (final recovery) using normalized data. **A)** Plots of nNOS α -EGFP and EGFP fluorescence recovery vs. time are presented and show that both proteins have similar mobilities at 40 sec and 290 sec; **B)** To study the effect of HSP90 on nNOS trafficking, cultures were treated with the HSP90 inhibitor, geldanamycin, or vehicle for 3 hours before photobleaching. A plot of nNOS α -EGFP fluorescence recovery vs. time is presented. Geldanamycin causes nNOS α -EGFP to recover faster compared to the control at 40 sec. *, $p \leq 0.05$. Bars represent the standard error. $n = 6$.

3.3.1. Effects of HSP90 on nNOS trafficking

In order to study the effect of HSP90 on nNOS α -EGFP mobility, an HSP90 inhibitor, the antibiotic geldanamycin, or vehicle was added for 3 hours to primary cortical cultures transfected with nNOS α -EGFP. The mobility of nNOS α -EGFP after treatment was more rapid than that of the control (Figure 11B). After 40 seconds of imaging, nNOS α -EGFP signal recovered ~80% of the pre-bleached intensity while the control recovered only ~30% (Figure 11B).

3.3.2. Effects of estrogen on nNOS trafficking

To better understand the role of estrogen on nNOS mobility in neurons, different concentrations of 17- β -estradiol (E2) or vehicle were added for 10 minutes to primary cortical cultures transfected with nNOS α -EGFP. Doses of 500 nM and 1000 nM of E2 significantly decreased nNOS mobility while 5 nM did not have an effect (Figure 12A). In addition, after 290 seconds of imaging, nNOS α -EGFP signal did not reach full recovery when cells were treated with 500 nM and 1000 nM E2 for 10 minutes (Figure 12A). To study the duration of action of E2 effect, cultures were treated with E2 (1000 nM) for 1 or 2 hours before the photobleaching experiments. This treatment did not significantly affect nNOS α -EGFP mobility at 40 sec and 390 sec (Figure 12B).

3.4. nNOS localization to aggregates

3.4.1. Characterization of nNOS aggregates

Primary cortical cultures grown for 8 or 14 days were fixed and processed for immunofluorescence against endogenous nNOS. Some immunopositive cells

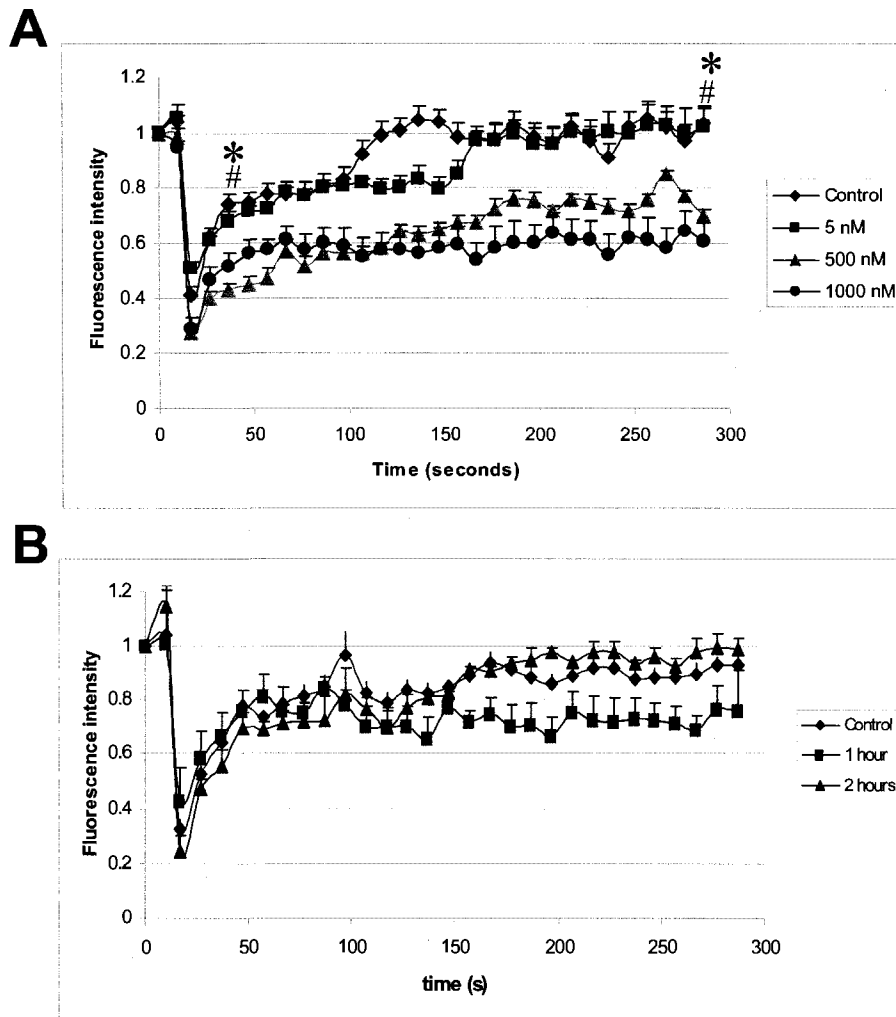


Figure 12. Effect of estrogen on nNOS α -EGFP trafficking in primary cortical neurons. nNOS α -EGFP or EGFP were transfected into 13 DIV primary cortical neurons. The FRAP experiment was carried on as described in Figure 10. Statistical testing was performed comparing the fluorescence only at 40 sec (half of the recovery) and at 290 sec (final recovery) using normalized data. **A)** Cultures were treated with 5 nM, 500 nM or 1000 nM of estrogen (E2) for 10 minutes. A plot of nNOS α -EGFP fluorescence recovery vs. time is presented. Treatment with 500 nM and 1000 nM of E2 significantly decreases nNOS recovery when compared to control; the control treatment was significantly different from 1000 μ M (*) and 500 μ M (#) estrogen treatments at both, 40 and 290 seconds. *,#, $p \leq 0.05$. **B)** To understand the duration of action of estrogen effect, cultures were treated with E2 (1000 nM) for 1 or 2 hours. Estrogen did not affect nNOS mobility after 1 or 2 hours of treatment when compared to control. Bars represent the standard error. $n = 6$

presented clear nNOS aggregations that were mostly rounded and varied in size and number from cell to cell. An example of neurons presenting aggregations is shown in Figure 13A. To evaluate the formation of these aggregations over time, nNOS distribution in neurons at 6, 10 and 14 DIV was evaluated. Results show that nNOS aggregations were not present in 6 DIV cells but present in 10 and 14 DIV cells (Figure 13B). In addition, I observed that the number of cells presenting nNOS aggregates increased with time in culture (Figure 13B).

3.4.1.1. Correlation between nNOS aggregates and aggresomes

To investigate whether nNOS accumulations are aggresomes, 14 DIV primary cortical cultures were fixed and processed for immunofluorescence against different proteins that have been previously shown to be accumulated in aggresomes such as HSP90, intermediate filaments and ubiquitin (Johnston et al., 1998). Results show that neither HSP90 (Figure 14A and 14B) nor neurofilament-M (Figure 14E and 14F) aggregate in neurons containing nNOS aggregations. I also observed that ubiquitin was aggregated in puncta in cells containing nNOS aggregates. Some of these puncta colocalized with nNOS aggregations (Figure 14C and 14D).

3.4.2. nNOS aggregations and neuronal survival

To study whether neurons containing nNOS aggregates show signs of degeneration, primary cortical cultures were processed for immunofluorescence for activated cleaved caspase-3, MAP-2, or the Golgi marker p115. Neurons containing nNOS aggregates were not reactive for activated Caspase-3 (Figure 15A) and displayed strong staining for MAP-2 in soma and dendrites (Figure 15B). In addition, MAP-2 signal was not detected in the regions where nNOS accumulated

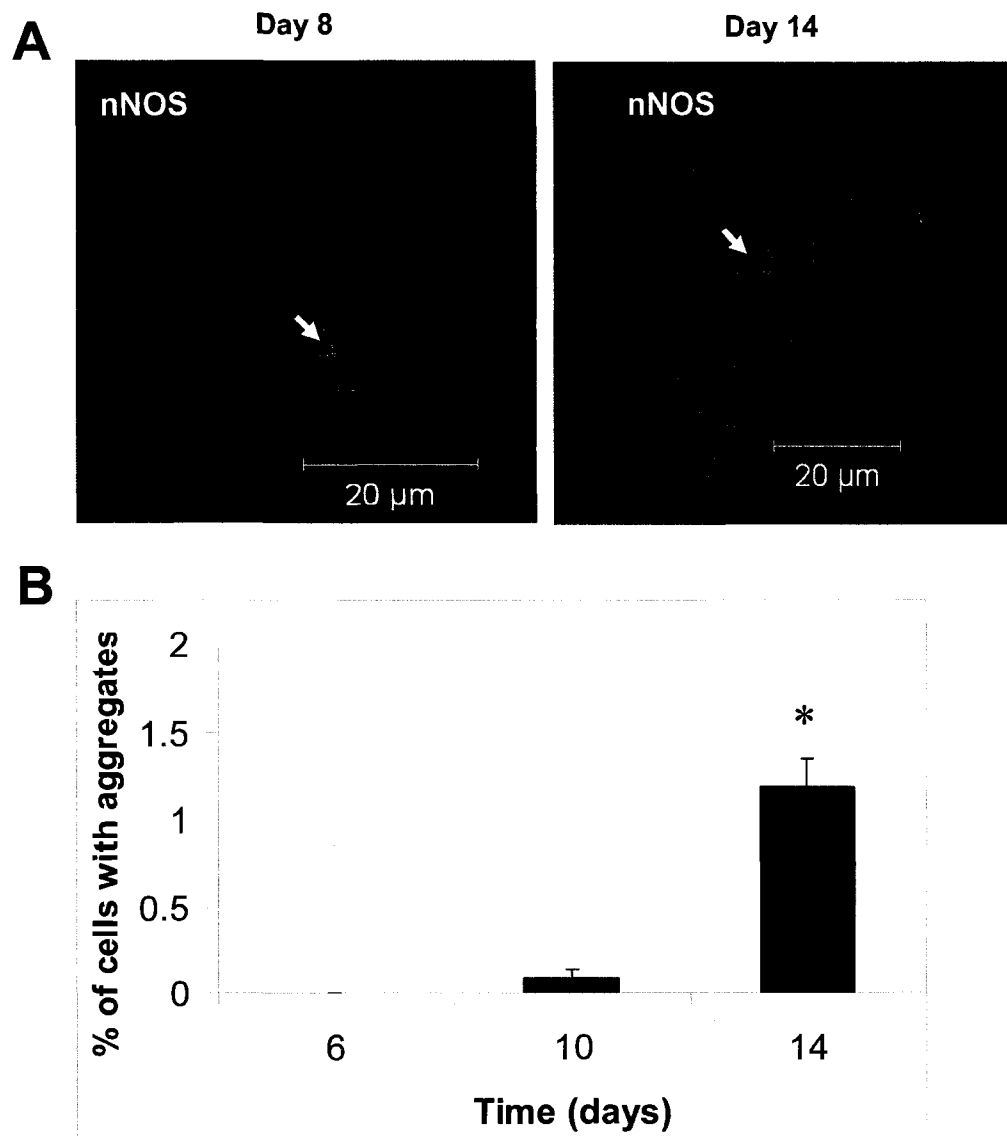


Figure 13. Endogenous nNOS aggregates in primary cortical cultures. A) Neurons grown for 8 or 14 DIV were processed by indirect immunofluorescence using anti-nNOS antibody. Arrows indicate nNOS cytoplasmic aggregations. **B)** Histogram depicting percentage of neurons containing nNOS aggregations relative to the total number of cells. The number of neurons containing nNOS aggregates increases with time in culture. Each repetition was carried out using a different culture. $n = 4$; The number of cells with aggregates is significantly larger at 14 DIV compared to 10 DIV *, $p < 0.05$.

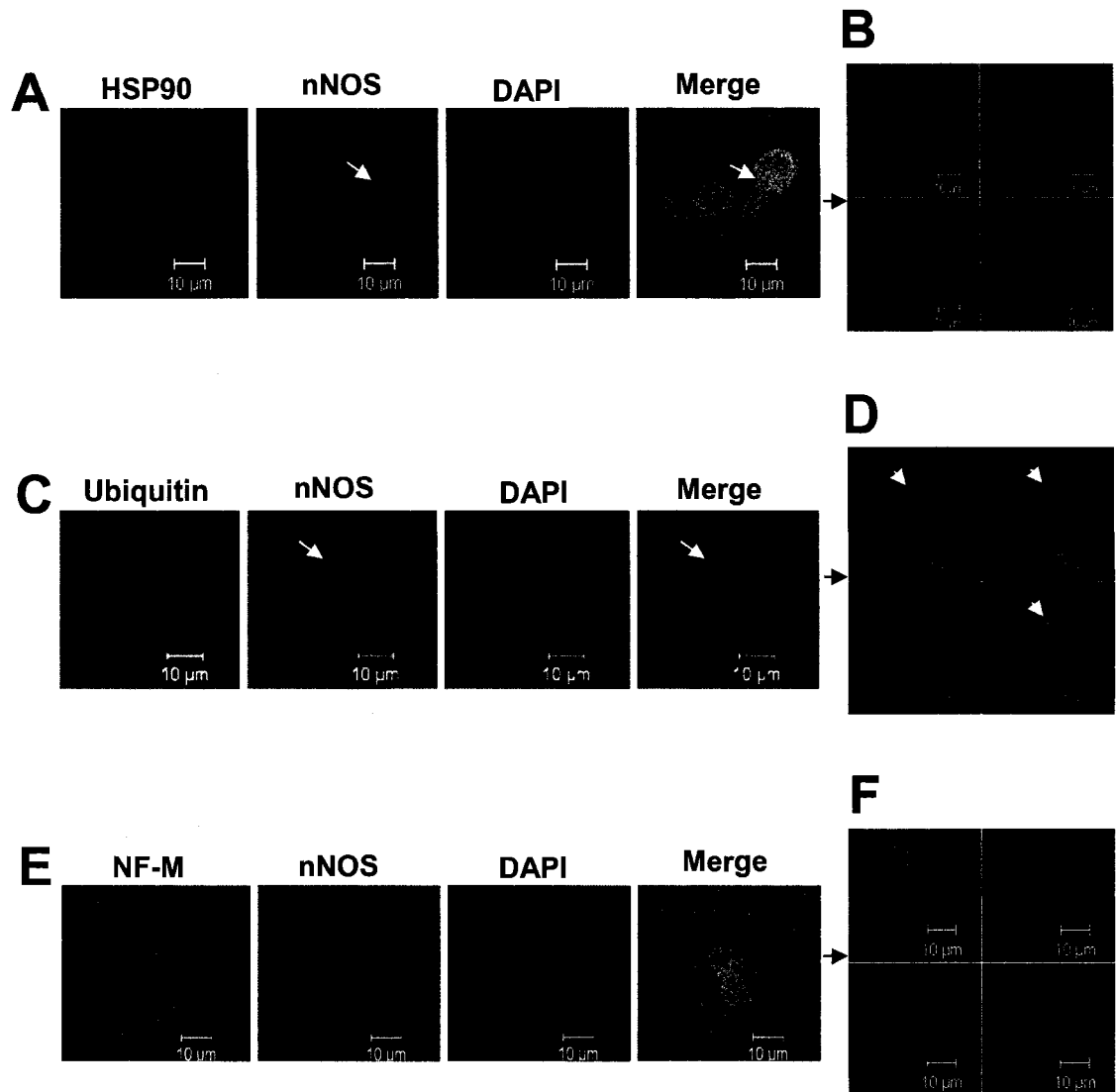


Figure 14. Characterization of nNOS aggregates. To determine whether nNOS aggregates have characteristics of aggresome formations, neurons grown for 14 DIV were processed for immunofluorescence against the aggresome markers, HSP90, ubiquitin or neurofilament-M. Arrows indicate nNOS aggregates. **A)** HSP90 is not aggregated in nNOS aggregates (arrows); **C)** Ubiquitin is aggregated in neurons containing nNOS aggregates; **E)** Neurofilament-M is not aggregated in nNOS aggregates. **B, D** and **F** are confocal images from **A, C** and **F** respectively. In **D**, arrow heads show aggregations of co-localized ubiquitin and nNOS.

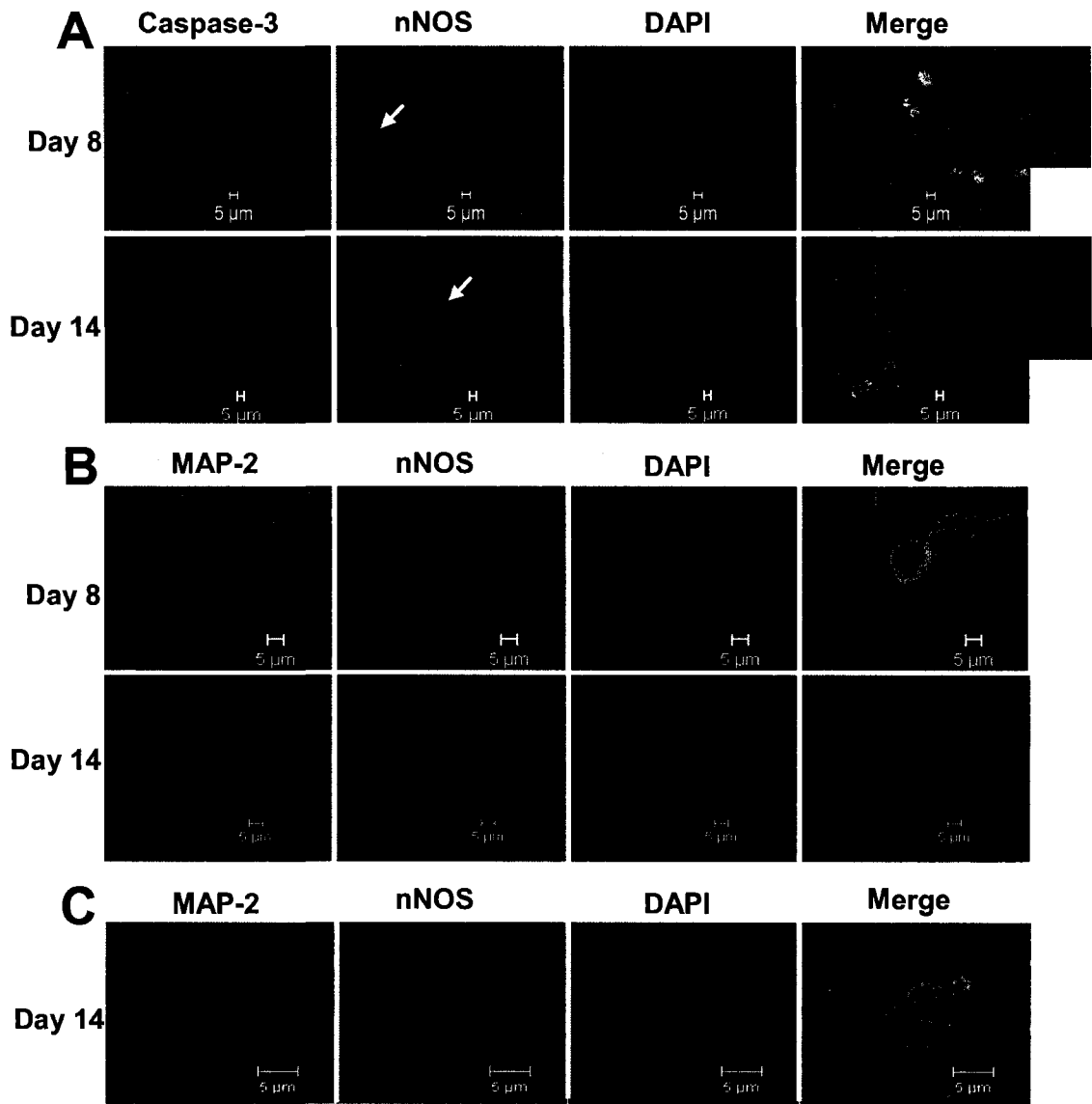


Figure 15. Survival of neurons containing nNOS aggregates. To determine whether neurons containing nNOS aggregates are degenerating, young (8 DIV) and mature (14 DIV) neurons were co-labeled with antibodies against nNOS and activated caspase-3 or microtubule associated protein 2 (MAP-2). **A)** Activated caspase-3 is not detected in young or mature cells presenting nNOS aggregates. Arrows indicate nNOS aggregates. A higher magnification of the neurons containing aggregates (orange square) is presented. **B)** MAP-2 is detected in the cytoplasm and dendrites of young and mature neurons containing aggregates. **C)** A 3 μ m slice of the neuron in B shows nNOS aggregations devoid of MAP-2.

(Figure 15C). The Golgi apparatus was not fragmented in 8 DIV neurons and was found close to nNOS aggregates (Figure 16A). In 14 DIV cells, the Golgi was fragmented in some cells containing nNOS aggregations (Figure 16B). Nevertheless, other nNOS immunoreactive 14 DIV cells that lacked nNOS aggregations also showed Golgi fragmentation suggesting that this fragmentation is independent of nNOS aggresome formation (Figure 16C).

3.4.3. Correlation between nNOS aggregates and nNOS localization to neuronal compartments

Primary cortical neurons grown for 14 DIV were fixed and processed for immunofluorescence against nNOS and MAP-2. The distribution of nNOS was punctate throughout the cytoplasm in neurons lacking nNOS aggregates (Figure 17A). In some neurons containing nNOS aggregates, the distribution of nNOS was restricted to nNOS aggregations and no longer present in neurites and soma (Figure 17B).

3.4.4. α -synuclein and nNOS aggregations

α -synuclein can form aggresome-like inclusions in cortical neurons (Olanow et al., 2004). To establish whether α -synuclein was also trafficked to somal aggregations, I performed immunostaining against α -synuclein and nNOS in 14 DIV primary cortical neurons. Results show that α -synuclein was not found in the same aggregations that contained nNOS (Figure 18A and 18B).

3.4.5. HSP90 effects on nNOS aggregation

To study the effects of HSP90 on nNOS trafficking to aggregates, nNOS α -EGFP, nNOS β -EGFP or EGFP were transfected into primary neuronal cultures.

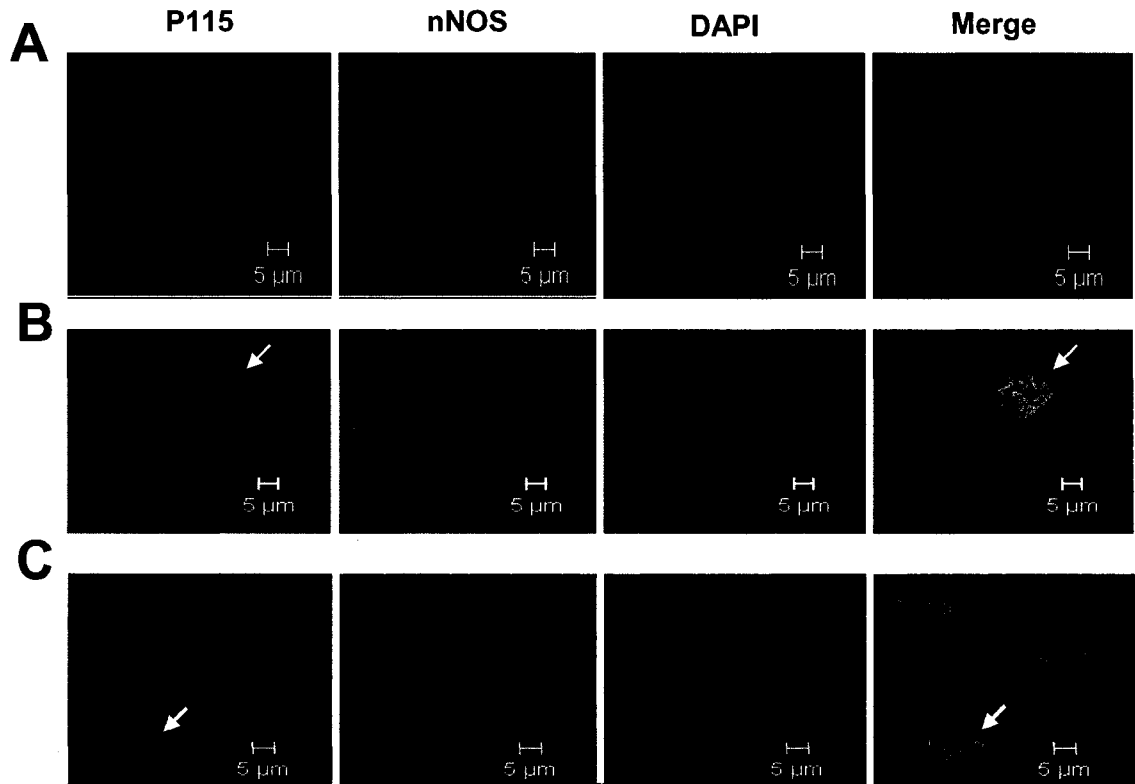


Figure 16. Golgi apparatus and nNOS aggregations. To determine whether neurons containing nNOS aggregates are undergoing a degenerative process, young (8 DIV) and mature (14 DIV) neurons were co-labeled with antibodies against nNOS and the Golgi marker p115. **A)** Golgi show no fragmentation in young neurons containing nNOS aggregates; **B)** Golgi is fragmented (arrow) in mature neurons containing nNOS aggregates; **C)** Golgi can be fragmented (arrow) in mature neurons that lack nNOS aggregates

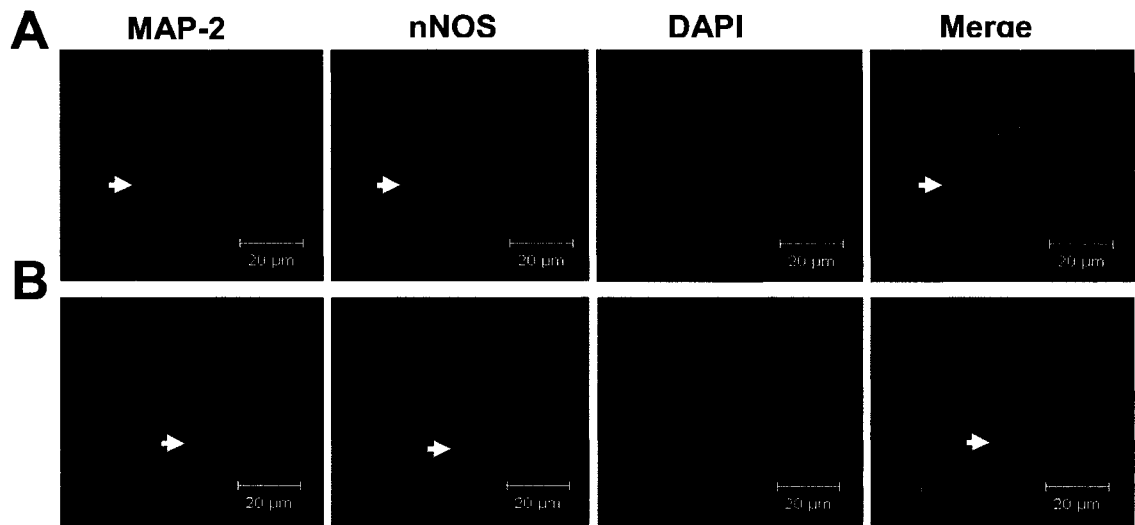


Figure 17. Correlation between nNOS aggregates and nNOS localization to neuronal compartments. To determine the distribution of nNOS in neurons with and without nNOS aggregates, mature (14 DIV) neurons were co-labeled with antibodies against nNOS and MAP-2. **A)** nNOS is distributed throughout the neuronal cytoplasm in neurons lacking nNOS aggregates. Arrows show nNOS signal in neurites. **B)** nNOS distribution is limited to the aggregates. Arrows show absence of nNOS signal in neurites.

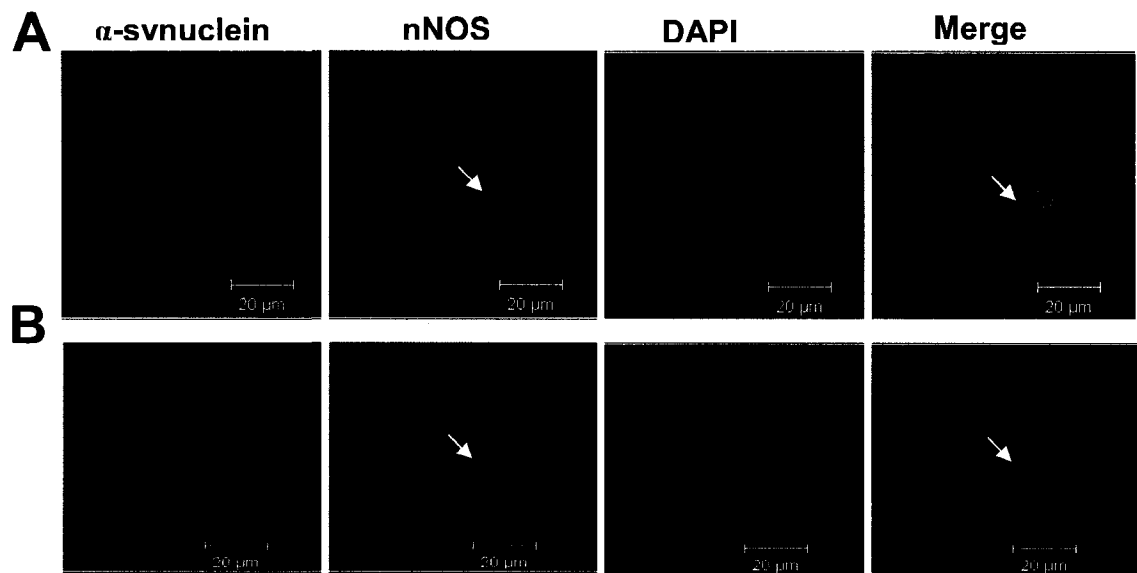


Figure 18. Specificity of nNOS aggregations. To establish if α -synuclein is trafficked to somal aggregates, mature (14 DIV) neurons were co-labeled with antibodies against nNOS and α -synuclein. **A)** Alpha-synuclein is not present in the same aggregates as nNOS. Arrows indicate nNOS aggregates. **B)** Confocal slice through neuronal soma of the neuron depicted in A. Arrows indicate nNOS aggregates.

Twenty four hours after transfection, cultures were treated for 6 hours with the HSP90 inhibitor, geldanamycin. Results show that nNOS α -EGFP and nNOS β -EGFP but not EGFP aggregated in neurons (Figure 19A). When the same experiment was performed in HEK293 cells, both splice variant chimeras formed clear perinuclear inclusions whereas EGFP did not aggregate (Figure 19B).

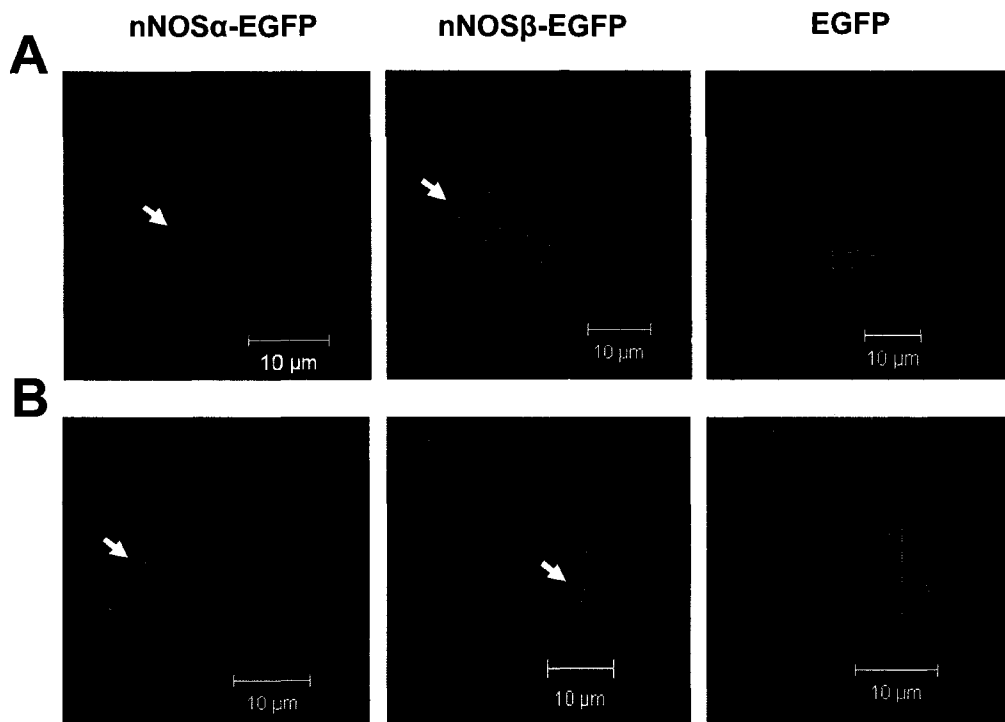


Figure 19. HSP90 inhibition induces nNOS aggregation. To study the effect of HSP90 on the formation of nNOS aggregates, cells were treated with an HSP90 inhibitor, geldanamycin. **A)** Primary cortical neurons were grown for 13 DIV and transfected with nNOS α -EGFP, nNOS β -EGFP or EGFP. Twenty four hours after transfection, neurons were treated with geldanamycin for 6 hours. Geldanamycin induced aggregation of both nNOS chimaeras in the neuronal cell bodies (arrows) but had no effect on EGFP; **B)** HEK293 cells were transfected and treated as in A. Geldanamycin induced formation of one nNOS perinuclear aggregation in each cell (arrows). EGFP distribution remained unchanged.

CHAPTER 4

DISCUSSION

4.1. Overview

Nitric oxide (NO) is a highly reactive gas required for a multitude of physiological processes (Oess et al., 2006). Three temporally and spatially regulated nitric oxide synthases mediate its production (Alderton et al., 2001). Neuronal nitric oxide synthase (nNOS) is present in the brain and is involved in the production of NO in neurons (Eliasson et al., 1997). In these cells, NO is involved in synaptic plasticity and neurotransmitter release (Prast et al., 1998; Sergeeva O et al., 2007). NO is also important for the regulation of neuronal survival. While NO can be neuroprotective (Guix et al., 2005) its over-production leads to cell death (Pacher et al., 2007).

To regulate the production of such a reactive gas, neurons modulate nNOS activation in different ways including phosphorylation (Adak et al., 2001; Song et al., 2007), degradation (Hajimohammadreza et al., 1997; Averna et al., 2007) and sub-cellular localization (Brenman et al., 1996; Jaffrey et al., 2002). In neurons, nNOS sub-cellular localization depends on its interaction with different proteins, such as the post-synaptic scaffold protein, PSD95, that tethers nNOS to the synaptic membrane (Brenman et al., 1996). The specific cellular signaling that mediates nNOS interactions and trafficking to different cellular compartments is poorly understood.

Here, I showed that nNOS α and nNOS β splice variants are present in the same sub-cellular compartments in primary cortical neurons. In addition, I demonstrated that nNOS α trafficking is regulated by the hormone estrogen and the chaperone HSP90. I also showed that nNOS α and nNOS β aggregate in perinuclear and/or somal regions of the cell. In the following section, I will discuss nNOS α trafficking and

address the sub-cellular localization of nNOS α and nNOS β , putting emphasis on their localization to aggregates.

4.2. Subcellular localization and trafficking of nNOS

4.2.1. Sub-cellular localization of neuronal nitric oxide synthase alpha (nNOS α)

Even though nNOS α is the most abundant and studied nNOS splice variant in the brain, its regulation and sub-cellular localization in neurons are still not completely understood. Here, I showed that endogenous nNOS is present in the soma, neurites and nuclei of young and mature primary cortical neurons. To support these findings, I also showed that constructed nNOS α chimeras were distributed in the same neuronal compartments. The over-expressed nNOS α chimeras followed a diffuse pattern as opposed to the punctuate pattern of endogenous nNOS. This difference in pattern may suggest that nNOS α lacks an intrinsic signal to be preferentially trafficked to specific organelles and/or that nNOS α chimeras are in excess relative to their endogenous protein partners.

The localization of nNOS α to the neuronal cytoplasm has been previously reported (Batista et al., 2001). Nevertheless, the localization of nNOS to the nuclear compartment has just been mentioned in cultured astrocytes and neutrophils with no distinction of the specific splice variant implicated (Yuan et al., 2004; Saini et al., 2006). In this study, I showed that, while a small pool of endogenous nNOS is present in the neuronal nucleus, in some cells nNOS is found only in this compartment and is

not present in the cytoplasm. In agreement with this result, I also showed that nNOS α -GFP was accumulated in the nucleus of some HEK293 cells.

Trafficking of nNOS α to the nuclear compartment could represent another mechanism of nNOS regulation and/or a mechanism by which nNOS regulates expression of nuclear proteins. nNOS trafficking to the nucleus could be useful to decrease NO production by sequestering nNOS away from calcium sources. This sequestering could become significant under stressful conditions such as oxidative stress, when NO can easily react with free radicals to form peroxynitrite and other harmful reactive species (Malinski et al., 2007). In addition, the function of nNOS in the nucleus could be to regulate nuclear protein localization. Interestingly, nNOS regulates the transcriptional co-repressor, CtBP, changing its localization from the nuclear to the cytosolic compartment (Riefler et al., 2001). Furthermore, nNOS could contribute to the production of NO in the nucleus to affect the function of nuclear proteins. This idea is supported by the fact that different transcription factors are regulated by the NO-mediated post-transcriptional modification, S-nitrosylation (De la Torre et al., 1998; Zhuravliova et al., 2007).

In summary, in accordance with previous results in the literature, I show that the nNOS α splice variant is present in the neuronal cytoplasm. I also report that nNOS α can be found in the nuclear compartment. The trafficking of nNOS α to this compartment may represent a new mechanism of enzyme regulation or function that has not been previously described.

4.2.2. Trafficking of neuronal nitric oxide synthase alpha (nNOS α)

The cellular cytoskeleton is designed to provide rapid trafficking of proteins over long distances where diffusion is not an option (Pfister et al., 1999). Because neurons have long dendrites and axons many proteins employ the cytoskeleton to reach their final destination (Guzik et al., 2004). Since nNOS is present in the axonal and dendritic compartments and has been shown to localize to actin and microtubules (Loesch et al., 1994), it is possible that its trafficking is also mediated by the neuronal cytoskeleton. To begin understanding the trafficking of nNOS α in neurons, I studied the mobility of nNOS α -EGFP in primary cortical neuronal cultures and its regulation by the chaperone HSP90 and the hormone estrogen.

EGFP is a small fluorescent protein that diffuses freely in the intracellular environment without using the cytoskeleton (Swaminathan et al., 1997). Here I show that nNOS α -EGFP movement in primary cortical neurons was very rapid and comparable to EGFP alone. Interestingly, proteosomes, which are large protein complexes, diffuse freely and comparably to the small GFP in HEK293 cells (Reits et al., 1997). Therefore, it is not surprising that a large protein like nNOS α -EGFP diffuses in a similar fashion as a smaller protein like EGFP. Similarities between nNOS and EGFP mobilities suggest that nNOS trafficking is mediated by simple diffusion as well. In support of this idea, the NOS isoform, eNOS, which shares 50% structural similarity with nNOS, diffuses freely in the cytosol of endothelial cells when it is not post-transcriptionally modified by palmitoyl groups that target it to the plasma membrane (Sowa et al., 1999).

HSP90 is a non-conventional chaperone that binds to nNOS (Bender et al., 1999) and affects the trafficking of different proteins such as Rab GTPases and the glucocorticoid receptor (Galigniana et al., 2004; Chen et al., 2006). In this study, inhibition of HSP90 increased nNOS mobility suggesting that HSP90 binding to nNOS may modulate the enzyme trafficking and interaction with other proteins. Since HSP90 facilitates nNOS maturation and stabilization (Osawa et al., 2003), I raise the possibility that HSP90 regulates nNOS trafficking by stabilizing the nNOS enzyme and facilitating its interaction with other proteins.

nNOS activity is regulated by the steroid hormone, estrogen (Alexaki et al., 2004). In this study, estrogen was shown to significantly delay nNOS mobility in primary cortical neurons. One potential explanation for this effect is that estrogen treatment increases nNOS protein-protein interactions, which, in turn, affect nNOS mobility. In agreement with this idea, estrogen was reported to influence nNOS association with PSD95 in rat brains (d'Anglemont de Tassigny et al., 2007). Effects of estrogen on nNOS mobility occurred within 10 minutes and did not last more than one hour. This rapid effect suggests that estrogen did not act through the classical genomic pathway in which estrogen receptors are translocated to the nuclear compartment to initiate gene transcription (Marino et al., 2006).

In summary, I show that nNOS α diffuses very rapidly in neurons and that this diffusion may be regulated by the chaperone, HSP90, and the hormone, estrogen. These findings provide new insights on the possible mechanisms by which nNOS is regulated in neurons.

4.2.3. Sub-cellular localization of neuronal nitric oxide synthase beta (nNOS β)

The nNOS β splice variant is present in discrete areas of the brain and only in neurons that contain the nNOS α variant (Eliasson et al., 1997). Because a specific antibody for nNOS β is lacking, no previous studies have been done on its distribution in neurons at the immunocytochemical level.

My data show that the distribution of nNOS β chimeras is very similar to that of the nNOS α variant. nNOS β diffuses throughout the neuronal cytoplasm including the neurites and nucleus. As I proposed for nNOS α , nNOS β may lack an intrinsic signal for preferential trafficking to specific organelles and its over-expression may saturate its binding partners. Here I showed that, while a small pool of nNOS β -EGFP is present in the neuronal nucleus, in some cells nNOS β -EGFP is present in this compartment to a similar extent to that of the cytoplasm. This localization of nNOS β -EGFP is interesting since it indicates that nNOS β may have a variety of functions in the cell such as the regulation of nuclear proteins as I previously hypothesized for nNOS α variant.

Because nNOS lacks a classical nuclear localization signal (NLS), the nuclear localization of nNOS α and nNOS β might be mediated by an unconventional NLS yet to be found or by another protein that binds to nNOS. Nuclear transport of proteins that lack an NLS has been shown for proteins such as the Id family of helix-loop-helix (HLH) transcriptional regulators (Deed et al., 1996). nNOS nuclear localization might not depend on the nNOS PDZ domain since the nNOS β variant lacks this domain (Brenman et al., 1996).

In summary, I show that nNOS β localization in the neuron is similar to that of nNOS α . Over-expressed nNOS β was not specifically targeted to any neuronal compartment, which suggests that nNOS β localization may also depend on protein-protein interactions for its trafficking to specific regions of the neuron under certain physiological circumstances. These interactions cannot be mediated by the PDZ domain, which mediates most of the known protein interactions found for nNOS α . Interestingly, nNOS β is also found in the nucleus, which opens a new perspective on the role of this splice variant in the brain.

4.2.4. Interactions of neuronal nitric oxide synthase alpha (nNOS α) and beta (nNOS β) with PSD95

Postsynaptic density protein 95 (PSD95) is a scaffold protein with multiple protein-protein interaction domains that organizes receptors and signal transduction molecules at the synapse (Dosemeci et al., 2007). PSD95 accumulates in distinct synaptic foci (puncta) when it is over-expressed in mature neurons (Gerrow et al., 2006).

Interestingly, nNOS α -HA and nNOS β -HA displayed a punctate pattern when they were co-expressed with PSD95 in primary cortical neurons. nNOS α -HA colocalized with PSD95 puncta suggesting that the two proteins interact. This is not unexpected since nNOS α interaction with PSD95 is well established (Brenman et al., 1996).

Surprisingly, nNOS β -HA was also colocalized with PSD95 in puncta. This colocalization was unforeseen as nNOS β lacks the PDZ domain which is known to mediate the nNOS α -PSD95 interaction. This co-localization also raises the possibility

that nNOS β binds PSD95 through another protein. In this case, a very attractive hypothesis is that nNOS β and nNOS α form a heterodimer. Dimer formation is indispensable for nNOS activity (Panda et al., 2003) and it has been shown that nNOS α is capable of inter-isoformal dimerization with iNOS when overexpressed in COS-7 cells (Watanabe et al., 1998). In further support of this idea, it was demonstrated that, unlike eNOS and iNOS, the N-terminal leader sequences lacking in nNOS β are not required to form a nNOS dimer (Panda et al., 2003). Furthermore, nNOS homodimer formation was disrupted by chimeras made only of mutant heme and reductase domains (Phung et al., 1999). I raise the possibility that heterodimerization may be a way by which splice variants are regulated. This heterodimerization may affect nNOS protein-protein interactions and the overall trafficking and activity of the enzyme.

In summary, in this study I show that nNOS α co-localizes with the important scaffold protein, PSD95. nNOS binding to PSD95 has been reported by others (Brenman et al., 1996). In addition, I report the unexpected finding that nNOS β also co-localizes with this scaffold protein. This finding is important because it suggests that nNOS β also participates in the synapse, adding more complexity to the functions of nNOS in regulating synaptic strength.

4.3. nNOS is trafficked to aggregates in primary cortical neurons

4.3.1. nNOS aggregations are aggresome-like structures

In this study, nNOS was seen aggregated in perinuclear and/or somal inclusions that were found near the Golgi apparatus in primary cortical neurons. The

numbers of cells containing nNOS aggregations were higher in mature neurons in comparison to young neurons suggesting that these aggregations are related to neuronal maturation or a consequence of expected stress related to longer culture times (King et al., 2006). Nevertheless, as I will explain below, I did not detect signs of degeneration in neurons bearing nNOS aggregates.

Interestingly, in some neurons containing nNOS aggregations, nNOS was not present throughout the soma and neurites suggesting that nNOS aggregations may deplete nNOS from the sub-cellular regions where it is normally found, and thus decrease NO production.

Aggresomes are a cellular response to misfolded or aggregated proteins (Johnston et al., 1998). Their formation involves trafficking of aggregated proteins along microtubules to perinuclear sites, reorganization of intermediate filaments, and recruitment of components of the proteasome machinery such as ubiquitin and heat shock proteins (Johnston et al., 1998). In this study, neurons containing nNOS aggregates also contained aggregated ubiquitin which indicate that nNOS aggregates could be aggresomes. However, neither HSP90 nor neurofilament-M were aggregated with nNOS. Interestingly, HSP90 is not always present in aggresomes (Kovacs et al., 2006), so other studies focusing on the presence of other chaperones are necessary to further characterize nNOS aggregations.

In summary, the perinuclear localization and ubiquitin distribution support the idea that nNOS aggregates are aggresome inclusions, whereas HSP90 and neurofilament distribution exclude them from this category. Therefore, I will refer to these inclusions as aggresome-like.

4.3.2. Neurons containing nNOS aggregations may not be degenerating

In this study, neurons containing nNOS aggregates did not show signs of activation of caspase-3, abnormal MAP-2 staining, or specific Golgi fragmentation. Because caspase-3 is a pro-apoptotic protein, I conclude that neurons containing nNOS aggregates are not undergoing caspase-dependent cell death. In addition, since MAP-2 is very sensitive to proteolysis and its staining is lost or its distribution is modified after neuronal exposure to different cellular stressors (Miñana et al., 1998; Pirondi et al., 2005), I conclude that a major degenerative process is likely not occurring in neurons presenting aggregates. Finally, Golgi fragmentation, which has been proposed to be involved in non-apoptotic neurodegenerative processes (Gonatas et al., 2006), is not specifically occurring in cells containing nNOS aggregations, suggesting again that cell death is not occurring in these neurons.

In support of these conclusions, α -synuclein, a protein that form aggresome-like inclusions (called Lewi bodies) in cortical neurons of Parkinson's disease patients (Olanow et al., 2004), did not form similar inclusions as those seen for nNOS in primary cortical neurons. Over-expressed α -synuclein, on the other hand, has been shown to aggregate in primary neurons (McLean et al., 2001).

Taken together, these results suggest that nNOS aggregations are not the consequence of cell death mechanisms occurring in the neurons but rather a nNOS-specific phenomenon.

4.3.3. Mechanism of formation of aggresome-like inclusions

HSP90 is a known unconventional chaperone that controls NO production by regulating nNOS activity (Song et al., 2001) and degradation (Osawa et al., 2003). In

this study HSP90 inhibition induced the formation of nNOS α -EGFP and nNOS β -EGFP aggregates in primary cortical neurons and HEK293 cells. Interestingly, inhibition of HSP90 in nNOS-transfected HEK293 cells has been previously shown to decrease the amount of nNOS protein in the soluble fraction and greatly increase it in the insoluble fraction (Peng et al., 2004). nNOS presence in the insoluble fraction may be due to its trafficking to detergent-insoluble aggresomes (García-Mata et al., 1999). Therefore, this work follows that of others who have demonstrated that HSP90 is a strong regulator of nNOS stability.

Here, I show that, after treatment with the HSP90 inhibitor geldanamycin, nNOS α -EGFP and nNOS β -EGFP form one typical perinuclear aggresome in each HEK293 cell, and numerous somal aggregates in neurons. This difference in aggregate number suggests that the mechanisms of protein aggregation in neurons may differ from those present in other cells. In support of this idea, it has been shown that in the presence of proteasome inhibitors, overexpressed α -synuclein forms a perinuclear aggregate in COS cells (Tanaka et al., 2004) but small aggregates distributed in the cytoplasm in primary neurons (McLean et al., 2001).

The physiological signaling that can trigger nNOS aggregation is likely very complex. Based on previous studies and the results of the present study, I propose that the monomeric form of nNOS is preferentially trafficked to the perinuclear or somal inclusions seen in this work. I base this hypothesis on my results regarding the effect of HSP90 inhibition on the induction of nNOS aggregates, and on previous reports which show that HSP90 has a role in nNOS stabilization regulating the nNOS dimer

formation through the facilitation of heme insertion in the nNOS monomer (Billecke et al., 2004).

In addition, I propose that the ubiquitylation of the nNOS monomer may be involved in nNOS aggregation. I base this hypothesis on the fact that HSP90 inhibition was shown to induce ubiquitylation of the nNOS monomer, which induces nNOS degradation by the proteasome complex (Bender et al., 2000), and on my results regarding the presence of ubiquitin aggregations in cells containing nNOS aggregates.

Since ubiquitylation is a label for nNOS degradation by the proteasome (Bender et al., 2000), it is possible that nNOS aggregates are a consequence of excess ubiquitylated nNOS that was not degraded by the proteasome. Interestingly, ubiquitylation is not just a marker for degradation as monoubiquitylation has also been found to regulate protein trafficking (Hicke et al., 1999). Therefore, it is an attractive possibility that nNOS ubiquitylation can specifically mediate nNOS trafficking to aggregates.

The monomeric form of nNOS was induced here artificially by the HSP90 inhibitor geldanamycin. nNOS monomerization can also occur in response to nNOS inhibition (Noguchi et al., 2000). In addition, nNOS monomerization can occur physiologically in response to different stimuli including heme availability (Albakri et al., 1996), tetrahydrobiopterin depletion (Reif et al., 1999), dimerization inhibition (McMillan et al., 2000), S-nitrosylation (Ravi et al., 2004), and PIN binding (Fan et al., 1998). In addition, HSP90 can also be inhibited physiologically by S-nitrosylation (Martínez-Ruiz et al., 2005). Therefore, nNOS may autoregulate itself by mediating

HSP90 inhibition, and it is likely that nNOS degradation and aggregation are similarly regulated.

The mechanism by which nNOS is trafficked to these somal aggregations may depend on dynein and microtubules as both have been shown to be important for aggresome formation (Johnston et al., 2002). Interestingly, the nNOS interactor PIN, which inhibits nNOS activity, is a dynein light chain (Liang et al., 1999), so it is an attractive possibility that it could mediate nNOS movement to perinuclear inclusions.

In summary, I show here that inhibition of HSP90 induces the formation of nNOS aggregates. HSP90 has been shown to be important for the stabilization of the nNOS dimer (Billecke et al., 2002). Therefore, I hypothesize that nNOS monomerization is involved in nNOS trafficking to aggregates (Figure 20). In this case, a hypothesis for this phenomenon is that the trafficking of nNOS monomers to aggregates may prevent dimer reconstitution and subsequent NO production. This idea is supported by the fact that nNOS monomer can easily reconstitute the dimer. For example, nNOS expressed in heme depleted insect cells is activated from the non-functional monomer to the dimer upon addition of exogenous heme to the culture medium (Billecke et al., 2004).

4.3.4. Implications of nNOS aggregations

Importantly, eNOS and iNOS isoforms, which share 50% homology with nNOS, have been reported to be trafficked to somal aggregations (Jiang et al., 2003; Kolodziejaska et al., 2005). iNOS formed aggresomes after its expression was induced

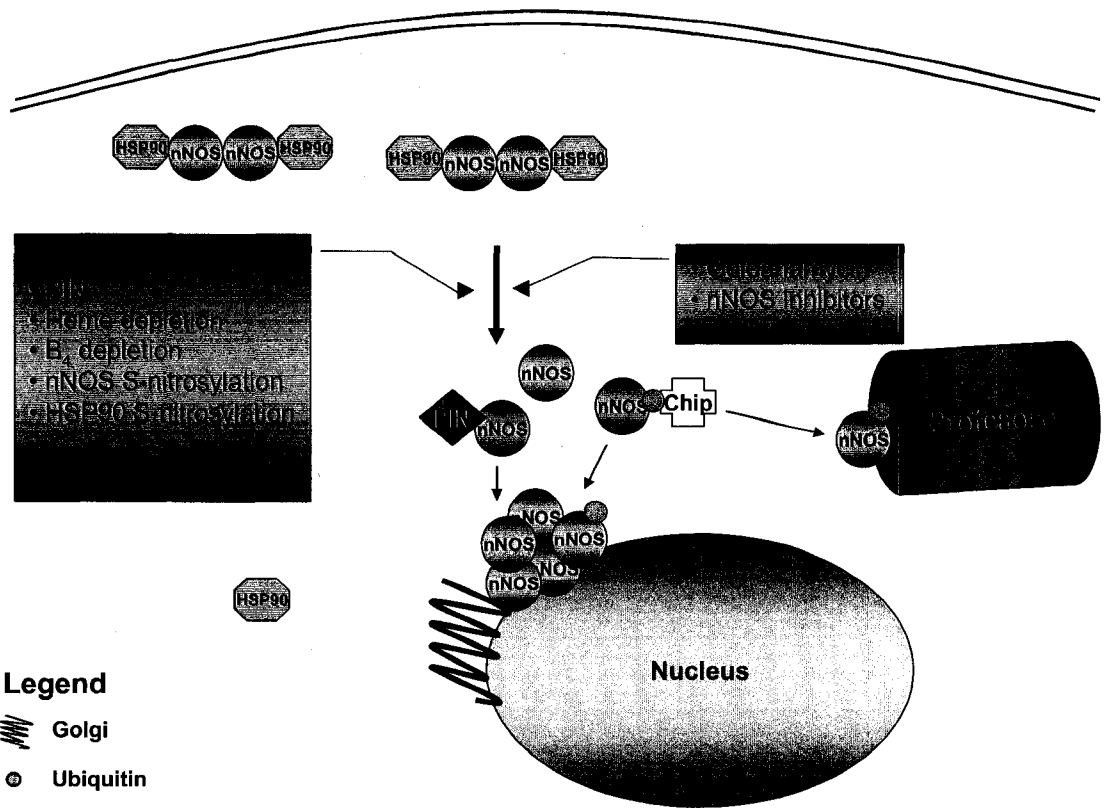


Figure 20. nNOS monomerization induces aggregation. The active nNOS dimer can undergo monomerization under different physiological conditions or artificial conditions as with the HSP90 inhibitor geldanamycin or nNOS inhibitors. nNOS monomers can bind the ubiquitin ligase CHIP which may ubiquitylate them. Ubiquitylation targets nNOS to the proteasome-complex or to perinuclear aggresomes. In addition, the dynein light chain, PIN, may mediate trafficking of the monomers to the perinuclear aggregates.

with various cytokines in different cell lines. In addition, overexpressed iNOS-EGFP in HEK293 cells formed aggresomes after cells were treated with the HSP90 inhibitor geldanamycin. These iNOS aggregations may constitute a form of enzyme regulation called “physiological aggresome” by the authors of the study (Kolodziejaska et al., 2005). iNOS does not need calcium for its activation and this mechanism of regulation may represent a rapid way of preventing NO production when iNOS is expressed in the cell (Kolodziejaska et al., 2005). Nevertheless, iNOS was also found in complexes with HSP90 (Antonova et al., 2007) and inhibition of HSP90 decreased NO production and toxicity in macrophages (Yoshida et al., 2003). Therefore, HSP90 may also be involved in iNOS stabilization and it is possible that the iNOS aggresome shown by Kolodziejaska in 2005 after geldanamycin treatment was directly related to iNOS protein instability.

Similarly, eNOS was shown to be trafficked to insoluble inclusions when the C-terminus of Hsp70 interacting protein (CHIP) was overexpressed in endothelial cells (Jiang et al., 2003). The authors concluded that eNOS trafficking to an inactive detergent-insoluble pool prevents normal trafficking of eNOS to different sub-cellular compartments.

In the present study, I report for the first time the localization of an endogenous protein to intracellular aggresome-like inclusions in primary neuronal cultures. I conclude that nNOS, as its counterparts, eNOS and iNOS, can be regulated by aggregation. However, I do not rule out the possibility that the presence of nNOS aggregates could have repercussions on the neuronal survival as has been proposed for protein aggregations in general (Ross et al., 2005). Interestingly, nNOS has been

reported to be present in neurofilament accumulations during amyotrophic lateral sclerosis (Chou et al., 1996). It is also noteworthy that a clear idea of the circumstances in which protein aggregates are toxic or protective in neurons is lacking. An example of a non-toxic aggregation in neurons is the transient localization of the glutamate receptor subunit 1 (GluR1) to aggresome-like structures in the gray matter of normal developing rat spinal cord (Serrando et al., 2002).

Since protein aggregation can be detrimental or beneficial for neurons, it is premature to speculate about the overall cellular effects of nNOS aggregations. Nevertheless, based on my results regarding the absence of signs of neuronal degeneration in nNOS aggregate-bearing cells, and on others' findings regarding iNOS and eNOS regulation by aggregation, I raise the possibility that nitric oxide synthases share a common aggregation-prone characteristic that may contribute to a rapid mechanism for NO downregulation. This mechanism could have important consequences in neurons as nNOS is involved in different neuronal functions (Prast et al., 1998; Sergeeva et al., 2007) and is a key player in neuronal survival (Guix et al., 2005; Pacher et al., 2007).

4.4. Concluding remarks

Overall, my results demonstrate new mechanisms by which nNOS may be regulated. Here, I show that the nNOS β splice variant may have a more widespread function than previously thought since it can localize to neuronal synaptic sites through PSD95 and to different neuronal compartments including the nucleus. I also show that both nNOS α and nNOS β are regulated by HSP90 and localize to somal

aggregations. Nevertheless, more studies are required to understand the mechanisms and physiological importance of these findings.

Interestingly, the use of HSP90 inhibitors has been proposed for the treatment of neurodegenerative diseases such as polyQ-mediated motor neuron degeneration, (Waza et al., 2006) and multiple sclerosis (Dello Russo et al., 2006). In addition, HSP90 inhibitors have been proposed to be used to inhibit c-Jun N-terminal kinases (JNK) signaling involved in diseases such as Parkinson and Alzheimer disease (Gallo et al., 2006). Furthermore, aggregation of α -synuclein, which is involved in Parkinson's disease (Olanow et al., 2004), is prevented by HSP90 inhibition (McLean et al., 2004). Therefore, it would be important to further study the effects of HSP90 inhibition on other HSP90 client proteins such as nNOS that play a key role in neuronal survival.

The aggregation of nNOS in neurons is a very important finding because it may represent another level of nNOS regulation. A better understanding of nNOS mechanisms of action and regulation will contribute to the design of strategies to manipulate its activity during disease.

4.5. Future directions

Several different directions are worth pursuing based on the findings presented in this thesis. I propose future experiments to be focused on answering the following questions: 1) What is the physiological significance of nNOS trafficking to the nuclear compartment? 2) How is nNOS β trafficked to PSD95 puncta? and 3) What are the characteristics of nNOS α and nNOS β aggregates in neurons?

4.5.1. What is the physiological significance of nNOS trafficking to the nuclear compartment?

nNOS trafficking to the nuclear compartment has not been studied before. Nevertheless, there are a few reports mentioning this trafficking in astrocytes and neutrophils (Yuan et al., 2004; Saini et al., 2006). To start assessing the relevance or mechanism of this trafficking, nNOS protein chimeras with a nuclear localization signal can be designed and transfected into a cell line. After crosslinking treatments, pull down experiments can be performed to recover the proteins that are bound to nNOS in the nuclear compartment. Mass spectrometry analysis could reveal new interactors of nNOS in this compartment, thus helping to clarify the significance of nNOS in the nucleus.

4.5.2. How is nNOS β trafficked to PSD95 puncta?

My result regarding nNOS β interaction with PSD95 indicates that the participation of nNOS at the synapse may be more regulated than was thought before. To follow up on this result it would be important to first confirm that nNOS β is actually present in PSD95 clusters. To accomplish this, I would over-express nNOS β and PSD95 in primary neuronal cultures and lyse the cells to obtain the synaptic fraction (Yoshimura et al., 2004). I would perform a western blot with this fraction to determine if nNOS β is present in postsynaptic density clusters. In addition, it would be interesting to confirm the hypothesis that nNOS α and nNOS β heterodimerize. To test for NOS α and nNOS β heterodimerization, a cell line can be transfected with different combinations of nNOS α , nNOS β and PSD95 constructs. Pull-down assays can be performed to show whether nNOS β requires nNOS α to bind to PSD95.

4.5.3. What are the characteristics of nNOS α and nNOS β aggregates in neurons?

nNOS trafficking to aggregates may represent an alternate mechanism by which nNOS protein is regulated. To further elucidate the nature of nNOS aggregates, it is important to determine which characteristics of aggresomes are shared by nNOS aggregates. Because aggresomes are rich in heat shock proteins and localize to the centrosome (Johnston et al., 1998), it would be important to evaluate if γ -tubulin and heat shock protein 70 (HSP70) are also present in nNOS aggregates. In addition, since aggresomes depend on microtubules for their formation (Johnston et al., 2002), I would study whether nNOS aggregates also depend on microtubules for their trafficking by treating nNOS expressing cells with a microtubule disruption agent together with geldanamycin.

Experiments can also focus on identifying the events that trigger nNOS trafficking to those aggregations. It would be important to elucidate whether the monomeric form of nNOS is preferentially trafficked to aggregates, using other dimer destabilizing agents instead of geldanamycin, such as nNOS inhibitors like the irreversible inhibitor guanabenz (Noguchi et al., 2000) or PIN (Fan et al., 1998). Conversely, the artificial stabilization of the nNOS homodimer with compounds such as 7-nitroindazole (Noguchi et al., 2000) in conjunction with geldanamycin treatment would clearly establish if enzyme instability is important for nNOS formation of aggresome-like inclusions.

REFERENCES

Adak S, Santolini J, Tikunova S, Wang Q, Johnson JD, Stuehr DJ. Neuronal nitric-oxide synthase mutant (Ser-1412 --> Asp) demonstrates surprising connections between heme reduction, NO complex formation, and catalysis. *J Biol Chem*. 2001 Jan; 276(2):1244-52.

Afanas'ev IB. Signaling Functions of Free Radicals Superoxide & Nitric Oxide under Physiological & Pathological Conditions. *Mol Biotechnol*. 2007 Sep; 37(1):2-4.

Albakri QA, Stuehr DJ. Intracellular assembly of inducible NO synthase is limited by nitric oxide-mediated changes in heme insertion and availability. *J Biol Chem*. 1996 Mar; 271(10):5414-21.

Alderton WK, Cooper CE, Knowles RG. Nitric oxide synthases: structure, function and inhibition. *Biochem J*. 2001 Aug; 357(Pt 3):593-615. Review

Alexaki VI, Charalampopoulos I, Kampa M, Vassalou H, Theodoropoulos P, Stathopoulos EN, Hatzoglou A, Gravanis A, Castanas E. Estrogen exerts neuroprotective effects via membrane estrogen receptors and rapid Akt/NOS activation. *FASEB J*. 2004 Oct; 18(13):1594-6.

Antonova G, Lichtenbeld H, Xia T, Chatterjee A, Dimitropoulou C, Catravas JD. Functional significance of hsp90 complexes with NOS and sGC in endothelial cells. *Clin Hemorheol Microcirc*. 2007;37(1-2):19-35.

Audesirk T, Cabell L, Kern M, Audesirk G. Enhancement of dendritic branching in cultured hippocampal neurons by 17beta-estradiol is mediated by nitric oxide. *Int J Dev Neurosci*. 2003 Jun;21(4):225-33.

Averna M, Stifanese R, De Tullio R, Salamino F, Bertuccio M, Pontremoli S, Melloni E. Proteolytic degradation of nitric oxide synthase isoforms by calpain is modulated by the expression levels of HSP90. *FEBS J*. 2007 Dec;274(23):6116-27. Epub 2007 Oct 29.

Balligand JL, Cannon PJ. Nitric oxide synthases and cardiac muscle. Autocrine and paracrine influences. *Arterioscler Thromb Vasc Biol*. 1997 Oct;17(10):1846-58. Review

Barouch LA, Harrison RW, Skaf MW, Rosas GO, Cappola TP, Kobeissi ZA, Hobai IA, Lemmon CA, Burnett AL, O'Rourke B, Rodriguez ER, Huang PL, Lima JA, Berkowitz DE, Hare JM. Nitric oxide regulates the heart by spatial confinement of nitric oxide synthase isoforms. *Nature*. 2002 Mar 21;416(6878):337-9.

Batista CM, de Paula KC, Cavalcante LA, Mendez-Otero R. Subcellular localization of neuronal nitric oxide synthase in the superficial gray layer of the rat superior colliculus. *Neurosci Res*. 2001 Sep;41(1):67-70.

Bauser-Heaton HD, Bohlen HG. Cerebral microvascular dilation during hypotension and decreased oxygen tension: a role for nNOS. *Am J Physiol Heart Circ Physiol*. 2007 Oct;293(4):H2193-201.

Bender AT, Silverstein AM, Demady DR, Kanelakis KC, Noguchi S, Pratt WB, Osawa Y. Neuronal nitric-oxide synthase is regulated by the Hsp90-based chaperone system in vivo. *J Biol Chem*. 1999 Jan 15;274(3):1472-8.

Bender AT, Demady DR, Osawa Y. Ubiquitination of neuronal nitric-oxide synthase in vitro and in vivo. *J Biol Chem*. 2000 Jun 9;275(23):17407-11.

Billecke SS, Draganov DI, Morishima Y, Murphy PJ, Dunbar AY, Pratt WB, Osawa Y. The role of hsp90 in heme-dependent activation of apo-neuronal nitric-oxide synthase. *J Biol Chem*. 2004 Jul 16;279(29):30252-8.

Boullerne AI, Benjamins JA. Nitric oxide synthase expression and nitric oxide toxicity in oligodendrocytes. *Antioxid Redox Signal*. 2006 May-Jun;8(5-6):967-80. Review

Bredt DS, Snyder SH. Nitric oxide: a physiologic messenger molecule. *Annu Rev Biochem*. 1994;63:175-95. Review.

Brenman JE, Chao DS, Gee SH, McGee AW, Craven SE, Santillano DR, Wu Z, Huang F, Xia H, Peters MF, Froehner SC, Bredt DS. Interaction of nitric oxide synthase with the postsynaptic density protein PSD-95 and alpha1-syntrophin mediated by PDZ domains. *Cell*. 1996 Mar 8;84(5):757-67

Brenman JE, Xia H, Chao DS, Black SM, Bredt DS. Regulation of neuronal nitric oxide synthase through alternative transcripts. *Dev Neurosci*. 1997;19(3):224-31. Review.

Brewer GJ, Torricelli JR, Evege EK, Price PJ. Optimized survival of hippocampal neurons in B27-supplemented Neurobasal, a new serum-free medium combination. *J Neurosci Res*. 1993 Aug 1;35(5):567-76.

Browne, S. E. & Beal, M. F. Oxidative damage in Huntington's disease pathogenesis *Antioxid. Redox Signal*. 8, 2061–2073 (2006).

Calabrese V, Mancuso C, Calvani M, Rizzarelli E, Butterfield DA, Stella AM. Nitric oxide in the central nervous system: neuroprotection versus neurotoxicity. *Nat Rev Neurosci*. 2007 Oct;8(10):766-75. Review

Cantoni O, Palomba L, Persichini T, Mariotto S, Suzuki H, Colasanti M. Pivotal role of arachidonic acid in the regulation of neuronal nitric oxide synthase activity and inducible nitric oxide synthase expression in activated astrocytes. *Methods Enzymol*. 2008;440:243-52.

Catania MV, Aronica E, Yankaya B, Troost D. Increased expression of neuronal nitric oxide synthase spliced variants in reactive astrocytes of amyotrophic lateral sclerosis human spinal cord. *J Neurosci*. 2001 Jun 1;21(11):RC148

Chanrion B, Mannoury la Cour C, Bertaso F, Lerner-Natoli M, Freissmuth M, Millan MJ, Bockaert J, Marin P. Physical interaction between the serotonin transporter and neuronal nitric oxide synthase underlies reciprocal modulation of their activity. *Proc Natl Acad Sci U S A*. 2007 May 8;104(19):7739-40.

Cheah JH, Kim SF, Hester LD, Clancy KW, Patterson SE 3rd, Papadopoulos V, Snyder SH. NMDA receptor-nitric oxide transmission mediates neuronal iron homeostasis via the GTPase Dexas1. *Neuron*. 2006 Aug 17;51(4):431-40.

Chen CY, Balch WE. The Hsp90 chaperone complex regulates GDI-dependent Rab recycling. *Mol Biol Cell*. 2006 Aug;17(8):3494-507.

Cheng, A., Wang, S., Cai, J., Rao, M.S., Mattson, M.P. Nitric oxide acts in a positive feedback loop with BDNF to regulate neural progenitor cell proliferation. *Dev Biol*. 2003 Jun 15;258(2):319-33.

Cherney, A., H. Edgell, and T.L. Krukoff. NO mediates effects of estrogen on central regulation of blood pressure in restrained, ovariectomized rats. *Am J Physiol Regul Integr Comp Physiol*, 2003. 285(4):842-9.

Chou SM, Wang HS, Komai K. Colocalization of NOS and SOD1 in neurofilament accumulation within motor neurons of amyotrophic lateral sclerosis: an immunohistochemical study. *J Chem Neuroanat*. 1996 Jun;10(3-4):249-58.

Chung KK, Thomas B, Li X, Pletnikova O, Troncoso JC, Marsh L, Dawson VL, Dawson TM. S-nitrosylation of parkin regulates ubiquitination and compromises parkin's protective function. *Science*. 2004 May 28;304(5675):1328-31.

Contestabile A, Ciani E. Role of nitric oxide in the regulation of neuronal proliferation, survival and differentiation. *Neurochem Int*. 2004 Nov;45(6):903-14. Review

d'Anglemont de Tassigny X, Campagne C, Dehouck B, Leroy D, Holstein GR, Beauvillain JC, Buée-Scherrer V, Prevot V. Coupling of neuronal nitric oxide synthase to NMDA receptors via postsynaptic density-95 depends on estrogen and contributes to the central control of adult female reproduction. *J Neurosci*. 2007 Jun 6;27(23):6103-14.

De la Torre A, Schroeder RA, Bartlett ST, Kuo PC. Differential effects of nitric oxide-mediated S-nitrosylation on p50 and c-jun DNA binding. *Surgery*. 1998 Aug;124(2):137-41; discussion 141-2.

- Deed RW, Armitage S, Norton JD. Nuclear localization and regulation of Id protein through an E protein-mediated chaperone mechanism. *J Biol Chem.* 1996 Sep 27;271(39):23603-6.
- Degerman E, Belfrage P, Manganiello VC. Structure, localization, and regulation of cGMP-inhibited phosphodiesterase (PDE3). *J Biol Chem.* 1997 Mar 14;272(11):6823-6. Review
- Dello Russo C, Polak PE, Mercado PR, Spagnolo A, Sharp A, Murphy P, Kamal A, Burrows FJ, Fritz LC, Feinstein DL. The heat-shock protein 90 inhibitor 17-allylamino-17-demethoxygeldanamycin suppresses glial inflammatory responses and ameliorates experimental autoimmune encephalomyelitis. *J Neurochem.* 2006 Dec;99(5):1351-62.
- Denninger JW, Marletta MA. Guanylate cyclase and the .NO/cGMP signaling pathway. *Biochim Biophys Acta.* 1999 May 5;1411(2-3):334-50. Review
- Dinerman, J.L., Dawson, T.M., Schell, M.J., Snowman, A., Snyder, S.H. Endothelial nitric oxide synthase localized to hippocampal pyramidal cells: implications for synaptic plasticity. *Proc Natl Acad Sci U S A.* 1994 May 10;91(10):4214-8.
- Domek-Łopacińska K, Strosznajder JB. Cyclic GMP metabolism and its role in brain physiology. *J Physiol Pharmacol.* 2005 Mar;56 Suppl 2:15-34. Review
- Dosemeci A, Makusky AJ, Jankowska-Stephens E, Yang X, Slotta DJ, Markey SP. Composition of the synaptic PSD-95 complex. *Mol Cell Proteomics.* 2007 Oct;6(10):1749-60.
- Dreyer J, Schleicher M, Tappe A, Schilling K, Kuner T, Kusumawidijaja G, Müller-Esterl W, Oess S, Kuner R. Nitric oxide synthase (NOS)-interacting protein interacts with neuronal NOS and regulates its distribution and activity. *J Neurosci.* 2004 Nov 17;24(46):10454-65.
- Duan S., Chen C. S-nitrosylation/denitrosylation and apoptosis of immune cells. *Cell Mol Immunol.* 2007 Oct;4(5):353-8. Review
- Dunbar AY, Kamada Y, Jenkins GJ, Lowe ER, Billecke SS, Osawa Y. Ubiquitination and degradation of neuronal nitric-oxide synthase in vitro: dimer stabilization protects the enzyme from proteolysis. *Mol Pharmacol.* 2004 Oct;66(4):964-9.
- Eliasson MJ, Blackshaw S, Schell MJ, Snyder SH. Neuronal nitric oxide synthase alternatively spliced forms: prominent functional localizations in the brain. *Proc Natl Acad Sci U S A.* 1997 Apr 1;94(7):3396-401.

- Evergren E, Benfenati F, Shupliakov O. The synapsin cycle: a view from the synaptic endocytic zone. *J Neurosci Res.* 2007 Sep;85(12):2648-56. Review
- Fan JS, Zhang Q, Li M, Tochio H, Yamazaki T, Shimizu M, Zhang M. Protein inhibitor of neuronal nitric-oxide synthase, PIN, binds to a 17-amino acid residue fragment of the enzyme. *J Biol Chem.* 1998 Dec 11;273(50):33472-81
- Faraci FM. Protecting the brain with eNOS: run for your life. *Circ Res.* 2006 Nov 10;99(10):1029-30.
- Feron, O., Belhassen, L., Kobzik, L., Smith, T. W., Kelly, R. A. and Michel, T. Endothelial nitric oxide synthase targeting to caveolae. Specific interactions with caveolin isoforms in cardiac myocytes and endothelial cells. *J Biol Chem.* 1996 Sep 13;271(37):22810-4
- Firestein BL, Bredt DS. Interaction of neuronal nitric-oxide synthase and phosphofructokinase-M. *J. Biol Chem.* 1999 Apr 9;274(15):10545-50.
- Förstermann U, Münzel T. Endothelial nitric oxide synthase in vascular disease: from marvel to menace. *Circulation.* 2006 Apr 4;113(13):1708-14. Review.
- Galigniana MD, Harrell JM, Housley PR, Patterson C, Fisher SK, Pratt WB. Retrograde transport of the glucocorticoid receptor in neurites requires dynamic assembly of complexes with the protein chaperone hsp90 and is linked to the CHIP component of the machinery for proteasomal degradation. *Brain Res Mol Brain Res.* 2004 Apr 7;123(1-2):27-36
- Gallo KA. Targeting HSP90 to halt neurodegeneration. *Chem Biol.* 2006 Feb;13(2):115-6.
- García-Mata R, Bebök Z, Sorscher EJ, Sztul ES. Characterization and dynamics of aggresome formation by a cytosolic GFP-chimera. *J Cell Biol.* 1999 Sep 20;146(6):1239-54.
- Garthwaite J, Charles SL, Chess-Williams R. Endothelium-derived relaxing factor release on activation of NMDA receptors suggests role as intercellular messenger in the brain. *Nature.* 1988 Nov 24;336(6197):385-8.
- Gebicke-Haerter PJ. Microglia in neurodegeneration: molecular aspects. *Microsc Res Tech.* 2001 Jul 1;54(1):47-58. Review
- Gerrow K, Romorini S, Nabi SM, Colicos MA, Sala C, El-Husseini A. A preformed complex of postsynaptic proteins is involved in excitatory synapse development. *Neuron.* 2006 Feb 16;49(4):547-62.

Getting, S. J., Segieth, J., Ahmad, S., Biggs, C. S. & Whitton, P. S. Biphasic modulation of GABA release by nitric oxide in the hippocampus of freely moving rats in vivo. *Brain Res.* 1996 Apr 22;717(1-2):196-9.

Gonatas NK, Stieber A, Gonatas JO. Fragmentation of the Golgi apparatus in neurodegenerative diseases and cell death. *J Neurol Sci.* 2006 Jul 15;246(1-2):21-30. Review

Griffith TM, Edwards DH, Davies RL, Harrison TJ, Evans KT. EDRF coordinates the behaviour of vascular resistance vessels. *Nature.* 1987 Oct 1-7; 329(6138):442-5
Grozdanovic Z. NO message from muscle. *Microsc Res Tech.* 2001 Nov 1;55(3):148-53. Review

Grove JR, Price DJ, Banerjee P, Balasubramanyam A, Ahmad MF, Avruch J. Regulation of an epitope-tagged recombinant Rsk-1 S6 kinase by phorbol ester and erk/MAP kinase. *Biochemistry.* 1993 Aug 3;32(30):7727-38.

Gu, Z., Kaul, M., Yan, B., Kridel, S.J., Cui, J., Strongin, A., Smith, J.W., Liddington, R.C., Lipton, S.A., 2002. S-Nitrosylation of matrix metalloproteinases: signaling pathway to neuronal cell death. *Science* 297,1186–1190.

Guix FX, Uribealago I, Coma M, Muñoz FJ. The physiology and pathophysiology of nitric oxide in the brain. *Prog Neurobiol.* 2005 Jun;76(2):126-52. Review

Guzik BW, Goldstein LS. Microtubule-dependent transport in neurons: steps towards an understanding of regulation, function and dysfunction. *Curr Opin Cell Biol.* 2004 Aug;16(4):443-50. Review

Hajimohammadreza I, Raser KJ, Nath R, Nadimpalli R, Scott M, Wang KK. Neuronal nitric oxide synthase and calmodulin-dependent protein kinase IIalpha undergo neurotoxin-induced proteolysis. *J Neurochem.* 1997 Sep;69(3):1006-13.

Hess DT, Matsumoto A, Kim SO, Marshall HE, Stamler JS. Protein S-nitrosylation: purview and parameters. *Nat Rev Mol Cell Biol.* 2005 Feb;6(2):150-66. Review

Hicke L. Getting down with ubiquitin: turning off cell-surface receptors, transporters and channels. *Trends Cell Biol.* 1999 Mar;9(3):107-12. Review

Hirata Y, Hayakawa H, Suzuki Y, Suzuki E, Ikenouchi H, Kohmoto O, Kimura K, Kitamura K, Eto T, Kangawa K, et al. Mechanisms of adrenomedullin-induced vasodilation in the rat kidney. *Hypertension.* 1995 Apr;25(4 Pt 2):790-5.

Huang, P. L., Dawson, T. M., Bredt, D. S., Snyder, S. H. & Fishman, M. C. Targeted disruption of the neuronal nitric oxide synthase gene. *Cell.* 1993 Dec 31;75(7):1273-86.

Ignarro LJ, Buga GM, Wood KS, Byrns RE, Chaudhuri G. Endothelium-derived relaxing factor produced and released from artery and vein is nitric oxide. *Proc Natl Acad Sci U S A*. 1987 Dec;84(24):9265-9.

Ishikawa Y, Iida H, Ishida H. The muscarinic acetylcholine receptor-stimulated increase in aquaporin-5 levels in the apical plasma membrane in rat parotid acinar cells is coupled with activation of nitric oxide/cGMP signal transduction. *Mol Pharmacol*. 2002 Jun;61(6):1423-34.

Jaffrey SR, Snyder SH. PIN: an associated protein inhibitor of neuronal nitric oxide synthase. *Science*. 1996 Nov 1;274(5288):774-7.

Jaffrey SR, Snowman AM, Eliasson MJ, Cohen NA, Snyder SH. CAPON: a protein associated with neuronal nitric oxide synthase that regulates its interactions with PSD95. *Neuron*. 1998 Jan;20(1):115-24.

Jaffrey SR, Erdjument-Bromage H, Ferris CD, Tempst P, Snyder SH. Protein S-nitrosylation: a physiological signal for neuronal nitric oxide. *Nat Cell Biol*. 2001 Feb;3(2):193-7.

Jaffrey SR, Benfenati F, Snowman AM, Czernik AJ, Snyder SH. Neuronal nitric-oxide synthase localization mediated by a ternary complex with synapsin and CAPON. *Proc Natl Acad Sci U S A*. 2002 Mar 5;99(5):3199-204.

Jiang J, Cyr D, Babbitt RW, Sessa WC, Patterson C. Chaperone-dependent regulation of endothelial nitric-oxide synthase intracellular trafficking by the co-chaperone/ubiquitin ligase CHIP. *J Biol Chem*. 2003 Dec 5;278(49):49332-41. Epub 2003 Sep 24.

Johnston JA, Ward CL, Kopito RR. Aggresomes: a cellular response to misfolded proteins. *J Cell Biol*. 1998 Dec 28;143(7):1883-98.

Johnston JA, Illing ME, Kopito RR. Cytoplasmic dynein/dynactin mediates the assembly of aggresomes. *Cell Motil Cytoskeleton*. 2002 Sep;53(1):26-38.

Kahlos K, Zhang J, Block ER, Patel JM. Thioredoxin restores nitric oxide-induced inhibition of protein kinase C activity in lung endothelial cells. *Mol Cell Biochem*. 2003 Dec;254(1-2):47-54.

Kim E, Sheng M. PDZ domain proteins of synapses. *Nat Rev Neurosci*. 2004 Oct;5(10):771-81. Review

Kim WK, Choi YB, Rayudu PV, Das P, Asaad W, Arnette DR, Stamler JS, Lipton SA. Attenuation of NMDA receptor activity and neurotoxicity by nitroxyl anion, NO⁻. *Neuron*. 1999 Oct;24(2):461-9.

King AE, Chung RS, Vickers JC, Dickson TC. Localization of glutamate receptors in developing cortical neurons in culture and relationship to susceptibility to excitotoxicity. *J Comp Neurol*. 2006 Sep 10;498(2):277-94.

Kitamura Y, Furukawa M, Matsuoka Y, Tooyama I, Kimura H, Nomura Y, Taniguchi T. In vitro and in vivo induction of heme oxygenase-1 in rat glial cells: possible involvement of nitric oxide production from inducible nitric oxide synthase. *Glia*. 1998 Feb;22(2):138-48.

Knowles RG, Moncada S. Nitric oxide synthases in mammals. *Biochem J*. 1994 Mar 1;298 (Pt 2):249-58. Review

Kolesnikov YA, Pan YX, Babey AM, Jain S, Wilson R, Pasternak GW. Functionally differentiating two neuronal nitric oxide synthase isoforms through antisense mapping: evidence for opposing NO actions on morphine analgesia and tolerance. *Proc Natl Acad Sci U S A*. 1997 Jul 22;94(15):8220-5.

Kolodziejaska KE, Burns AR, Moore RH, Stenoien DL, Eissa NT. Regulation of inducible nitric oxide synthase by aggresome formation. *Proc Natl Acad Sci U S A*. 2005 Mar 29;102(13):4854-9.

Komeima K, Hayashi Y, Naito Y, Watanabe Y. Inhibition of neuronal nitric-oxide synthase by calcium/ calmodulin-dependent protein kinase IIalpha through Ser847 phosphorylation in NG108-15 neuronal cells. *J Biol Chem*. 2000 Sep 8;275(36):28139-43.

Kovacs I, Lentini KM, Ingano LM, Kovacs DM. Presenilin 1 forms aggresomal deposits in response to heat shock. *J Mol Neurosci*. 2006;29(1):9-19.

Kröncke KD, Fehsel K, Kolb-Bachofen V. Inducible nitric oxide synthase and its product nitric oxide, a small molecule with complex biological activities. *Biol Chem Hoppe Seyler*. 1995 Jun;376(6):327-43. Review

Kröncke KD, Fehsel K, Kolb-Bachofen V. Inducible nitric oxide synthase in human diseases. *Clin Exp Immunol*. 1998 Aug;113(2):147-56. Review

Krukoff TL. Central actions of nitric oxide in regulation of autonomic functions. *Brain Res Brain Res Rev*. 1999 Jul;30(1):52-65. Review

Lee SY, Andoh T, Murphy DL, Chiuch CC. 17beta-estradiol activates ICI 182,780-sensitive estrogen receptors and cyclic GMP-dependent thioredoxin expression for neuroprotection. *FASEB J*. 2003 May;17(8):947-8.

Liang J, Jaffrey SR, Guo W, Snyder SH, Clardy J. Structure of the PIN/LC8 dimer with a bound peptide. *Nat Struct Biol*. 1999 Aug;6(8):735-40.

- Lippincott-Schwartz J, Snapp E, Kenworthy A. Studying protein dynamics in living cells. *Nat Rev Mol Cell Biol.* 2001 Jun;2(6):444-56. Review
- Loesch A, Belai A, Burnstock G. An ultrastructural study of NADPH-diaphorase and nitric oxide synthase in the perivascular nerves and vascular endothelium of the rat basilar artery. *J Neurocytol.* 1994 Jan;23(1):49-59.
- Lonart G, Wang J, Johnson KM. Nitric oxide induces neurotransmitter release from hippocampal slices. *Eur J Pharmacol.* 1992 Sep 22;220(2-3):271-2.
- Lorrain DS, Hull EM. Nitric oxide increases dopamine and serotonin release in the medial preoptic area. *Neuroreport.* 1993 Oct 25;5(1):87-9.
- Luconi M, Forti G, Baldi E. Genomic and nongenomic effects of estrogens: molecular mechanisms of action and clinical implications for male reproduction. *J Steroid Biochem Mol Biol.* 2002 Apr;80(4-5):369-81. Review
- Luo W, Dou F, Rodina A, Chip S, Kim J, Zhao Q, Moulick K, Aguirre J, Wu N, Greengard P, Chiosis G. Roles of heat-shock protein 90 in maintaining and facilitating the neurodegenerative phenotype in tauopathies. *Proc Natl Acad Sci U S A.* 2007 May 29;104(22):9511-6.
- Magee T, Fuentes AM, Garban H, Rajavashisth T, Marquez D, Rodriguez JA, Rajfer J, Gonzalez-Cadavid NF. Cloning of a novel neuronal nitric oxide synthase expressed in penis and lower urinary tract. *Biochem Biophys Res Commun.* 1996 Sep 4;226(1):145-51.
- Malinski T. Nitric oxide and nitroxidative stress in Alzheimer's disease. *J Alzheimers Dis.* 2007 May;11(2):207-18. Review
- Mancuso C, Scapagini G, Currò D, Giuffrida Stella AM, De Marco C, Butterfield DA, Calabrese V. Mitochondrial dysfunction, free radical generation and cellular stress response in neurodegenerative disorders. *Front Biosci.* 2007 Jan 1;12:1107-23. Review
- Marino M, Galluzzo P, Ascenzi P. Estrogen signaling multiple pathways to impact gene transcription. *Curr Genomics.* 2006 Nov;7(8):497-508.
- Martínez-Ruiz A, Villanueva L, González de Orduña C, López-Ferrer D, Higuera MA, Tarín C, Rodríguez-Crespo I, Vázquez J, Lamas S. S-nitrosylation of Hsp90 promotes the inhibition of its ATPase and endothelial nitric oxide synthase regulatory activities. *Proc Natl Acad Sci U S A.* 2005 Jun 14;102(24):8525-30.
- Matus A. Microtubule-associated proteins: their potential role in determining neuronal morphology. *Annu Rev Neurosci.* 1988;11:29-44. Review

McLean PJ, Kawamata H, Hyman BT. Alpha-synuclein-enhanced green fluorescent protein fusion proteins form proteasome sensitive inclusions in primary neurons. *Neuroscience*. 2001;104(3):901-12.

McLean PJ, J. Klucken, Y. Shin, and B.T. Hyman. Geldanamycin induces Hsp70 and prevents a-synuclein aggregation and toxicity in vitro. *Biochem. Biophys. Res. Comm.* 2004; 321(3): 665-669.

McMillan K, Masters BS. Prokaryotic expression of the heme- and flavin-binding domains of rat neuronal nitric oxide synthase as distinct polypeptides: identification of the heme-binding proximal thiolate ligand as cysteine-415. *Biochemistry*. 1995 Mar 21;34(11):3686-93.

McMillan K, Adler M, Auld DS, Baldwin JJ, Blasko E, Browne LJ, Chelsky D, Davey D, Dolle RE, Eagen KA, Erickson S, Feldman RI, Glaser CB, Mallari C, Morrissey MM, Ohlmeyer MH, Pan G, Parkinson JF, Phillips GB, Polokoff MA, Sigal NH, Vergona R, Whitlow M, Young TA, Devlin JJ. Allosteric inhibitors of inducible nitric oxide synthase dimerization discovered via combinatorial chemistry. *Proc Natl Acad Sci U S A*. 2000 Feb 15;97(4):1506-11.

McNeill AM, Kim N, Duckles SP, Krause DN, Kontos HA. Chronic estrogen treatment increases levels of endothelial nitric oxide synthase protein in rat cerebral microvessels. *Stroke*. 1999 Oct;30(10):2186-90.

Melino G, Bernassola F, Knight RA, Corasaniti MT, Nistico G, Finazzi-Agro A. S-nitrosylation regulates apoptosis. *Nature*. 1997 Jul 31;388(6641):432-3.

Mendelsohn ME. Genomic and nongenomic effects of estrogen in the vasculature. *Am J Cardiol*. 2002 Jul 3;90(1A):3F-6F. Review

Michel T. Targeting and translocation of endothelial nitric oxide synthase. *Braz J Med Biol Res*. 1999 Nov;32(11):1361-6. Review

Miñana MD, Montoliu C, Llansola M, Grisolia S, Felipo V. Nicotine prevents glutamate-induced proteolysis of the microtubule-associated protein MAP-2 and glutamate neurotoxicity in primary cultures of cerebellar neurons. *Neuropharmacology*. 1998 Jul;37(7):847-57.

Monti JM, Jantos H. Effects of L-arginine and SIN-1 on sleep and waking in the rat during both phases of the light-dark cycle. *Life Sci*. 2004 Sep 10;75(17):2027-34.

Motterlini R, Green CJ, Foresti R. Regulation of heme oxygenase-1 by redox signals involving nitric oxide. *Antioxid Redox Signal*. 2002 Aug;4(4):615-24. Review
Mungrue IN, Bredt DS. nNOS at a glance: implications for brain and brawn. *J Cell Sci*. 2004 Jun 1;117(Pt 13):2627-9. Review

Navarro-Lérida I, Corvi MM, Barrientos AA, Gavilanes F, Berthiaume LG, Rodríguez-Crespo I. Palmitoylation of inducible nitric-oxide synthase at Cys-3 is required for proper intracellular traffic and nitric oxide synthesis. *J Biol Chem*. 2004 Dec 31;279(53):55682-9.

Noguchi S, Jianmongkol S, Bender AT, Kamada Y, Demady DR, Osawa Y. Guanabenz-mediated inactivation and enhanced proteolytic degradation of neuronal nitric-oxide synthase. *J Biol Chem*. 2000 Jan 28;275(4):2376-80.

Nurminen M.L, A. Ylikorkala, and H. Vapaatalo. Central inhibition of nitric oxide synthesis increases blood pressure and heart rate in anesthetized rats. *Methods Find Exp Clin Pharmacol*, 1997;19(1):35-41.

Oess S, Icking A, Fulton D, Govers R, Müller-Esterl W. Subcellular targeting and trafficking of nitric oxide synthases. *Biochem J*. 2006 Jun 15;396(3):401-9. Review

Okamura, H., M. Yokosuka, and S. Hayashi. Estrogenic induction of NADPH-diaphorase activity in the preoptic neurons containing estrogen receptor immunoreactivity in the female rat. *J Neuroendocrinol*, 1994. 6(6): p. 597-601.

Olanow CW, Perl DP, DeMartino GN, McNaught KS. Lewy-body formation is an aggresome-related process: a hypothesis. *Lancet Neurol*. 2004 Aug;3(8):496-503. Review

Osawa Y, Lowe ER, Everett AC, Dunbar AY, Billecke SS. Proteolytic degradation of nitric oxide synthase: effect of inhibitors and role of hsp90-based chaperones. *J Pharmacol Exp Ther*. 2003 Feb;304(2):493-7. Review

Pacher, P., Beckman, J. S. & Liaudet L. Nitric oxide and peroxynitrite in health and disease. *Physiol Rev*. 2007 Jan;87(1):315-424.

Panda K, Adak S, Aulak KS, Santolini J, McDonald JF, Stuehr DJ. Distinct influence of N-terminal elements on neuronal nitric-oxide synthase structure and catalysis. *J Biol Chem*. 2003 Sep 26;278(39):37122-31.

Pelligrino DA, Ye S, Tan F, Santizo RA, Feinstein DL, Wang Q. Nitric-oxide-dependent pial arteriolar dilation in the female rat: effects of chronic estrogen depletion and repletion. *Biochem Biophys Res Commun*. 2000 Mar 5;269(1):165-71.

Peng HM, Morishima Y, Jenkins GJ, Dunbar AY, Lau M, Patterson C, Pratt WB, Osawa Y. Ubiquitylation of neuronal nitric-oxide synthase by CHIP, a chaperone-dependent E3 ligase. *J Biol Chem*. 2004 Dec 17;279(51):52970-7.

Persechini A, McMillan K, Leakey P. Activation of myosin light chain kinase and nitric oxide synthase activities by calmodulin fragments. *J Biol Chem*. 1994 Jun 10;269(23):16148-54.

- Pfister KK. Cytoplasmic dynein and microtubule transport in the axon: the action connection. *Mol Neurobiol*. 1999 Oct-Dec;20(2-3):81-91. Review
- Phung YT, Black SM. Use of chimeric forms of neuronal nitric-oxide synthase as dominant negative mutants. *IUBMB Life*. 1999 Sep;48(3):333-8.
- Pierrefiche O, Abdala AP, Paton JF. Nitric oxide and respiratory rhythm in mammals: a new modulator of phase transition?. *Biochem Soc Trans*. 2007 Nov;35(Pt 5):1258-63. Review
- Pike MC, Pearce CL, Wu AH. Prevention of cancers of the breast, endometrium and ovary. *Oncogene*. 2004 Aug 23;23(38):6379-91. Review
- Pirondi S, Fernandez M, Schmidt R, Hökfelt T, Giardino L, Calzà L. The galanin-R2 agonist AR-M1896 reduces glutamate toxicity in primary neural hippocampal cells. *J Neurochem*. 2005 Nov;95(3):821-33.
- Poulos TL. Soluble guanylate cyclase. *Curr Opin Struct Biol*. 2006 Dec;16(6):736-43. Review
- Prast, H., Tran, M. H., Fischer, H. & Philippu, A. Nitric oxide-induced release of acetylcholine in the nucleus accumbens: role of cyclic GMP, glutamate, and GABA. *J Neurochem*. 1998 Jul;71(1):266-73.
- Rameau GA, Chiu LY, Ziff EB. NMDA receptor regulation of nNOS phosphorylation and induction of neuron death. *Neurobiol Aging*. 2003 Dec;24(8):1123-33.
- Rameau GA, Tukey DS, Garcin-Hosfield ED, Titcombe RF, Misra C, Khatri L, Getzoff ED, Ziff EB. Biphasic coupling of neuronal nitric oxide synthase phosphorylation to the NMDA receptor regulates AMPA receptor trafficking and neuronal cell death. *J Neurosci*. 2007 Mar 28;27(13):3445-55.
- Rauhala P, Lin AM, Chiueh CC. Neuroprotection by S-nitrosoglutathione of brain dopamine neurons from oxidative stress. *FASEB J*. 1998 Feb;12(2):165-73.
- Ravi K, Brennan LA, Levic S, Ross PA, Black SM. S-nitrosylation of endothelial nitric oxide synthase is associated with monomerization and decreased enzyme activity. *Proc Natl Acad Sci U S A*. 2004 Feb 24;101(8):2619-24.
- Reif A, Fröhlich LG, Kotsonis P, Frey A, Bömmel HM, Wink DA, Pfeleiderer W, Schmidt HH. Tetrahydrobiopterin inhibits monomerization and is consumed during catalysis in neuronal NO synthase. *J Biol Chem*. 1999 Aug 27;274(35):24921-9.
- Reiter TA. NO* chemistry: a diversity of targets in the cell. *Redox Rep*. 2006;11(5):194-206. Review

- Reits EA, Benham AM, Plougastel B, Neefjes J, Trowsdale J. Dynamics of proteasome distribution in living cells. *EMBO J*. 1997 Oct 15;16(20):6087-94.
- Riefler GM, Firestein BL. Binding of neuronal nitric-oxide synthase (nNOS) to carboxyl-terminal-binding protein (CtBP) changes the localization of CtBP from the nucleus to the cytosol: a novel function for targeting by the PDZ domain of nNOS. *J Biol Chem*. 2001 Dec 21;276(51):48262-8.
- Rivier, C. Role of gaseous neurotransmitters in the hypothalamic–pituitary–adrenal axis. *Ann N Y Acad Sci*. 2001 Mar;933:254-64.
- Roberts CK, Barnard RJ, Scheck SH, Balon TW. Exercise-stimulated glucose transport in skeletal muscle is nitric oxide dependent. *Am J Physiol*. 1997 Jul;273(1 Pt 1):E220-5.
- Rodriguez-Crespo I, Straub W, Gavilanes F, Ortiz de Montellano PR. Binding of dynein light chain (PIN) to neuronal nitric oxide synthase in the absence of inhibition. *Arch Biochem Biophys*. 1998 Nov 15;359(2):297-304.
- Ross CA, Poirier MA. Opinion: What is the role of protein aggregation in neurodegeneration? *Nat Rev Mol Cell Biol*. 2005 Nov;6(11):891-8. Review
- Lohmann SM, Vaandrager AB, Smolenski A, Walter U, De Jonge HR. Distinct and specific functions of cGMP-dependent protein kinases. *Trends Biochem Sci*. 1997 Aug;22(8):307-12. Review
- Saha RN, Pahan K. Signals for the induction of nitric oxide synthase in astrocytes. *Neurochem Int*. 2006 Jul;49(2):154-63. Review
- Saini R, Patel S, Saluja R, Sahasrabudde AA, Singh MP, Habib S, Bajpai VK, Dikshit M. Nitric oxide synthase localization in the rat neutrophils: immunocytochemical, molecular, and biochemical studies. *J Leukoc Biol*. 2006 Mar;79(3):519-28.
- Saitoh F, Tian QB, Okano A, Sakagami H, Kondo H, Suzuki T. NIDD, a novel DHHC-containing protein, targets neuronal nitric-oxide synthase (nNOS) to the synaptic membrane through a PDZ-dependent interaction and regulates nNOS activity. *J Biol Chem*. 2004 Jul 9;279(28):29461-8.
- Sánchez F, Martínez ME, Rubio M, Carretero J, Moreno MN, Vázquez R. Reduced nicotinamide adenine dinucleotide phosphate-diaphorase activity in the paraventricular nucleus of the rat hypothalamus is modulated by estradiol. *Neurosci Lett*. 1998 Sep 4;253(2):75-8.

- Sattler R, Xiong Z, Lu WY, Hafner M, MacDonald JF, Tymianski M. Specific coupling of NMDA receptor activation to nitric oxide neurotoxicity by PSD-95 protein. *Science*. 1999 Jun 11;284(5421):1845-8.
- Schulz E, Anter E, Zou MH, Keaney JF Jr. Estradiol-mediated endothelial nitric oxide synthase association with heat shock protein 90 requires adenosine monophosphate-dependent protein kinase. *Circulation*. 2005 Jun 28;111(25):3473-80.
- Schuman, E.M. and D.V. Madison. A requirement for the intercellular messenger nitric oxide in long-term potentiation. *Science*, 1991. 254(5037):1503-6.
- Sergeeva OA, Doreulee N, Chepkova AN, Kazmierczak T, Haas HL. Long-term depression of cortico-striatal synaptic transmission by DHPG depends on endocannabinoid release and nitric oxide synthesis. *Eur J Neurosci*. 2007 Oct;26(7):1889-94.
- Serrando M, Casanovas A, Esquerda JE. Occurrence of glutamate receptor subunit 1-containing aggresome-like structures during normal development of rat spinal cord interneurons. *J Comp Neurol*. 2002 Jan 1;442(1):23-34.
- Shaul PW, Smart EJ, Robinson LJ, German Z, Yuhanna IS, Ying Y, Anderson RG, Michel T. Acylation targets endothelial nitric-oxide synthase to plasmalemmal caveolae. *J Biol Chem*. 1996 Mar 15;271(11):6518-22.
- Shu X, Shaner NC, Yarbrough CA, Tsien RY, Remington SJ. Novel chromophores and buried charges control color in mFruits. *Biochemistry*. 2006 Aug 15;45(32):9639-47.
- Silvagno F, Xia H, Bredt DS. Neuronal nitric-oxide synthase-mu, an alternatively spliced isoform expressed in differentiated skeletal muscle. *J Biol Chem*. 1996 May 10;271(19):11204-8.
- Singh P, Deng A, Weir MR, Blantz RC. The balance of angiotensin II and nitric oxide in kidney diseases. *Curr Opin Nephrol Hypertens*. 2008 Jan;17(1):51-6. Review
- Song T, Sugimoto K, Ihara H, Mizutani A, Hatano N, Kume K, Kambe T, Yamaguchi F, Tokuda M, Watanabe. p90 RSK-1 associates with and inhibits neuronal nitric oxide synthase. *Biochem J*. 2007 Jan 15;401(2):391-8.
- Song Y, Zweier JL, Xia Y. Heat-shock protein 90 augments neuronal nitric oxide synthase activity by enhancing Ca²⁺/calmodulin binding. *Biochem J*. 2001 Apr 15;355(Pt 2):357-60.
- Soszynski D. Molecular mechanism of emotional fever--the role of nitric oxide. *J Physiol Pharmacol*. 2006 Nov;57 Suppl 8:51-9.

Squadrito F, Calapai G, Altavilla D, Cucinotta D, Zingarelli B, Arcoraci V, Campo GM, Caputi AP. Central serotonergic system involvement in the anorexia induced by NG-nitro-L-arginine, an inhibitor of nitric oxide synthase. *Eur J Pharmacol.* 1994 Apr 1;255(1-3):51-5.

Sultana R, Poon HF, Cai J, Pierce WM, Merchant M, Klein JB, Markesbery WR, Butterfield DA. Identification of nitrated proteins in Alzheimer's disease brain using a redox proteomics approach. *Neurobiol Dis.* 2006 Apr;22(1):76-87.

Swaminathan R, Hoang CP, Verkman AS. Photobleaching recovery and anisotropy decay of green fluorescent protein GFP-S65T in solution and cells: cytoplasmic viscosity probed by green fluorescent protein translational and rotational diffusion. *Biophys J.* 1997 Apr;72(4):1900-7.

Tanaka M, Kim YM, Lee G, Junn E, Iwatsubo T, Mouradian MM. Aggresomes formed by alpha-synuclein and synphilin-1 are cytoprotective. *J Biol Chem.* 2004 Feb 6;279(6):4625-31.

Toda N, Ayajiki K, Okamura T. Nitric oxide and penile erectile function. *Pharmacol Ther.* 2005 May;106(2):233-66. Review

Tonini M, De Giorgio R, De Ponti F, Sternini C, Spelta V, Dionigi P, Barbara G, Stanghellini V, Corinaldesi R. Role of nitric oxide- and vasoactive intestinal polypeptide-containing neurones in human gastric fundus strip relaxations. *Br J Pharmacol.* 2000 Jan;129(1):12-20.

Zagotta WN, Siegelbaum SA. Structure and function of cyclic nucleotide-gated channels. *Annu Rev Neurosci.* 1996;19:235-63. Review.

Walters EH, Soltani A, Reid DW, Ward C. Vascular remodelling in asthma. *Curr Opin Allergy Clin Immunol.* 2008 Feb;8(1):39-43. Review

Wandinger SK, Richter K, Buchner J. The Hsp90 chaperone machinery. *J Biol Chem.* 2008 Jul 4;283(27):18473-7.

Wang Y, Newton DC, Robb GB, Kau CL, Miller TL, Cheung AH, Hall AV, VanDamme S, Wilcox JN, Marsden PA. RNA diversity has profound effects on the translation of neuronal nitric oxide synthase. *Proc Natl Acad Sci U S A.* 1999 Oct 12;96(21):12150-5.

Watanabe Y, Nishio M, Hamaji S, Hidaka H. Inter-isoformal regulation of nitric oxide synthase through heteromeric dimerization. *Biochim Biophys Acta.* 1998 Oct 14;1388(1):199-208.

Watanabe Y, Song T, Sugimoto K, Horii M, Araki N, Tokumitsu H, Tezuka T, Yamamoto T, Tokuda M. Post-synaptic density-95 promotes calcium/calmodulin-

dependent protein kinase II-mediated Ser847 phosphorylation of neuronal nitric oxide synthase. *Biochem J.* 2003 Jun 1;372(Pt 2):465-71.

Waza M, Adachi H, Katsuno M, Minamiyama M, Tanaka F, Sobue G. Alleviating neurodegeneration by an anticancer agent: an Hsp90 inhibitor (17-AAG). *Ann N Y Acad Sci.* 2006 Nov;1086:21-34. Review

Weiner CP, Lizasoain I, Baylis SA, Knowles RG, Charles IG, Moncada S. Induction of calcium-dependent nitric oxide synthases by sex hormones. *Proc Natl Acad Sci U S A.* 1994 May 24;91(11):5212-6.

Wen Y, Perez EJ, Green PS, Sarkar SN, Simpkins JW. nNOS is involved in estrogen mediated neuroprotection in neuroblastoma cells. *Neuroreport.* 2004 Jun 28;15(9):1515-8.

Wolff DJ, Lubeskie A, Gauld DS, Neulander MJ. Inactivation of nitric oxide synthases and cellular nitric oxide formation by N6-iminoethyl-L-lysine and N5-iminoethyl-L-ornithine. *Eur J Pharmacol.* 1998 Jun 5;350(2-3):325-34.

Xie, Q.W., Kashiwabara, Y., Nathan, C., 1994. Role of transcription factor NF-kappa B/Rel in induction of nitric oxide synthase. *J. Biol. Chem.* 269, 4705–4708.

Yang SN. Presynaptic involvement of nitric oxide in dopamine D1/D5 receptor-induced sustained enhancement of synaptic currents mediated by ionotropic glutamate receptors in the rat hippocampus. *Neurosci Lett.* 1999 Jul 30;270(2):87-90.

Yang, S., L. Bae, and L. Zhang. Estrogen increases eNOS and NOx release in human coronary artery endothelium. *J Cardiovasc Pharmacol*, 2000. 36(2):242-7.

Yoshida M, Xia Y. Heat shock protein 90 as an endogenous protein enhancer of inducible nitric-oxide synthase. *J Biol Chem.* 2003 Sep 19;278(38):36953-8.

Yoshimura Y, Yamauchi Y, Shinkawa T, Taoka M, Donai H, Takahashi N, Isobe T, Yamauchi T. Molecular constituents of the postsynaptic density fraction revealed by proteomic analysis using multidimensional liquid chromatography-tandem mass spectrometry. *J Neurochem.* 2004 Feb;88(3):759-68.

Yuan Z, Liu B, Yuan L, Zhang Y, Dong X, Lu J. Evidence of nuclear localization of neuronal nitric oxide synthase in cultured astrocytes of rats. *Life Sci.* 2004 May 14;74(26):3199-209.

Zhuravliova E, Barbakadze T, Narmania N, Ramsden J, Mikeladze D. Inhibition of nitric oxide synthase and farnesyltransferase change the activities of several transcription factors. *J Mol Neurosci.* 2007;31(3):281-7.